The Roles of Polo-like kinase A in Cell Cycle Regulation and Development in *Aspergillus nidulans*

Klarita Mogilevsky

A Thesis

in

The Department

of

Biology

Presented in Partial Fulfillment of the Requirements

for the Degree of Master of Science (Biology) at

Concordia University

Montreal, Quebec, Canada

April 2008

Your file Votre référence
ISBN: 978-0-494-40854-4
Our file Notre référence
ISBN: 978-0-494-40854-4

Abstract

The Roles of Polo-Like Kinase A in Cell Cycle Regulation and Development in *Aspergillus nidulans*

Klarita Mogilevsky

The Polo-Like Kinases (PLK) comprises a family of conserved serine/threonine kinases that play critical roles throughout the cell cycle. PLK are up-regulated in various cancers, and thus are being targeted by several anti-cancer therapies. While higher organisms contain multiple PLK homologues, lower organisms contain a single copy, which is essential. *Aspergillus nidulans* is a filamentous fungus that is used as a model organism for eukaryotic cell cycle research. A previous study isolated PLKA in *A. nidulans*, the first polo-like kinase reported in any filamentous fungus, but the functions were not clear. In this study, we explored the function of PLKA through constructing strains deleted for *plkA* or carrying a single copy under control of the regulatable *alcA* promoter. Surprisingly, our results show that *plkA* is not essential, despite being the single PLK in *A. nidulans*. However, it is required for proper colony growth and polar axis formation in hyphae, since colonies were compact and hyphae were multi-branched with split tips in the absence of the gene. The absence of *plkA* also resulted in numerous abnormal spindle patterns and an abnormally high proportion of cells with telophase spindles, suggesting roles in spindle formation and possibly mitotic exit, as seen with other PLK. Chromosome segregation was also abnormal in a significant proportion of cells, which has not been seen with other PLK mutants. Nuclear division could occur in the absence of *plkA*, suggesting that it is not essential for nuclear division. However, absence of *plkA* partially suppressed the G2/M block in $nimT^{Cdc25C}$ cells at restrictive temperature, suggesting a novel role for PLKA in negatively regulating the G_2/M transition.

Surprisingly, PLKA was not required for septation/cytokinesis, unlike all other PLK. PLKA may be carrying out its functions in part through regulating microtubule dynamics, since the compact growth phenotype was cold-sensitive, and could be suppressed by low doses of the microtubule-destabilizing drug benomyl. Finally, the absence of *plkA* also resulted in a repression of asexual development but induction of sexual structures, suggesting a novel role for this cell cycle regulator in controlling developmental processes. Thus, despite the fact that PLKA is not essential in *A. nidulans*, we have demonstrated that the gene has conserved but also novel functions in regulating the cell cycle and, intriguingly, development. The results expand our current knowledge of the functions of an important group of cell cycle regulators, and thus have important implications for the control of cell growth and the relationship between the cell cycle and development.

Acknowledgements

First and foremost, thank you Dr. C. Bachewich! Without you this work would not have been possible. Your excitement over our discoveries has been infectious. You have helped me in so many ways and have taught me so much. Your patience and understanding are immeasurable. Thank you!

Secondly, to my committee members, Dr. M. Herrington and Dr. R. Storms, thank you for the time, help and guidance that you have provided me over the last few years.

To Dr. M. Champagne, thank you for your endless help, chats and assistance, especially during the long hours on the microscope.

To my colleagues and lab members, thank you for the moral support throughout this amazing rollercoaster ride. I will never forget our endless trips for more caffeine.

Finally, I wish to extend my thanks to my closest friends, my mother and my love Jamie. Without your love and support, I would not have had the energy to continue.

Table of Contents

List of Figures

List of Tables

1. Introduction

1.1 Cell Cycle: General

The eukaryotic cell cycle is the process by which two daughter cells form from one mother cell (Murray and Hunt, 1993). Details of the cycle may vary from one organism to another, but the foundation remains conserved. The cell will first duplicate its DNA so that there are two copies of the entire genome, followed by separation of DNA and then the physical separation of the cell into two identical daughter cells. Different cancers can be caused by the deregulation of the cell cycle, where one or more of the regulatory players no longer functions properly. Therefore an understanding of the regulation of the cell cycle has important implications for the fundamental process of cell growth, as well as cancer.

The cell cycle is divided into two distinct phases, interphase and mitosis. Interphase takes up 90% of the cell cycle time (Murray and Hunt, 1993) and is composed of G1, G2 and S phases. Chromosomes and spindle pole bodies duplicate during S (synthesis) phase, where as growth occurs during G1 and G2 phases, depending on the organism (Murray and Hunt, 1993). Mitosis takes up the remaining 10% of the cell cycle time and is characterized by the segregation of chromosomes to opposite poles of the spindle in order for them to be sequestered into separate daughter cells during cytokinesis (Murray and Hunt, 1993). Cytokinesis follows the completion of mitosis allowing the physical separation of the two daughter cells. There are five sub phases to mitosis. Prophase begins with condensation of the chromosomes and the break down of the nuclear envelope (Murray and Hunt, 1993). At metaphase, chromosomes align at the center of the spindle via their kinetochores which attach to the spindle microtubules. During

anaphase, the chromosomes separate and move to opposite poles of the cell in part through spindle elongation. At telophase, the nuclear envelope re-forms and the chromosomes become uncoiled. Cytokinesis follows, where the contractile ring pinches the cell apart, creating two identical daughter cells (Murray and Hunt, 1993).

1.2 Major regulators of the cell cycle

Cyclins and their partner cyclin dependent kinases (CDK's) regulate major transitions in the cell cycle. Cyclins are proteins that are constantly synthesized and degraded, resulting in a rise and fall in their protein levels throughout the cell cycle (Murray and Hunt, 1993). In contrast, the levels of CDK's are not cyclic during the cell cycle and are therefore found at constant levels throughout the cycle (Murray and Hunt, 1993). Entry into mitosis is regulated by association of cyclin B with its appropriate CDK (Cdc2), forming the mitosis promoting factor (MPF) (Murray and Hunt, 1993). MPF, in turn, is activated by Cdc25, a protein phosphatase that removes an inhibitory phosphate from Cdc2 at threonine 161 (Lee et al., 2005). The Wee1 kinase phosphorylates this residue to maintain Cdc2 in an inactive state, preventing the onset of mitosis (Lee et al., 2005). After triggering mitosis, MPF activity is required for the destruction of cyclin B, leading to the inactivation of MPF, and activation of mitotic exit.

The cell cycle is also regulated by targeted proteolysis. For example, the anaphase-promoting complex (APC) is another major regulator of the cell cycle. It is composed of an E3 ubiquitin ligase that marks proteins for degradation via the proteosome. This activity is required for progression through mitosis. For example, cyclin B and securin, the "glue" that holds sister chromatids together, are targeted by the APC for degradation,

which in turn allows the onset of anaphase. Specific APC activators, such as Cdc20p, target APC activity during anaphase onset, while other factors, such as Cdh1, associate with APC and help activate mitotic exit (Zachariae and Nasmyth, 1999).

The SCF ubiquitin ligase complex is another example of cell cycle regulation control, and is composed of Skp1, Cullin1p and F-box (Wang et al., 2005). In *S. cerevisiae*, the SCF complex targets CDK1/cyclin proteins such as Cdc28p/Cln1 or Cdc28p/Cln2 for degradation, which facilitates activation of the Cdk2-cyclin E complex and thus transition into S phase (Wang et al., 2005). The SCF complex is also found in other organisms where it also targets Cdk1p homologues for degradation to allow transition into S phase.

The cell cycle is also regulated by various checkpoints, which utilize the major players discussed above. Checkpoints are in place to ensure that the cell has successfully completed all the necessary steps prior to entry into the next cell cycle stage. For example, a checkpoint exists in G1 phase that verifies that there are no problems with either the DNA or the spindle pole bodies (Sherr and Roberts, 2004). In the absence of any defects, cells pass the checkpoint and proceed into S phase, where the DNA and the spindle pole bodies duplicate. This checkpoint is known as Start in unicellular eukaryotes and the Restriction Point in higher organisms (Murray and Hunt, 1993). The DNA replication and DNA damage checkpoints ensure that DNA replication is finished without errors and that there is no damage before mitosis is allowed to begin. If errors or damage is discovered, checkpoint factors such as tumor suppressor factor p53 will phosphorylate Cdc2, therefore ensuring that MPF is off. Mitosis will not begin until DNA is properly repaired (Murry and Hunt, 1993). Checkpoints also exist in mitosis, where the mitotic spindle checkpoint will not allow anaphase to begin until the

chromosomes have been correctly aligned on the spindle. This checkpoint is controlled by Mad2p (mitotic arrest deficient), which binds each kinetochore until microtubules attach to it. If this does not occur, then Mad2p remains on the kinetochore and blocks entry into anaphase via binding and inactivating Cdc20p (Zachariae and Nasmyth, 1999). Therefore multiple checkpoints exist throughout the cell cycle and are vital to the integrity of the process.

1.3 Polo-like kinases: major regulators of the cell cycle

1.3.1 General

The polo-like kinases (PLK) comprise a family of major regulators of multiple stages of the cell cycle (Lee et al., 2005). The first polo-like kinase to be discovered was Polo in *Drosophila melanogaster* (Sunkel and Glover, 1998). Mutations resulted in a mitotic block, and abnormalities in spindle formation and nuclear distribution (Sunkel and Glover 1988). Family members from other organisms have since been found, including Cdc5p (Kitada et al., 1993) and Plo1p (Okhura et al., 1995) in *S. cerevisiae* and *S. pombe*, respectively, and CaCdc5p in *C. albicans* (Bachewich et al., 2003). In higher organisms, multiple copies of the gene exist. For example, mammals have four polo-like kinase genes designated Plk1, Plk2, Plk3 and Plk4 (Golsteyn et al., 1994), while *Xenopus laevis* has three, named Plx1, Plx2 and Plx3 (Kumagai and Dunphy, 1996). PLK's in organisms with multiple copies show functions in G1 and S. The fact that PLK have multiple functions during multiple stages of the cell cycle makes them somewhat similar to CDKs.

1.3.2 Structure

PLKs are defined by two conserved domains, the catalytic domain and polo box domain (PBD) (Nigg, 1998). The catalytic domain at the N-terminus is found in all kinases, but has PLK-specific features, including a GxGGFAxC motif, while other kinases have a different motif, GxGxxGxV (Nigg, 1998). The PBD at the C-terminal is found exclusively in the polo-like kinase family and is a highly conserved sequence of 30 amino acids (Li and Li, 2006). The functions of PBD appear to be conserved from yeast to mammals, and include localizing PLK to cellular substructures and regulating PLK activity (Cheng et al., 2003; Elie et al., 2003). The sequence between the domains has no known functional motif and is not conserved among family members.

1.3.3 Functions

PLKs have multiple functions, which appear to be conserved throughout evolution. The main roles are in regulating the G_2/M transition, anaphase onset, mitotic exit and cytokinesis. As well, PLKs have roles in DNA repair, spindle formation and microtubule regulation.

i. G_2/M Transition

There is controversial evidence that PLKs are involved in the G_2/M transition. For example, in vertebrates, Cdc25 removes a phosphate from Cdc2 allowing activation of MPF activity and mitosis. Plk1 can phosphorylate Cdc25 at serine 198 *in vitro*, resulting in its activation (Lee, 2005). However, RNAi results have shown that when Plk1 is silenced, cells arrest in metaphase with incompletely separated chromatids (Xie et al.,

2005), questioning whether PLK1 plays any direct role in regulating the G_2/M transition.

In *S. cerevisiae*, the PLK Cdc5p can also phosphorylate the Cdc25 homologue Mih1, as well as the Wee1 homologue Swe1, which negatively regulates Cdc2/Cdc28 activity (Figure 1). This suggests that Cdc5p may play some role in regulating the G_2/M transition. However, cells lacking Cdc5 can still enter mitosis (Nigg, 1998), which is consistent with the results found in mammals. Therefore Plks may play some positive role in the G_2/M transition, but their necessity is still questionable.

ii. Anaphase Onset

In order for anaphase to begin, where sister chromatids migrate to opposite poles of the cell, the "glue" that keeps the chromatids together or cohesin, must be degraded (Alexandru et al., 2001). Polo-like kinases have functions in this process. For example, Plk1 in mammals will phosphorylate cohesin which results in a reduction in affinity between cohesin and chromatin. This occurs at the metaphase/anaphase transition, preliminary action occurs at prophase (Lee et al, 2005). Similarly, in *S. cerevisiae*, Cdc5p phosphorylates the cohesin Scc1, which promotes its cleavage via the separase Esp1 (Funabiki et al., 1996). This only occurs at anaphase (Lee et al., 2005).

iii. Mitotic Exit

Once sister chromatids have migrated to opposite poles, cells must exit from mitosis. Polo-like kinases are major regulators of this process. For example, in *S. cerevisiae,* the CDK Cdc28p must be inactivated to allow for mitotic exit. The inactivation is achieved through the FEAR (Cdc Fourteen Early Anaphase Release) and MEN (Mitotic Exit

Network) pathways, in which Cdc5p is a major player (Lee et al., 2005). Cdc14p is a phosphatase that is released from the nucleolus in small quantities during early anaphase (FEAR) by Cdc5p activity. Cdc14p dephosphorylates Cdc28p, which inhibits Cdc28p activity. Cdc5p also helps activate the MEN pathway by phosphorylating and inhibiting an antagonizer of MEN, Bfa1/Bub2. Inactivation of Bfa1/Bub2 allows the MEN pathway to release the rest of Cdc14p that was bound in the nucleolus. Cdc14p activity is responsible for the activation of the APC complex, stabilization of the Cdk1 inhibitor Sic1, and nuclear entry of a Sic1 transcription factor, Swi5, leading to further inhibition of Cdc28p activity (Lee et al., 2005). Activation of the APC complex leads to the degradation of both cyclin B and Cdc5p (Zachariae and Nasmyth, 1999), resulting in total inactivation of the Cdc28-Clb2p (MPF), and release of the cell from mitosis. PLKs are also believed to participate in a similar pathway in higher organisms (Figure 3). Mammalian Plks need to be degraded for proper mitotic exit, as shown when Plk3 was overexpressed and cells were unable to undergo cytokinesis (Wang et al., 2002). Therefore PLKs have important functions in both the FEAR and MEN pathways that allow mitosis to end.

iv. Cytokinesis

Polo-like kinases are also involved in cytokinesis in higher organisms and the equivalent process of septation in fungi, but the precise mechanisms of action are not fully understood. In mammals, Plk1 may regulate cytokinesis via its interaction with and phosphorylation of MK1p2 (mitotic kinesin-like protein 2), which is essential for cytokinesis, since depletion of this enzyme caused binucleated cells (Neef et. al., 2003).

When Plk1 is overexpressed, septation becomes random and appears at any stage of the cell cycle (Glover et al., 1998). As well, Plk3 might regulate cytokinesis since it was found to be localized to the midbody at telophase and ectopic expression of a mutant form caused cells to remain attached at the midbody (Wang et al., 2002).

In *S. cerevisiae*, Cdc5p is believed to contribute to septation because *cdc5* temperature-sensitive mutants were defective in membrane closure and septum formation, even when mitotic exit was bypassed (Park et al., 2003). As well, localization studies have determined that Cdc5p is localized to the bud neck from G_2 until late mitosis, after which it localizes to the SPB (Park et al., 2003). Cdc5p appears to exert its function in septation through MEN-dependent and MEN-independent mechanisms.

The role of PLK in septation in *S. pombe* was shown very clearly, where loss of Plo1p function resulted in multinucleated cells with no septa and defective actin rings (Toyoshima-Morimoto et al., 2001). Overexpression of Plo1p induced septation in interphase cells (Nigg, 1998). The septum initiation network (SIN) is the pathway used by *S. pombe* to go through the final phase of mitosis and regulate septation, and involves Plo1p activity (Figure 3) (Lee et al., 2001). The contraction of the actomyosin ring and formation of the septum is initiated by Plo1p. Thus, PLK are clearly important for cytokinesis and septation in all organisms studied, but the exact mechanisms are not yet fully understood.

v. Spindle formation and Microtubule regulation

Spindles are composed of microtubules of α and β tubulin subunits (Murray and Hunt, 1993), while γ tubulin plays an important role in nucleating microtubule

polymerization (Morris and Enos, 1992). One of the hallmark functions of PLK is in the regulation of bipolar spindle formation. For example, plo1 mutants in *S. pombe* caused cells to arrest in mitosis with monopolar spindles (Toyoshima-Morimoto et al., 2001). In *S. cerevisiae*, certain *cdc5* temperature-sensitive mutants contained spindles that were noticeably bent and often discontinuous. As well, the spindles were shorter than normal and defective cytoplasmic microtubule dynamics were observed in the population (Park et al., 2008). In vertebrates, expression of a dominant negative PBD of Plk1 caused defects in proper bipolar spindle formation (Lane and Nigg, 1996). Therefore, PLK might have roles in regulating spindle formation. To further support this role, Plks have been linked to numerous microtubule-associating proteins. For instance, Plk1 in vertebrates phosphorylates NIp (ninein-like protein) (Casenghi et al., 2003), TCTP (microtubule stabilizing protein) (Yarm, 2002) and Stathmin (microtubule destabilizing protein) (Budde et al., 2001), which are required at different stages of the cell cycle to promote microtubule dynamics.

vi. DNA damage/repair

PLKs have been shown to be involved in the DNA damage and repair checkpoint pathways, and specifically in mammals by Plk1 (Smits et al., 2000). Ataxia telangiectasia mutated kinase (ATM) responds to cell damage caused by ionizing radiation, and is involved in a G_2 phase cell cycle arrest. A second enzyme, ATM-Rad3–related kinase (ATR), responds to other cell cycle damage, such as DNA replication errors. Plk1, in mammals, is inhibited by DNA damage in an ATM/ATR–dependent fashion. For example, when cells are treated with caffeine, a known inhibitor of ATM,

they arrest in G2 and PLK1 is inhibited (van Vugt et al., 2001). However, it is not clear how PLK1 is regulated during M phase DNA damage. Recent studies have shown that when mitotic cells are treated with DNA damaging agents, this will cause dephosphorylation of Plk1, thus inhibiting its activity (Yuan et al., 2004). However, inhibition of ATM activity will not inhibit Plk1 activity in these mitotic cells, thus Plk1 might not have a direct function in the mitotic cell damage response (Yuan et al., 2004).

PLKs also have a role in DNA repair. In mammals, Plk3 can regulate the activity of DNA polymerase β (Xie et al., 2005), which is known to be a key component in repairing DNA damage. In *S. cerevisiae*, Cdc5p is a target of Rad53p, a DNA-damage checkpoint component. Rad53 phosphorylates and inhibits Cdc5 activity. However, Cdc5p can also inhibit Rad53 by means of a feedback loop, therefore allowing the cell cycle to continue (Cheng et al., 1998). Therefore polo like kinases have important roles in both arresting the cell cycle after DNA damage and repairing it.

vii. Cancer

PLK function has been linked to various cancers. For example, Plk1 plays important roles in prostate cancer and depletion of Plk1 in these cancer cells results in apoptosis (Shaw and Ahmand, 2005). As well, PLKs are commonly overexpressed in many human tumor cells (Strebhardt and Ullrich, 2006). PLKs are therefore being investigated for their important roles in regulating the fundamental process of the cell cycle, but also as potential targets for anti-cancer therapies (Strebhardt and Ullrich, 2006). Specifically, the

unique polo box domain seen only in the polo-like kinase family has been postulated to be an ideal target for drug development.

1.4 Unanswered Questions

Despite the multiple functions of PLK, there still remain many questions regarding regulation and mechanisms of action. For example, phosphorylation of PLKs are required for their activation, but the identity of the Polo like kinase kinases (PLKKs) in most organisms remains elusive. In *Xenopus,* xPLKK1 was discovered, but we do not know its homologues in other organisms, especially in lower organisms. Another question is the importance of PLKs in the G_2/M transition. Early findings suggested that PLKs were required for progression into mitosis, whereas recent findings are putting this into question. Finally, another unanswered question is related to the identity of all the substrates of the PLKs. Many targets have been discovered, but with the vast potential of this kinase, there are likely many more effectors.

1.5 Life cycle of *Aspergillus nidulans*

Aspergillus nidulans is a filamentous fungus that has been used as a model organism for cell cycle research. It grows in a vegetative manner through hyphal formation but also has sexual and asexual development (Casselton and Zolan, 2002). During vegetative growth, asexual spores called conidia germinate and produce long hyphae, which grow in a polar manner. As the hypha grows, nuclear division occurs and septal walls are deposited, creating compartments along the hypha with three or four evenly spaced nuclei (Kaminskyj, 2001). The cells remain attached. The nucleus contributes to septa

placement by directing where morphological landmarks will be placed to form the septum. However, since each compartment is multinucleated, not every nucleus activates the formation of the septal wall (Kaminskyj, 2001). The apical cell compartment grows and this has an active cell cycle, while the subapical compartments remain arrested in interphase. Branching from subapical compartments reactivates mitosis, but how this is achieved is unknown (Kaminskyj, 2001). Cortical landmarks are visible in the areas where polarized growth will occur, such as the apical tip and the branch tip (Momany and Hamer, 1997). An example of the landmarks found at these points is the Spitzenkorper, an organization center that is composed of actin and microtubules and that directs vesicles for fusion with the hyphal tip (Momany, 2002).

In *Aspergillus nidulans*, asexual development begins approximately 20 hours after vegetative growth has started. At the center of a colony, aerial hyphae differentiate and produce aerial stalks, the apical tips of which swell and produce vesicles that contain multiple nuclei. This becomes the conidiophore head. Budding causes a primary metullae layer to appear on the surface of the vesicle and a single nucleus enters each cell. A single division follows and produces a secondary phialide layer, where nuclear division proceeds. One daughter cell remains at the tip of the phialide, whereas the other one buds off to form a conidium, or asexual spore. The process continues, producing a long chain of conidia at various stages of maturity (Boylan et al., 1987). The conidiophore head contains a vast amount of nuclei at various stages of maturation. As mature conidium bud off, they will begin to grow vegetatively and restart the process.

A. nidulans switches to sexual development after approximately one week of growth. At this time the carbon source has been depleted and specialized sexual structures called

cleistothecia become visible. Hülle cells surround the cleistothecia and might have a function in supporting fruiting body formation. Cleistothecia are fruiting bodies that contain thousands of asci, each containing eight binucleated ascospores (Adams et al., 1998). In the ascus sac, two haploid nuclei can fuse, form a diploid nucleus, undergoes meiosis and finally mitosis (Casselton and Zolan, 2002). However the mechanisms that control cleistothecial development have not been studied to the same extent as conidiation, and therefore many unanswered questions regarding regulation remain. Today, both sexual and asexual life cycles are used for experimental purposes.

1.6 Conditional cell cycle mutants

Aspergillus nidulans is an excellent model organism for studying the eukaryotic cell cycle. First, a large number of cell cycle mutants exist in *A. nidulans* that can be utilized for experimental purposes (Morris, 1975). Some of these mutants identified genes that were the first examples of conserved cell cycle associated factors. For example, γ tubulin which functions in initiating microtubule polymerization from the microtubule organization center was first discovered in *A. nidulans* (Morris and Enos, 1992). Secondly, *A. nidulans* is a fungus that is amenable to genetic and molecular manipulation, and it is easy to handle since it grows fast. Third, the genome was recently sequenced and annotated, which facilitates research. Finally, aspects of cell cycle regulation in *A. nidulans* are much more similar to mammals than to yeast. For example, the regulation of the G_2/M transition shows more similarity in *A. nidulans* and mammals than mammals and yeast. As well, spindle formation occurs at the G_2/M transition in *A. nidulans* and

mammals, whereas spindle formation occurs at the S phase in *S. cerevisiae* (Oakley and Osmani, 1993).

Morris et al., (1975) first described numerous cell cycle mutants in *A. nidulans*. These mutants were isolated based on temperature sensitivity, and therefore could not go through the cell cycle when placed at restrictive temperature (42^0C). However, at permissive temperature (32^0C), the cell cycle progressed normally. The mutants were categorized as being NIM (never in mitosis), BIM (blocked in mitosis) and NUD (nuclear distribution). The NIM mutant phenotype is characterized by a single nucleus with uncondensed chromosomes that is blocked in interphase. To date 26 *nim* mutants in 23 genes have been discovered (Osmani and Mirabito, 2004). The BIM mutant phenotype is characterized by a single nucleus with condensed chromosomes and divided spindle pole bodies. To date 9 *bim* mutants in 6 genes have been isolated (Osmani and Mirabito, 2004). The NUD mutants, can complete mitosis, but can not move the nuclei into the elongating hyphae. To date 7 *nud* genes have been discovered (Morris, 2000). Some conditional mutants that play important roles in the cell cycle are the *nimA, nimX, nimT*, *bimE* and *bimG*, and shall be discussed below.

Of the NIM genes, *nimA* has been the most extensively studied and is the defining member of the NIMA kinase family found in other organisms, including mammals. It is a protein kinase that is required in addition to cdc2 for entry into mitosis in *A. nidulans*. When *nimA* was overexpressed, cells were induced to enter mitosis, even if they were in S phase. The mRNA level of *nimA* increased significantly when the cell entered mitosis and decreased as the cell completed mitosis, supporting a role for NIMA in entry and exit from mitosis (Osmani and Mirabito, 2004). However, *nimA* works independently of the

MPF complex, because studies have shown that when *nimA* is placed at restrictive temperature, high levels of MPF are seen (Osmani, 1987). As well, MPF might function upstream of NIMA, therefore explaining why MPF levels remained high when NIMA was absent. The current opinion for the function of *nimA* is in bringing *nimX* and *nimE* (Cdc2 and cyclin B) to the nuclear pore complex (NPC) (Davies et al., 2004), and for regulating disassembly of NPC proteins at mitosis. For example, lower organisms such as filamentous fungi and yeast undergo a closed mitosis, where the nuclear envelope does not breakdown. Thus, transporters are required to bring the proper proteins to the nuclear pore complex for mitosis to begin. It was discovered in *A. nidulans* that this closed mitosis model was not entirely correct, because the nuclear pore complex is partially disassembled at mitosis, with five nucleoporins dispersing from the NPC (De Souza et al., 2004). NIMA kinase function is required for this disassembly, since inappropriate expression of NIMA promoted S phase NPC to resemble that of mitosis (De Souza et al., 2004).

Another important gene, *nimX*, is a homologue of cdc2 in *S. pombe* and *CDC28* in *S. cerevisiae*. The mutant is blocked in G1 phase at the restrictive temperature and the DNA morphology is abnormal (Osmani and Mirabito, 2004). The gene is the only mitotic cyclin-dependent kinase found in *A. nidulans* and is required at both G1 and G2 phases (Osmani and Mirabito, 2004).

NimT is the Cdc25C homologue in *A. nidulans* and is required to remove a phosphate from cdc2 for activation of MPF. When *nimT* mutants are placed at restrictive temperature, little MPF activity is seen (Osmani and Mirabito, 2004), therefore confirming its activity.

Of the BIM genes, *bimE* is a component of the APC/C complex (Osmani and Mirabito, 2004). Homologues of the gene are cut4 and *APC1* in *S. pombe* and *S. cerevisiae*, respectively. Another important gene is *bimG*. When conditional mutants are placed at restrictive temperature, they contain an increased number of phosphoproteins in the cell. Therefore *bimG* may be a protein phosphatase and its function in dephosphorylation could be important for mitotic exit (Osmani and Mirabito, 2004). No homologues for this gene have yet to be discovered.

Thus *A. nidulans* has been an invaluable organism that has helped identify important genes and elucidate many important functions in the regulation of the cell cycle.

1.7 PLKA in *A. nidulans*

The newest member of the polo-like kinase family was recently discovered in *A. nidulans*, called PLKA (Bachewich et al., 2005). Of the PLK family, PLKA has the longest sequence, nearly double that of POLO in *D. melanogaster*. The sequence contains the characteristic catalytic domain at the N terminus, the polo box at the C terminus and the conserved GxGGFAxC motif in the kinase domain. Similar to PLK in other organisms, the middle section has no homology to any known domains or genes. When the full PLKA sequence was compared to other organisms, it demonstrated 43% identity and 64% similarity to *CDC5* in *S. cerevisiae*, 44% identity and 63% similarity to plo1 in *S. pombe* and 42% identity and 61% similarity to Plk1 in *Homo sapiens* (Bachewich et al., 2005). Recent sequencing of the genome confirms that PLKA is the only bonafide PLK homologue in *A. nidulans* (Galagan et al., 2005).

To determine the function of PLKA, attempts were made to delete the gene or place it

under control of an inducible promoter, but were unsuccessful. The potential roles of PLKA were thus explored by overexpressing the gene (Bachewich et al., 2005). The overexpression of PLKA via the *alcA* promoter, which is induced by EtOH and repressed by glucose, demonstrated a nuclear division block, resulting in a *nim*-like phenotype. Interestingly, septation was also inhibited (Bachewich et al., 2005). Similar to that found in *A. nidulans*, overexpression of Plk1 blocked cytokinesis in mammals (Lee et al., 2005), whereas in yeast, such as *S. cerevisiae* and *S. pombe*, the overexpression of Cdc5p (Song et al., 2000) or Plo1p (Okhura et al., 1995) induced septa formation or septin deposition, respectively. The authors concluded that the absence of septa could either be a secondary effect due to absence of nuclear division, suggesting that PLKA is not important for septation, or that PLKA is required for the process, as seen with PLK in other systems.

When microtubules were visualized in *A. nidulans* cells overexpressing PLKA, most cells were blocked in interphase, as demonstrated by the presence of cytoplasmic microtubules and a visible nucleolus within the nucleus (Bachewich et al., 2005). However, approximately 3% of the *plkA* cells were in mitosis, and contained various defects in spindle formation, such as monopolar spindles. Abnormal segregation of chromosomes and uncondensed chromosomes were also seen in the overexpressed cells (Bachewich et al., 2005). Therefore PLKA was proposed to function in spindle formation like that seen with PLK in other organisms, but also in chromosome segregation.

While PLK in other systems localize to the spindle pole body during mitosis, PLKA was found to be localized to the spindle pole body throughout the entire cell cycle, suggesting that PLKA may have a different function or regulation (Bachewich et al.,

2005). To date, no other organism has demonstrated the presence of polo-like kinase throughout interphase. For instance, in *S. cerevisiae*, Cdc5p is localized to the spindle pole body from early S phase until cytokinesis (Cheng et al., 1998). In *S. pombe*, the Plo1p signal is only seen on the spindle pole body once Cdc2 is activated and the signal disappears once Cdc2 is inactivated in mid mitosis (Reynolds and Ohkura, 2002). In vertebrates, Plk1 is localized to the centrosome in late S or early G2 phase and the signal begins to disappear during anaphase (Lindon and Pines, 2004). Therefore the novel localization of PLKA suggests that it may have some novel function in interphase. This localization was independent of NIMA activity (Bachewich et al., 2005), whereas localization of Plo1p was found to be dependent in the NIMA homologue Fin1p (Grallert and Hagan, 2002). These novel aspects of localization suggest that regulation and function of PLKA may involve novel features.

Thus, PLKA appears to have conserved and novel functions, but the mechanisms of action are not understood. Due to the many benefits of the *A. nidulans* system for cell cycle research, continued investigations of PLKA will have the potential to expand our knowledge of an important group of cell cycle regulators, and identify novel functions.

We have thus continued to explore PLKA function, through construction of deletion and regulated strains. Our findings confirm many of the roles of PLKA suggested by overexpression studies, but have also uncovered novel and unexpected functions, which highlight the complex multi-functional nature of this important cell cycle regulatory kinase.

Thus, this thesis will explore the roles of PLKA in *Aspergillus nidulans*. A separate study on the roles of the TRAPP complex factor Trs120p in morphogenesis and cell cycle regulation in *C. albicans* is included in Appendix 2".

2. Materials and Methods

2.1 Strains, oligos, plasmids, media

Strains and plasmids are listed in Table 1 and Table 2, respectively. Oligos are listed in Table 3. Conidia were normally prepared from strains grown in YAG media containing 0.5% yeast extract, 1% glucose, 10mM $MgSO_4$, 0.1% trace elements (1mg/ml $FeSO_4$, 8.8mg/ml $ZnSO_4$, 0.4mg/ml $CuSO_4$, 0.15mg/ml $MnSO_4$, 0.1mg/ml $Na_2B_4O_7$, 0.05mg/ml $(NH_4)_6Mo_7O_2$) and the following vitamins (unless specified otherwise): 2ug/ml nicotinamide, 5uM para-aminobenzoic acid, 0.1ug/ml riboflavin, 0.05ug/ml pyridoxine and 0.02ug/ml biotin (Osmani et al., 1987). Strains that were auxotrophic for *pyrG* were grown in YAGuu media, consisted of YAG media supplemented with 10mM each of uracil and uridine. Alternatively, conidia from strains carrying a gene under the control of the *alcA* promoter were grown in minimal media containing 0.5M Urea, 0.35M KCl, 0.1M $MgSO_4$, 0.5M monobasic potassium phosphate, 0.5M dibasic potassium phosphate, 0.8M sodium thiosulfate, trace elements (as described above), all vitamins except riboflavin, and either 0.6% threonine and 0.9% fructose to induce or 2% glucose to repress the *alcA* promoter, respectively (Pontecorvo et al., 1953). YAG media was also utilized as a repressing medium, as it was reported to suppress the *alcA* promoter more strongly than minimal media containing glucose (Bussink and Osmani, 1999). Strains were also grown on rich MAG media to compare its effect on repression of the promoter. MAG consisted of 2% Malt extract, 0.2% peptone, 1% dextrose, trace elements (as described above), and all vitamins, as previously described. All solid media contained 2% agar, unless specified otherwise. Parental strains TN02A25, SO182 and ASH262 were grown on YAGuu, whereas strain LO879 was grown on YAG. *plkA*

deletion and control strains KM13, KM14 and KM25 were grown on YAG media. Strains carrying GFP-tagged PLKA, including KM1, KM10 or S-tagged PLKA, including KM8 and KM9 were grown on YAG media. Strains KM3, KM5, KM17, KM20, KM21 and KM22, which contained a single copy of *plkA* under control of the *alcA* promoter, were grown in minimal inducing or repressing media.

For experiments that required synchronous germination, conidia were streaked from glycerol stocks onto plates and allowed to grow for three days. The conidia were then collected, washed and subsequently inoculated ($1x10^7$ spores/ml) into 4mls of top agar, which consisted of the same media that was used on the plates, but contained only 0.8% agar. Top agar media was poured over a standard plate and incubated at 32°C for three days.

General preparation of conidia for inoculation on plates and liquid media was performed according to Kaminskyj (2001). Briefly, conidia were streaked from glycerol stocks on the desired plates and allowed to grow for three days at 32°C. Conidia were then harvested in 0.2% Tween 80 (Sigma-Aldrich) by rubbing the surface of the culture with a sterile plastic rod, centrifuged for 5 min, and subsequently washed twice with ddH_20. Since bacterial infections of strains were frequent, 50μg/ml kanamycin (Sigma) was added to plates used for conidia collection, as well as to liquid media from which conidia were collected for genomic DNA extraction. For short term storage up to two weeks, conidia were maintained in ddH_20 at 4°C. However, for long term storage, glycerol stocks consisting of 20% glycerol and 80% conidia suspension were prepared and kept at -80°C. For most studies, strains were grown at 32°C prior to transformation

or microscope analysis. For temperature sensitivity assays, conidia were plated and grown at 32°C, 37°C or 42°C.

Table 1: *Aspergillus nidulans* strains used in this study

Strains	Genotype	Source
SO182	*nimT, pyrG89, papaA6*	S.A. Osmani
ASH262	*bimE, pabaA6, yA2, pyrG89*	S.A. Osmani
LO879	*nimT23, histone H1-GFP, riboB2*	B. Oakley
TN02A25	*pyrG89, pabaA1, riboB2, nkuA*	B. Oakley
KM1	SO182 PLKA-GFP *(pyrG+)*	This study
KM2	SO182 PLKA-GFP *(pyrG+)*	This study
KM3	TN02A25-*alcA(p)::plkA* (*ribo+)* (Start B)	This study
KM4	TN02A25-*alcA(p)::plkA* (*ribo+)* (Start B)	This study
KM5	TN02A25 *(ribo+)*	This study
KM8	ASH262 PLKA-S-tag *(pyrG+)*	This study
KM9	ASH262 PLKA-S-tag *(pyrG+)*	This study
KM10	ASH262 PLKA-GFP *(pyrG+)*	This study
KM11	ASH262 PLKA-GFP *(pyrG+)*	This study
KM13	TN02A25 *plkA::pyr4+*	This study
KM14	TN02A25 *plkA::pyr4+*	This study
KM20	LO879-*alcA::plkA* (*ribo+*) (Start A)	This study
KM21	LO879-*alcA::plkA* (*ribo+*) (Start A)	This study
KM22	LO879-*alcA::plkA* (*ribo+*) (Start A)	This study
KM23	TN02A25-*alcA::plkA* (*ribo+)* (Start A)	This study
KM26	SO182 *plkA::pyr4+*	This study
KM31	SO182 (*pyr4+*)	This study

Table 2: Plasmids used in this study

Plasmid	Genotype	Sources
pSDW194	*A. nidulans alcA* promoter and A. fumigatus *riboB*	B. Oakley
pFN03	GA5-GFP and *A. fumigatus pyrG*	S.A. Osmani
pAO81	S-TAG and *A. fumigatus pyrG*	S.A. Osmani
pCB150	Upstream and downstream of *plkA* ORF and *pyr4*	C. Bachewich
pAL3	*alcA* and *N. crassa pyr4*	Waring et al., 1989
Cosmid231	*A. nidulans* genome	FGSC

Table 3: Oligos used in this study

Oligonucleotides	Sequence
KM2F	TAG ATA AAT ACA GAA GCA TAT GTG GTG TAT
KM2R	TAA AGT CGC TCG TTA TGT CGT CGG TCG TCA
KM3F	ATG GAG AGA CAC CTC CAA CCA ACA ATG GAA
KM3R	AGA TCG CGT CTT TCC CAC CGT CAA CAT TCC
KM4F	TGA CGA CCG ACG ACA TAA CGA GCG ACT TTA AAG AGG CCG TTC AGG AGT CTG GCT
KM4R	TTC CAT TGT TGG TTG GAG GTG TCT CTC CAT TTT TGA GGC GAG GTG ATA GGA TTG
KM5R	TGT TGG TTG GAG GTG TCT CTC CAT TAA AGT
KM6F	ATG GAA GCT CTA TCG CCG CGG TCA ACA AAC
KM7F	ACT TTA ATG GAG AGA CAC CTC CAA CCA ACA AAG AGG CCG TTC AGG AGT CTG GCT
KM7R	GTT TGT TGA CCG CGG CGA TAG AGC TTC CAT TTT TGA GGC GAG GTG ATA GGA TTG
KM9F	AGC TCG TGA GAC CAA GTT CT
KM9R	ACC GTC CCT TCT CTT GCA TC
CBGSP1	CGG ATA CCA GCG TTC TTT CTA GCA GAA GC
CBGSP2	TAA GCC CGC TAA TCG CAG TCG TTC CCT GAG
CBGSP3	TAA ATT ATG ACT GAT GAC CTT GGG TTG TAT
CBGSP4	TAC AGT CCA GAG CAG ACA AGG GAG GAA ACA
CBGFP1	CTC AGG GAA CGA CTG CGA TTA GCG GGC TTA GGA GCT GGT GCA GGC GCT GGA GCC
CBGFP2	ATA CAA CCC AAG GTC ATC AGT CAT AAT TTA GTC TGA GAG GAG GCA CTG ATG CG
CB2F	TCT TGG CGC ATT GTG CGT GT
CB2R	CAT CGC GCC GAA GCT ATA T
Polo5'F4	TAC ATA CGT CTG GCC AAA AG
Polo3'R5	GTC TTT CCC ACC GTC AAC AT
DpoloF4	GCA CAT CAC CTG GTT G
CB38Fa	GAC CTG TCG TAA AAG CC
CB38Ra	ATC TCG TCT TGG CCC AGT TC

2.2 DNA manipulation

To place *plkA* under the control of the *alcA* promoter (Bussink and Osmani, 1999), a two step PCR approach was utilized (Yang et al, 2004). Oligos KM2F and KM2R were used to amplify a 2kb fragment just upstream of the start codon of the *plkA* sequence from cosmid 231. Oligos KM3F and KM3R were used to amplify a 2kb fragment immediately downstream, including the start codon. Oligos KM4F and KM4R were used to amplify a 3kb fragment of the *alcA* promoter and *ribo* marker from the plasmid pSDW194 (a kind gift from B. and L. Oakley). The three products were then used as templates in a second PCR reaction in a 1:3:1 ratio (50:150:50 ng), where oligos KM2F and KM3R were used to create a 7kb final product. Since the reaction resulted in numerous bands, 6-7 PCR tube samples were run on a 0.9% agarose gel, and the desired 7kb band was cut and subsequently cleaned using a gel extraction kit (Qiagen). 5μg of the product was transformed into strains TN02A25 (Nayak et al, 2006) and LO879. This construct incorporated the original start site reported for *plkA*, which was identified by 5' RACE (Bachewich et al., 2005) and is referred to throughout the thesis as start site A. Since a second start site was suggested for *plkA* when the entire genome was later sequenced (Galagan et al., 2005), a second construct was made that included start site "B", which was 23 nucleotides downstream of start site A. Similar oligos were used for this construction, except that KM5R replaced KM2R, KM6F replaced KM3F, KM7F replaced KM4F and KM7R replaced KM4R. KM2F and KM3R were used with the products in a 1:3:1 ratio, to create the final 7kb transforming construct and transformed into strain TN02A25 (Nayak et al., 2006).

The running conditions for the PCR reaction for fragments 1 and 3 consisted of: 1 cycle of 94°C for 2 min, 10 cycles of 94°C for 10 sec, 45°C for 30 sec, and 68°C for 2 min, 15 cycles of the same conditions with a 20 sec extension, and 1 cycle of 68°C for 7 min. 10μM of oligos, 100mM of dNTP's, and 40ng of cosmid 231 were used in the reaction. Expand long template high fidelity Polymerase with Buffer 3 (Roche) was used for the reaction. PCR conditions for fragment 2 were similar except the extension time was 2 min and 40 sec, and 10ng of pSDW194 plasmid containing the *alcA* promoter and *ribo* as the selectable marker was used. The second fusion PCR consisted of 1 cycle of 95°C for 2 min, 10 cycles of 95°C for 10 sec, 45°C for 30 sec, and 68°C for 7 min, 15 cycles of the same conditions with a 20 sec extension included and extension of 69°C, and a final cycle of 69°C for 7 min. The same concentrations of dNTPs and enzymes were used, except that the templates, fragments 1 to 3, were used in a 1:3:1 ratio (50:150:50 ng).

To attempt to construct a *plkA* deletion strain, a previously-made deletion construct was utilized, which consisted of the *pyr4* marker surrounded by 2kb of 5' and 3' flanking sequence of *plkA*, in plasmid pCB150 (Bachewich et al., 2005). The 6.5kb deletion construct was liberated by cutting with *XbaI* and *StuI*, gel purified and 5μg of DNA was transformed into strain TN02A25, which lacks the *ku* gene and thus increases efficiency of correct integration (Nayak et al., 2006). In order to test the effects of *plkA* within a synchronous population of cells, plkA was also deleted from the temperature-sensitive $nimT^{Cdc25C}$ strain (SO182), which arrests in interphase at the restrictive temperature of 43°C.

In order to investigate PLKA localization in different strain backgrounds, the 3' end of *plkA* was tagged with GFP, using a construct derived from a two-step fusion PCR (Yang et al., 2004; Bachewich et al., 2005). Briefly, oligos CBGSP1 and CBGSP2 were used to amplify a 2kb sequence immediately before the stop codon of the *plkA* sequence, while oligos CBGSP3 and CBGSP4 amplified a 2kb sequence downstream including the stop codon. Oligos CBGFP1 and CBGFP2 amplified a 2.5kb sequence of GFP and the *pyrG* marker from plasmid pFNO3 (Yang et al., 2004).

The running conditions for the PCR reaction for fragments 1 and 3 consisted of: 1 cycle 94°C for 2 min, 10 cycles of 94°C for 10 sec, 51°C for 30 sec, and 68°C for 3 min, 15 cycles of the same conditions with 20 sec extension, and 1 cycle of 68°C for 7 min. 10μM of oligos, 100mM of dNTP's, and 40ng of cosmid 231 were used in the reaction. Expand Long Template Polymerase with Buffer 3 (Roche) was used in the reaction. PCR conditions for fragment 2 were similar except the extension temperature 46°C, and 10ng of GFP plasmid with *pyrG* as the selectable marker (pFN03) was used. The three products were then placed into a second PCR reaction in a 1:3:1 ratio, and oligos CBGSP1 and CBGSP4 amplified a 7kb final transforming construct. The second fusion PCR consisted of 1 cycle of 95°C for 2 min, 10 cycles of 95°C for 10 sec, 46°C for 30 sec, and 68°C for 8 min, 15 cycles of the same conditions with a 20 sec extension included and extension temperature of 69°C, and a final cycle of 69°C for 7 min. The same concentrations of dNTPs and enzymes were used, except that the templates, fragments 1 to 3, were used in a 1:3:1 ratio (50:150:50 ng). The DNA was then gel purified and 5ug was transformed into strain ASH262 to test whether BIME is required

for PLKA localization. A second transformation was done with a different strain background, SO182, to test whether NIMT is required for PLKA localization.

In order to purify PLKA for future affinity purification work, PLKA was tagged with the S-tag (Kim and Raines, 1993) at the 3' end using a construct created with a similar two-step PCR approach. The same oligos for GFP tagging were utilized, but plasmid pAO81 (Yang et al., 2004) was used instead of pFN03 to amplify the 2.5kb sequence of the S-tag and the *pyrG* marker. The three products (50:150:50 ng) were used in a final PCR reaction to create a 7kb product using the same PCR conditions described for GFP-tagging. The DNA was then gel purified and 5ug of DNA was transformed into strain ASH262 strain.

2.3 Transformation

Transformation was performed according to Osmani et al. (1987). Briefly, conidia from glycerol stocks were streaked onto plates and incubated for three days at 32°C. Conidia were then collected, washed, and $2x10^7$ spores/ml were inoculated into 50mls of YAGuu liquid media. After 5 hours (strain ASH262) or 5.5 hours (strains LO879,TN02A25 or SO182) at 32°C, when germ tubes began to emerge, the conidia were collected and transferred to 50ml of lytic mix, composed of 8 mg/ml B-D glucanase (Interspex Products Inc), 5mg/ml Driselase (Interspex Products Inc), and 2mg/ml BSA (Bovine Serum Albumin; Sigma) dissolved into 25ml of solution I (0.8M ammonium sulfate and 100mM citric acid, pH 6.0 with KOH) and 25ml of solution II (1% yeast extract, 2% sucrose, 20mM $MgSO_4$, trace elements and vitamins as required). After incubation at 32°C for two hours at 200rpm, the resulting protoplasts were collected,

washed twice with solution III (0.4M ammonium sulfate, 1% sucrose, 50mM citric acid, pH to 6.0 with KOH) and incubated overnight in 500µl of solution V (0.6M KCl, 50mM $CaCl_2$, 10mM MOPS pH to 6.0 with KOH) at 4°C, on ice. The following day, 100µl of protoplast suspension was mixed with 5µg of DNA and 50µl of solution IV (25% PEG 8000, 50 $CaCl_2$, 0.6M KCl and 10mM Tris pH 7.5) and incubated on ice for 20 min. 1ml of room temperature solution IV was then added and the suspension was incubated at room temperature for 20 min. Various volumes of protoplast suspension were mixed with 4ml of top agar, and plated on selective media containing 0.6M KCl (Osmani et al, 1987). Protoplast volumes ranging from 50-200µl were used. In the case of the *alcA*-regulated strains, selective media consisted of minimal media containing either 25 mM, 50mM or 100mM threonine with 50mM fructose in order to determine the best inducing concentration. For the *plkA*-deletion, GFP and S-tagged strains, selective media consisted of YAG. Transformation plates were left for three days at 32°C. *plkA*-deletion transformants required seven days at 32°C.

During transformation with the *ribo* marker, loss of *ribo* auxotrophy occurred. This could have been due to trace amounts of riboflavin in the media. To ensure that only transformed conidia would grow on the selective media, riboflavin was omitted from solution II. In addition, the volume of solution III wash was increased from 10mls to 50mls. Finally, untransformed protoplasts were also plated to test the selective media plate.

2.4 gDNA extraction

Transformants were streaked to single colony three times, after which $5x10^7$ conidia were collected and incubated in 50mls of liquid media overnight. Mycelia were collected on Miracloth (Calbiochem) using a buchner funnel, quickly frozen with liquid nitrogen, transferred to a 15ml conical tube and placed in a lyophilizer (ModulyoD Freeze Dryer) overnight. The next day, 50-100mg of dried mycelium was placed in an Eppendorf tube and ground to a fine powder using an autoclaved tooth pick. The genomic DNA was extracted using two different methods. The Wizard genomic DNA purification kit (Promega) was initially used. Briefly, 100mg of fine powdered mycelium was resuspended in 600µl of nuclei lysis solution, vortexed for 1-3 seconds and immediately incubated at 65°C for 15 min. After adding 3µl of RNase solution, the tube was inverted several times and then incubated at 37°C for 15 min. The samples were allowed to cool to room-temperature for 5 min. After adding 200µl of protein precipitation solution, the samples were vortexed vigorously for 20 sec at high speed, then centrifuged for 20 min at 14,000 x g. The supernatant was then removed, put into a new microcentrifuge tube, and centrifuged for 20 min. The supernatant was transferred to a new tube containing 600µl of room temperature isopropanol. The tubes were inverted gently until thread-like strands of DNA became visible, and then centrifuged at 14,000 x g for 3 min at room temperature. The solution was decanted and 600µl of 70% EtOH at room temperature was added. The tubes were inverted several times and centrifuged at 14,000 x g. The EtOH was carefully removed, the pellet was air dried for 15 min, dissolved in DNA rehydration solution, and incubated overnight at 4°C.

A phenol/chlorophorm method was later adopted with some modifications (Chow and Kafer, 1993) because a better yield was required. Briefly, 100mg of dried mycelium was grounded to a fine powder with an autoclaved tooth pick. The powder was then resuspended in 200µl of buffer (0.2M Tris-HCl pH 7.5, 0.5M NaCl, 0.01M EDTA and 1% SDS) and 200µl of phenol/cholorofom (1:1), and vortexed for 6 min. After adding 300µl of each buffer and phenol/choloroform, the samples were centrifuged at 14,000 x g for 1 min at room temperature. The supernatant was transfered to a fresh microcentrifuge tube containing 300µl of phenol/chloroform, vortexed for 1 min, and then centrifuged for 1 min. The supernatant was transferred to a new tube and the genomic DNA was precipitated overnight in 1ml of cold 95% EtOH at -20°C. The following day, the genomic DNA was washed in cold 70% EtOH and allowed to air dry for 15 min. The DNA was dissolved in TE (10mM Tris pH8.0 and 1mM EDTA) with 20mg/ml RNaseA (Fermentas Life Science) and incubated at 37°C for 30 min. Genomic DNA was quantified with a Fluorimeter (Hoefer DQ300) using Hoechst Dye.

2.5 Screening Transformants

For the *alcA*-regulated strains, oligos KM9F and KM3R were used with 100ng of gDNA to PCR screen the transformants for proper integration of the DNA construct for both start sites. PCR screening reaction consisted of 1 cycle of 94°C for 2 min, 10 cycles of 94°C for 30 sec, 42°C for 30 sec, and 68°C for 4 min and 20 sec, 15 cycles of the same conditions with 20 sec extension, and a final cycle of 68°C for 7 min. 10µM of oligos and 10mM of dNTP's was used. Expand Long Template Polymerase with Buffer 1 (Roche) was used for the reaction.

Oligos CB38Fa and CB38Ra were used with 100ng of gDNA to PCR screen the *plkA* deletion transformants. PCR screening reaction consisted of 1 cycle of 94°C for 2 min, 10 cycles of 94°C for 30 sec, 48°C for 30 sec, and 68°C for 7 min and 45 sec, 15 cycles of the same conditions including a 20 sec extension, and a final cycle of 68°C for 7 min. 10μM of oligos and 10mM of dNTP's were used. Expand Long Template Polymerase with Buffer 1 (Roche) was used for the reaction.

Oligos CB2R and CBGSP1 were used to PCR screen the GFP-tagged or S-tagged PLKA transformants. 100ng of DNA was used for each sample. PCR screening reaction consisted of 1 cycle of 94°C for 2 min, 10 cycles of 94°C for 30 sec, 41°C for 30 sec, and 68°C for 4 min and 20 sec, 15 cycles of the same conditions including a 20 sec extension, and a final cycle of 68°C for 7 min. The same concentrations or volumes of oligos, dNTPs, gDNA and Buffer 1 were used as previously described.

Southern analysis using the DIG Hybridization System (Roche Diagnostics, Mannheim, Germany) was also performed confirming whether the constructs were properly integrated into the strains. 3-4μg of genomic DNA was cut with 35U of *ClaI* for *alcA*-regulated strain, 140U of *NdeI* for *ΔplkA* strain or 140U *EcoRI* for GFP and S-tag strains overnight. The following day, 4μl of 5M NaCl and 400μl of 95% EtOH was added to the gDNA, which was precipitated overnight at -20°C. The following day, the gDNA was centrifuged at 4°C for 10min, washed with 70% EtOH, then air dried. DNA was dissolved in 20μl of TE and run overnight on a 0.7% agarose gel at 25V. The following day, the gel was denatured, neutralized and then allowed to transfer for a minimum of 5 hours onto a positive charged nylon membrane (Roche). Probe construction and hybridization were performed according to the DIG Hybridization

System (Roche Diagnostics, Mannheim, Germany). Oligos polo5'F4 and polo3'R5 (Bachewich et al., 2005) were used to amplify a product homologous to a sequence within the *plkA* orf. The product was labeled with DIG and used to screen *alcA*-regulated, GFP and S-tagged strains. Oligos DpoloF4 and CB2R (Bachewich et al., 2005) were used to amplify a product homologous to a sequence downstream of the stop codon. This probe was used to screen the *plkA* deletion strains. For probe construction, 500ng of PCR product was boiled for 5min, placed on ice for 5min, and mixed with 10µl of 10X hexanucleotide mix, 10µl of 10X dNTP labeling reaction and 5µl of Klenow polymerase enzyme (Roche). The microcentrifuge tube was gently mixed and incubated at 37°C overnight. The next day, 4µl of 0.5M EDTA, 1µl of 20mg/ml glycogen (Roche), 7.62µl of 5M LiCl and 300µl of cold 95% EtOH were added, and the contents were incubated overnight at -20°C. The following day, the tube was centrifuged at 14,000 x g for 10min (4°C), and the supernatant was removed. The pellet was washed with cold 70% EtOH and centrifuged at 14,000 x g for 5min (4°C). The pellet was allowed to air dry for 15 min, and then dissolved in 50µl of TE buffer. To quantify the probe, 1µl of probe DNA was diluted in 10µl of solution I (0.1M Maleic acid, 0.15M NaCl, 0.175M NaOH pH 7.5), and subsequently serial diluted 1/10, 1/100, 1/1000, 1/10 000 and 1/100 000 times in 50µl of solution I. A control probe at 5ng/ml was diluted to the same concentrations. 1µl of each sample was spotted on a positive charged membrane (Roche). The membrane was UV-cross linked in a UV linker (Stratagene) and then washed with solution I for 1 min. The membrane was then incubated in 50ml of solution II (1% blocking agent (Roche) diluted in solution I) for 30 min and then washed briefly with solution I. After 30 min incubation with a 1:5000 dilution of anti-DIG antibody

conjugated to alkaline phosphatase (Roche) in solution I, the membrane was washed twice for 15 min in solution I. The membrane was then equilibrated for 2 min in 20 ml of solution III (0.1M NaCl and 0.1M Tris-HCl pH9.5), and incubated in a dark container with 40µl of NBT/BCIP (Roche) and 2ml of solution III for up to 20 min. When the desired intensity of coloration was achieved, the membrane was washed with 5ml of solution IV (0.01M Tris-HCl pH8.0 and 0.001M EDTA) for 5 min to stop the reaction. Since the control concentration was known, the probe concentration could be estimated. The two probes were estimated to be 50ng/µl and, 50ng was used for each Southern.

2.6 Microscopy, cell staining

To examine nuclei and septa, $1x10^6$ fresh conidia were inoculated into 500 µl of media on clean coverslips. The cover slips were placed in petrie plates, and incubated at 32°C. To determine germination length and number of nuclei per germling for the *alcA*-regulated strains, conidia were incubated in either YAGuu media for 9 hours or in inducing or repressing minimal media 12 hours. To determine germination pattern, conidia were incubated in either YAGuu media for 10 hours or in inducing or repressing minimal media 15 hours. Finally, to investigate the length of subapical compartments, conidia were incubated in either YAGuu media for 12 hours or in inducing or repressing minimal media 19 hours. Deletion strains were grown in YAG media at 9 hours to determine germination lengths and number of nuclei per germling, 10 hours to determine germination pattern and 12 hours to determine length of subapical compartments. After incubation, cells that adhered to coverslips were fixed with 6% paraformaldehyde fixative for 30 min. Fix consisted of 6% paraformaldehype, 40mM PIPES pH 7.0, 40mM Hepes

pH 8.0, 9mM EGTA pH 7.0, 4.5mM $MgCl_2$, 5% DMSO (Dimethyl Sulfoxide, Fisher Scientific), 10μg/ml of leupeptin (MP Bio), 3μg/ml of aproptinin (MP Bio) and 200μM AEBSF (4-(2-aminoethyl) benzenesulfonyl fluoride, MP Bio). To dissolve paraformaldehyde in ddH_20, the solution was heated and 10μl of NaOH was added prior to the addition of the remaining components. Coverslips were washed twice with 1X PHEM (20mM PIPES pH 7.0, 20mM Hepes pH 8.0, 4.5mM EGTA pH 7.0 and 2.25mM $MgCl_2$) at 4°C, and incubated in 40ng/ml of DAPI (4', 6- Diamidino-2-phenylindole, Sigma) for 20 min. After washing with dH_2O, the cover slips were incubated in 10μg/ml of Calcofluor (Sigma) for 10 min, rinsed with dH_2O, and mounted on microscope slides that were sealed with nail polish. The slides were then examined on a Carl Zeiss microscope (Carl Zeiss, Axioplan) using 100X and 63X oil EC Plan-Neofluar objectives.

To observe microtubules, immunolocalization of α-tubulin was performed (Oakley and Osmani, 1993). Conidia were inoculated onto coverslips and grown in a similar manner as previously described, then fixed with 6% fixative for 30 min. Fix consisted of 6% paraformaldehyde, 50mM PIPES pH6.8, 25mM EGTA, 5mM $MgSO_4$, 5% DMSO, 10μg/ml of leupeptin (MP Bio), 3μg/ml of aprotinin (MP Bio), and 200μM AEBSF (4-(2-aminoethyl) benzenesulfonyl fluoride, (MP Bio). Coverslips were rinsed twice with PE buffer (50mM PIPES pH 6.8, 25mM EGTA pH 7.0) at 4°C, and then incubated in digestive solution (50mM sodium citrate buffer pH 6.0, 1mM $MgSO_4$, 2.5mM EGTA pH 7.0, 2% BSA, 10mg/ml Driselase, 1mg/ml Lyticase, 16mg/ml B-D-glucanse and 10μg/ml of leupeptin (MP Bio), 3μg/ml of aprotinin (MP Bio) and 200μM AEBSF (MP Bio)) for 30 min. Coverslips were then rinsed with PE buffer, and incubated in permeabilizer solution (0.1% Nonidet P40 Substitute (Fluka) in PE buffer, 10μg/ml of leupeptin (MP

Bio), 3μg/ml of aprotinin (MP Bio) and 200μM AEBSF (MP Bio)) for 5 min. After rinsing with PE buffer, cells were incubated overnight at room temperature in primary antibody solution (0.05% sodium azide, 2% BSA and 1:200 dilution of monoclonal anti-α tubulin (DM1A, Sigma) in PE buffer). The next day coverslips were rinsed twice with PE buffer and then incubated for 1 hour in secondary antibody solution (PE buffer, 0.05% sodium azide, 2% BSA and 1:200 dilution of anti-mouse IgG $F(ab')_2$ fragment-FITC, Sigma). Coverslips were rinsed twice with PE buffer, once with dH_20 and then incubated with 40ng/ml of DAPI for 20min. After rinsing with water, the coverslips were mounted on microscope slides that contained a drop of SlowFade gold antifade reagent (Invitrogen). The slides were then examined on a Leica microscope (DM6000B) using a 100X immersion oil objective and the DAPI (460nm) and FITC (520nm) filters.

2.7 Benomyl sensitivity assay

To test whether *ΔplkA* strains were sensitive to benomyl, YAG plates containing 0, 0.2, 0.4, 0.6, 0.8 and 1μg/ml of benomyl were prepared. Initially, a 1mg/ml benomyl stock (Chem Service Inc), diluted in 95% EtOH was made and stored at 4°C. 2000 spores of the deletion strains KM13, KM14 and the control strain KM25 were spot inoculated on each plate and incubated for three days at 32°C.

2.8 Localization of PLKA in *nimT* and *bimE* backgrounds

To test whether the cell cycle factors $nimT^{Cdc25C}$ and $bimE^{APC17}$ were required for PLKA localization, conidia of strains KM1 and KM10 were inoculated into YAG media for 12 hours at either the permissive temperature of 32°C or for 9 hours ($nimT^{Cdc25C}$) at

43°C to arrest the cell cycle at the respective stages. Due to slower growth at higher temperature, strain KM10 (*bimE*^{APC17}) required 15 hours incubation at 43°C. The cells were subsequently fixed with 6% paraformaldehyde, as previously described. Coverslips containg the cells were washed three times with 1X PHEM at 4°C and incubated in 40ng/ml of DAPI for 20min. After four vigourous washes with dH_20, the coverslips were mounted onto microscope slides that contained a drop of SlowFade gold antifad reagent (Invitrogen). The slides were then examined on the Leica microscope (DM6000B) using the 100X immersion oil objective. The GFP signal was seen with the FITC filter and was co-localized to the nucleus using the DAPI filter.

2.9 G_2 Block assay

To investigate the effect of cell synchronization on the rate of mitosis and spindle formation, $1x10^6$ condia from strains KM26 and KM31 strains were inoculated onto coverslips for 8 hours in YAG media at 43°C to induce the *nimT*-dependent block at the G_2/M transition. Sample coverslips were then transferred to permissive temperature of 32°C, for 10min, 15min or 20min. The coverslips were fixed with 6% paraformaldehyde, and α-tubulin was immunolocalized and DNA was stained with DAPI, as previously described. Coverslips were mounted onto microscope slides containing a drop of SlowFade gold antifade reagent (Invitrogen). The slides were then examined on a Leica microscope (DM6000B) using a 100X immersion oil objective and the DAPI (460nm) and FITC (520nm) filters.

2.10 Computer analysis

Image J was used to determine hyphal lengths in the cells (Rasband, W.S. 1997-2007). Statistical analyses were preformed using the SPSS software.

3. Results

3.1 Construction of an *alcA::plkA* regulated strain

In a previous study where *plkA* was first isolated, the functions of the gene were explored by overexpression, the results of which suggested potential dominant negative effects (Bachewich et al., 2005). This strategy was employed because attempts to delete the gene or place it under the control of the regulatable *alcA* (alcohol dehydrogenase) promoter using one-step approaches were not successful, suggesting that *plkA* was essential. This concept was further supported by the fact that when a diploid strain was made heterozygous for *plkA* and plated on benomyl to induce haploidization, viable spores lacking *plkA* could not be recovered (Bachewich et al., 2005).

In order to further investigate the functions of PLKA and to determine whether the gene was in fact essential, we repeated attempts to place *plkA* under control of the *alcA* promoter, but used a new strategy. In the previous study, attempts to create such a regulated strain involved transforming a circular plasmid that contained a 3' truncated copy of *plkA* following the regulatable *alcA* promoter. However, no positive transformants were isolated. In this study, we used fusion PCR (Yang et al., 2004) to create a linear promoter-replacement construct, and transformed it into the Δ*nku* strain background. The *ku* gene is essential for recombination of nonhomologous end joining, and in its absence the efficiency of homologous recombination is as high as 90% (Nayak et al, 2006).

The promoter replacement construct were made to take into account the two different putative translation start sites. Start site "A" (Figure 1) was reported in the first

sequencing of PLKA, which utilized RACE PCR (Bachewich et al., 2005). Start site "B" (Figure 1) was subsequently reported when the entire *Aspergillus nidulans* genome was sequenced, using the shot-gun approach (Galagan et al., 2005). These constructs were created by PCR-amplifying 2kb fragments immediately upstream and downstream of the start codon in *plkA*. A 3kb fragment that contained the *alcA* promoter and the *ribo* selectable marker was also amplified. The three resulting fragments were combined and PCR amplified to create a final 7kb product (Figure 2), which was subsequently transformed into the Δ*nku* strain TN02A25.

Figure 1: Start sites for PLKA
Two different start sites were reported for PLKA. Start A was determined using the 5' RACE method, whereas start B was determined during shotgun sequencing of the entire *A. nidulans* genome.

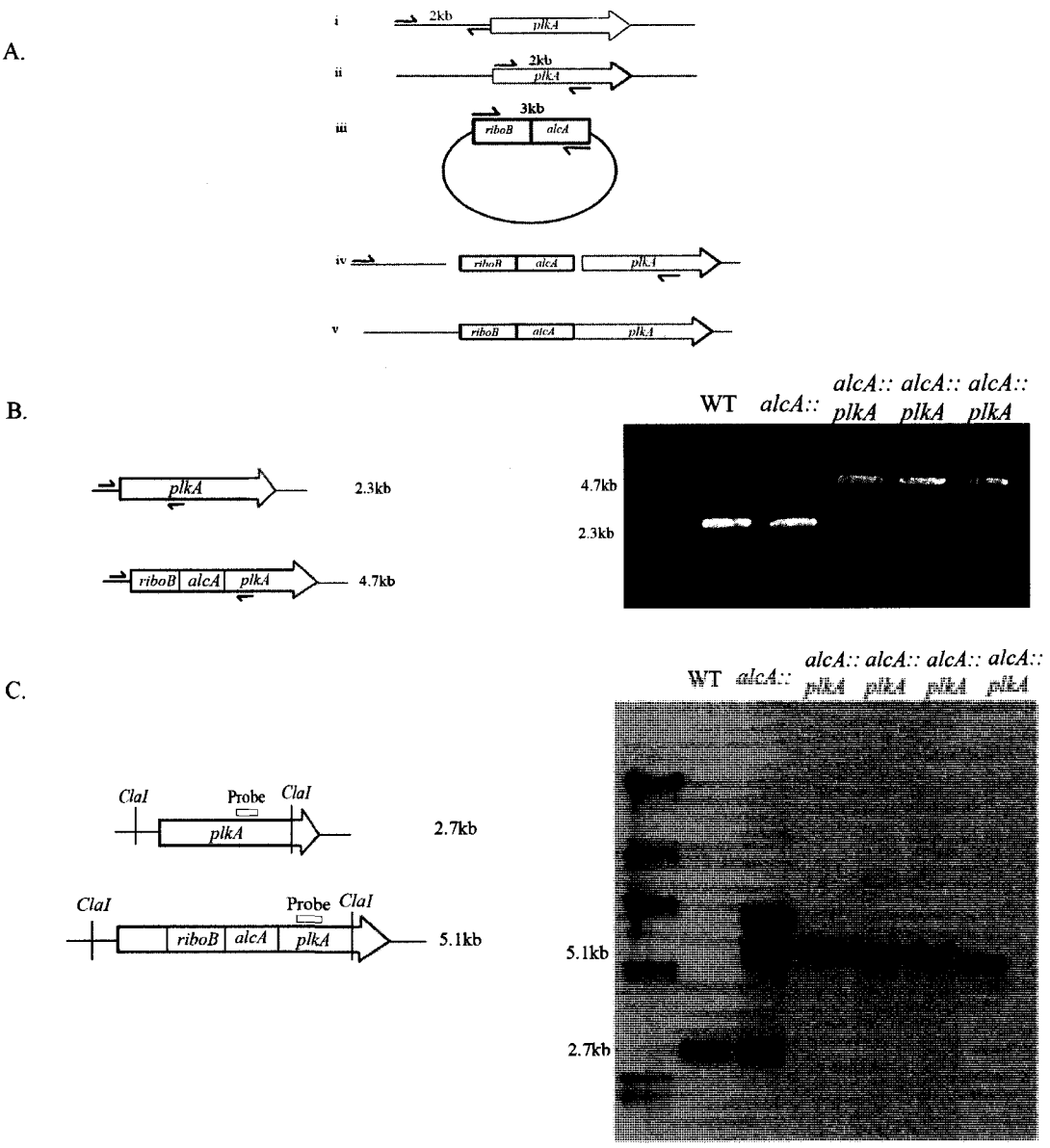

Figure 2: Placing PLKA under the control of the *alcA* promoter in strain TN02A25
(A) Strategy to construct the *alcA::plkA* regulated strain. (i) a 2kb fragment was PCR amplified upstream of the start site. (ii) a 2kb fragment including and downstream of the start site. (iii) a 3kb fragment PCR amplified the *riboB* marker and *alcA* promoter from the plasmid pSDW194. (iv-v) Three fragments were used as a template in a fusion PCR reaction to create a 7kb final product that was transformed into TN02A25 strain. (B) PCR screening demonstrated that strains KM3, KM4 and KM17 are positive (4.7kb), and KM5 is negative (2.3kb). (C) Southern analysis confirming that strains KM3, KM4, KM17 and KM23 are positive (5.1kb), and KM5 is negative (2.7kb).

Transformation with the promoter-replacement construct for start site A resulted in a few transformants. After streaking to single colony three times, strains were screened by PCR using flanking oligos lying outside the transferring DNA sequence (Figure 2B). Strain KM17 was positive, since a 4.7kb band was observed as opposed to a 2.3kb band as seen in the wild type strain. Southern analysis demonstrated the presence of a 2.7kb band in the wild-type TN02A25 strain, but a 5.1kb band in strains KM17 and KM23 (Figure 2C) confirmed proper integration of the promoter-replacement construct.

Transformation with the promoter replacement construct for start site B resulted in several transformants, of which three were streaked to single colony three times and screened by PCR (Figure 2B). Strains KM3 and KM4 were positive, whereas strain KM5 was negative. Southern analysis (Figure 2C) confirmed that proper integration occurred in strains KM3 and KM4, which contained a 5.1 kb band instead of the wild type band at 2.7kb. Strain KM5 contained the 2.7 kb wild type band, as well as two additional bands at 4.6kb and 6.3kb. This strain was subsequently used as a negative control for further analysis. Thus, the new strategy was successful in producing strains that contained a single copy of *plkA* under control of the *alcA* promoter.

3.2 Repressing PLKA does not inhibit growth, but results in abnormal colony morphology

In order to determine the effects of shutting off *plkA* expression, conidia from strains KM17 and KM3, which contained start sites A and B respectively, and the control strain KM5 were point inoculated onto solid repressing medium containing 2% glucose (mm-Glu) or inducing medium containing 0.6% threonine/ 0.9% fructose (mm-TF). The

strains were also tested on YAG repressing media, which has been reported to be a stronger repressor of the *alcA* promoter (Romero et al., 2003) and included point inoculation of the wild type strain TN02A25. After incubation at 32°C for 3 days, all strains demonstrated similar and normal growth on inducing media (Figure 3). On repressing media, however, strains KM17 and KM3 were able to grow but in an abnormal fashion, resulting in compact colonies. No differences were observed between the two strains, suggesting that both start sites were valid. In contrast, control strains TN02A25 and KM5 grew normally on repressing media (Figure 3).

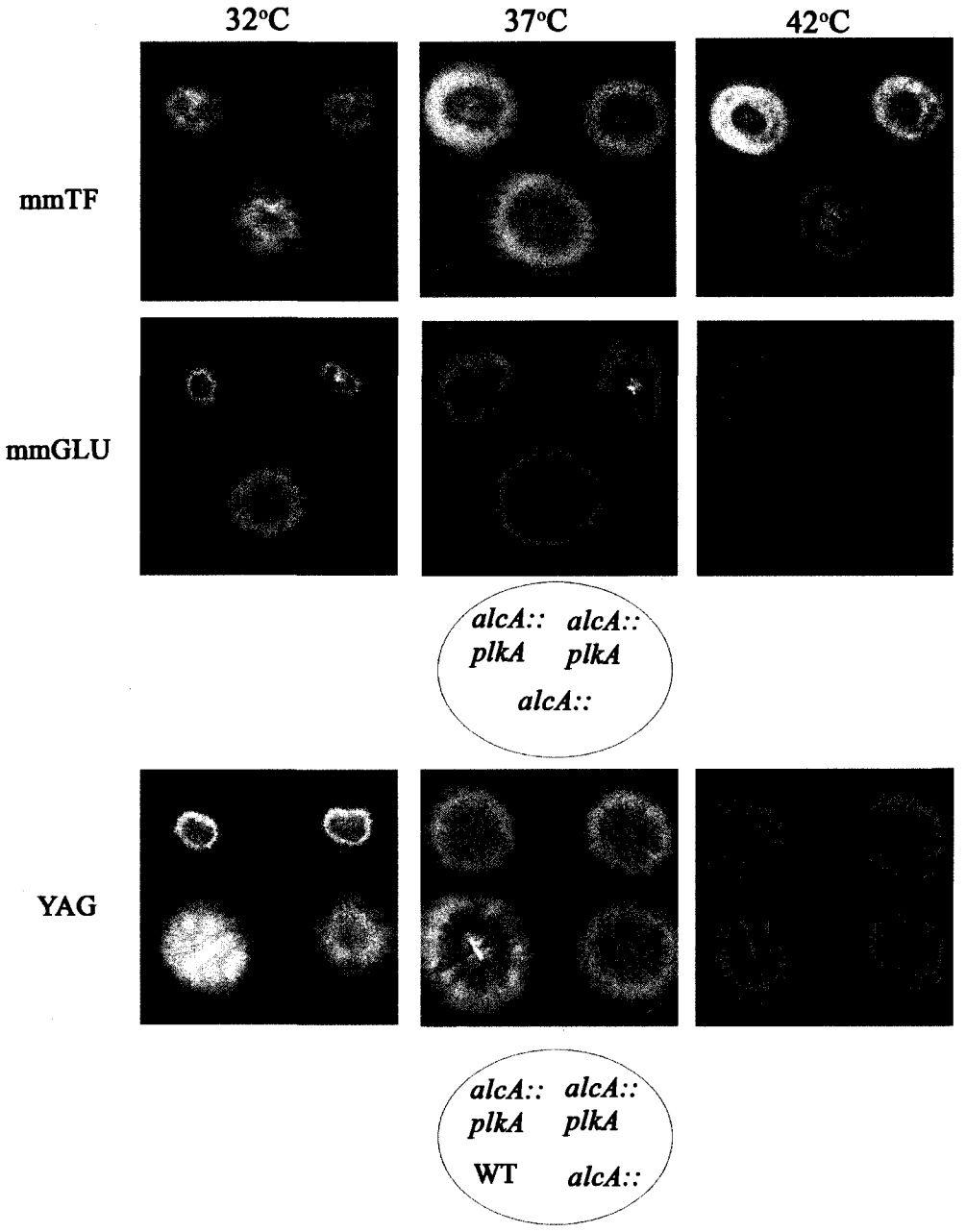

Figure 3: The *alcA::plkA* growth phenotype
Strains KM3 (*alcA::plkA*), KM17 (*alcA::plkA*) and KM5 (*alcA::*) were spot inoculated on mmTF and mmGlu plates, and incubated for three days at 32°C, 37°C and 42°C. Strains KM3, KM17, KM5 and wild type TN02A25 were spot inoculated on YAG plates and incubated for three days at 32°C, 37°C and 42°C.

In order to determine whether the shut-off phenotype was strain-dependent, the promoter replacement construct for start site A was also transformed into strain LO879, which was not deleted for the *nku* gene. This strain contained a GFP-tagged copy of histone H_2A, allowing for visualization of nuclei in living cells. Transformation resulted in 70 transformants, of which three were analyzed by Southern (Figure 4). Strain KM20 contained a wild-type band at 2.7 kb, while strain KM22 contained a single band at 5.1 kb, confirming proper integration. Strain KM21, on the other hand, contained the 5.1 kb band as well as a higher band just below 6.5 kb (Figure 4c). When conidia of strains KM20, KM21 and KM22 were plated on solid inducing media, growth was normal. However, strains KM21 and KM22 grew in a compact morphology on repressing minimal media, while strain KM20 grew in a normal manner (data not shown). The compact phenotype was similar to that seen with the strains created in the Δ*nku* background, suggesting that the effect was not strain-dependent. The fact that growth occurred, albeit abnormal, under repressing conditions suggests that either the *alcA* promoter is leaky, or that *plkA* is not essential.

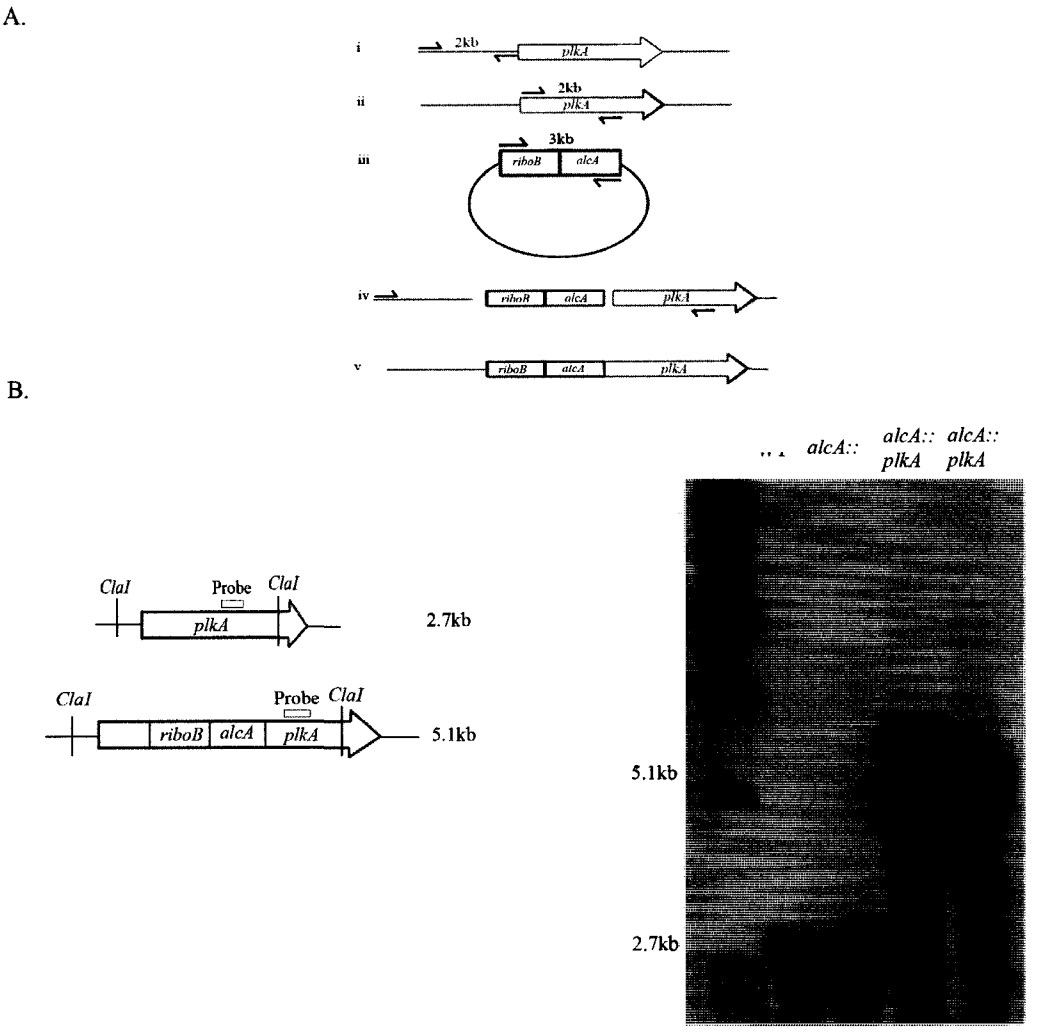

Figure 4: Placing *plkA* under the control of the *alcA* promoter in strain LO897
(A) Strategy to construct the *alcA::plkA* regulated strain. (i) a 2kb fragment was PCR amplified upstream of the start site. (ii) a 2kb fragment including and downstream of the start site. (iii) a 3kb fragment PCR amplified the *riboB* marker and *alcA* promoter from the plasmid pSDW194. (iv-v) Three fragments were used as a template in a fusion PCR reaction to create a 7kb final product that was transformed into TN02A25 strain. (B) Southern analysis demonstrating that two strains KM21 and KM23 are positive (5.1kb), and KM20 is negative (2.7kb).

3.3 Construction of a *plkA* deletion strain

PLK are essential in lower organisms that contain a single homologue, including *plo1* in *S. pombe* (Reynolds and Ohkura, 2002), *CDC5* in *S. cerevisiae* (Cheng et al., 1998) and *CaCDC5* in *C. albicans* (Bachewich et al., 2003). In higher organisms, however, multiple copies of PLK exist and may have some redundant functions, including PLK1, PLK2, PLK3 and PLK4 in mammals (Johnson et al., 2007). Since *A. nidulans* contains a single homologue of PLK, it was surprising to observe growth when gene expression was presumably shut off. In order to confirm that PLKA is not essential in *A. nidulans* and the previous results were not due to leakiness of the *alcA* promoter, attempts to make a deletion strain were repeated, utilizing the Δ*ku* strain background to increase homologous integration (Figure 5A). Upon transforming a *plkA* deletion construct containing 2kb of flanking DNA sequences and the *pyr4* marker (Bachewich et al., 2005) into strain TN02A25, multiple transformants were obtained (Figure 5B). Some transformants were compact, like that seen for the *alcA::plkA* regulated strains under repressing conditions, while others appeared normal. After streaking to single colony, PCR screening demonstrated that three transformants, including KM12, KM13 and KM14, contained a 5.3kb band, consistent with deletion of the gene, whereas the wild type strain TN02A25 and strain KM25 contained the wild-type band at 7.4kb (Figure 5D). KM25 also contained a very faint band at 5.3kb, which suggested some strain contamination, but subsequent Southern analysis demonstrated the presence of a wild-type band at 7.4 kb, and a second slightly smaller band, but this was not 2.9kb, which corresponds to deletion of the gene (Figure 5D). A similar band pattern was observed in a second independent negative strain (data not shown). Thus, KM25 was used as a negative control. Southern

analysis on the three positive transformants demonstrated the presence of a single 2.9kb band, confirming that *plkA* was replaced by *pyr4* (Figure 5F). Thus, the *plkA* gene was successfully deleted.

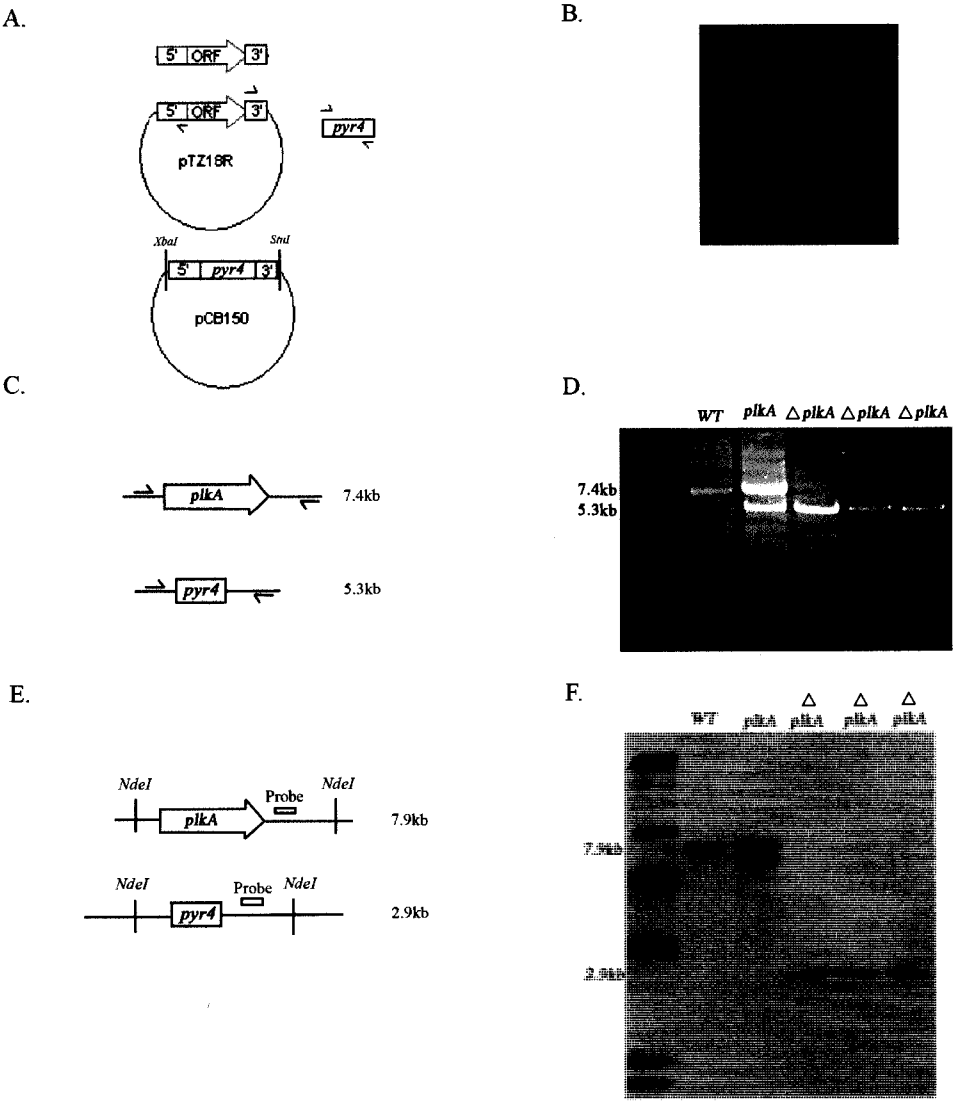

Figure 5: Deletion of *plkA* in strain TN02A25
(A) Deletion construct from plasmid was liberate with *XbaI* and *StuI*, and transformed into TN02A25 background. (B) A section of the transformation plate demonstrating the various colony morphologies. (C, D) PCR screening reaction demonstrating that strains KM12, KM13 and KM14 are positive (5.3kb), and KM25 is negative (7.4kb). (E, F) Southern analysis confirming that strains KM12, KM13 and KM14 are positive (2.9kb), and KM25 is negative (7.9kb).

3.4 *plkA* is not essential, and deletion results in compact colony growth, hyperbranching and split tips

To confirm that cells were able to grow without the *plkA* gene, conidia from deletion strains KM13, KM14 and control strains KM25 and TNO2A25 were inoculated onto YAGuu media and incubated for three days at 32°C. Strains KM13 and KM14 were able to grow and demonstrated the same compact growth phenotype as strains containing a single copy of *alcA::plkA* on repressing media (Figure 6). In contrast, control strains KM25 and TN02A25 grew normally. Thus, the phenotype of the deletion strain was consistent with that of the *alcA::plkA* regulated strain under repressing conditions, indicating that *plkA* is not essential.

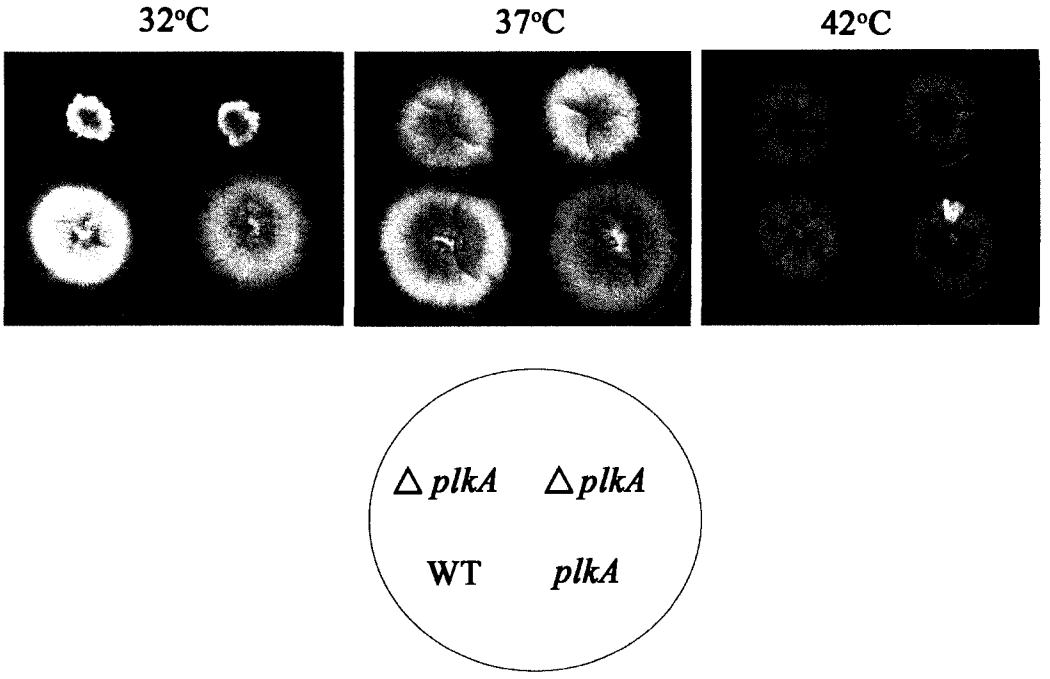

Figure 6: The *ΔplkA* growth phenotype
Strains KM13 (*ΔplkA*), KM14 (*ΔplkA*), KM25 (*plkA*) and wild type TN02A25 were spot inoculated on YAG plates and incubated for three days at 32°C, 37°C and 42°C.

Since compact colonies are often associated with hyperbranching (Inoue et al., 1998), we examined the colony margins for unusual growth patterns. In the *plkA* deletion strains KM13 and KM14, the colony edges demonstrated hyper-branched hyphae, often with split tips (Figure 7A). As well, hyphae grew in multiple directions. In contrast, the control strains KM25 and TN02A25 demonstrated less branching and split tips, and grew in a more constant direction.

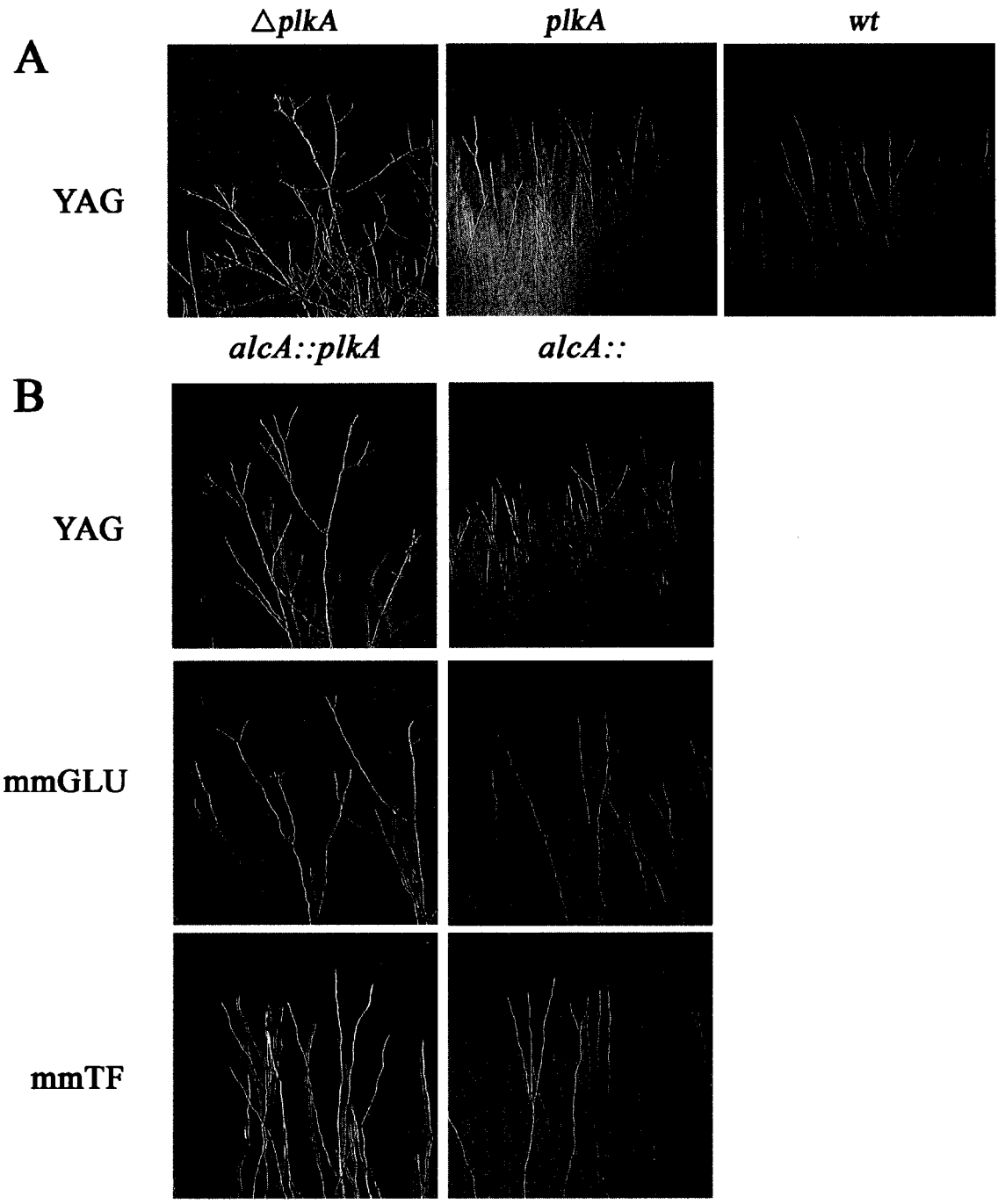

Figure 7: Absence or depletion of PLKA results in hyperbranching and split tips
(A) Strains KM14 (*ΔplkA*), KM25 (*plkA*) and wild type TN02A25 were spot inoculated on YAG plates and incubated for three days at 32°C. (B) Strains KM3 (*alcA::plkA*), and KM5 (*alcA::*) were spot inoculated on YAG, mmTF and mmGlu plates, and incubated for three days at 32°C.

To confirm that the effects were due to absence of *plkA*, the *alcA::plkA* regulated strains KM3 and KM17 and the control strain KM5 were spot inoculated on mmTF, mmGlu and YAG media for three days at 32°C. In repressing YAG media, the colony edges from the *alcA::plkA* regulated strains demonstrated hyper-branched hyphae, often with split tips and growth in multiple directions (Figure 7B). In repressing minimal media, a similar phenotype was observed, but hyperbranching was less dramatic. In contrast, hyphae grew in a normal fashion with less branching in inducing minimal media. The control strain KM5 grew in a normal manner under inducing and repressing conditions, although some split tips were observed in YAG media (Figure 7B). The results agree with those of the deletion strains.

Thus, PLKA is not essential for growth, but may be important for proper polar axis formation and growth direction in hyphae. Since PLKA is the first example of a PLK in a filamentous fungus, this is the first report indicating a potential role for a PLK in hyphal morphogenesis.

Since colony growth was affected in the absence of *plkA*, growth of individual hyphae was investigated in order to determine whether *plkA* is important for normal hyphal growth rate. Conidia from deletion strains KM13, KM14 and the negative control KM25 were inoculated into liquid YAG medium at 32°C. After 9 hours, cells were fixed and hyphal lengths were quantified. Strain KM25 hyphae were 42.12 μm ± 0.74 (n=298), while hyphae of strains KM13 and KM14 were slightly longer at 48.18 μm ± 0.97 (n=335; z=-3.89, $p<0.001$, Mann Whitney U) and 45.48 μm ± 0.98 (n=267; z=-2.17, $p<0.001$, Mann Whitney U), respectively (Table 4; Figure 8). Thus, a slight increase in growth was seen in the deletion strains compared to the control.

Table 4: Hyphal length in *plkA* deletion and *alcA::plkA* regulated cells[1]

Strain[2]	Time	Media	N	Length in μm ±S.E.M.	Mann-Whitney U Test
KM25	9h	YAG	298	42.12 ±0.74	-
KM13	9h	YAG	335	48.18 ±0.97	p<0.001
KM14	9h	YAG	267	45.48 ±098	p = 0.030
TN02A25	9h	YAGuu	337	50.65 ±1.07	-
KM5	9h	YAGuu	385	30.81 ±0.57	p<0.001
KM3	9h	YAGuu	362	32.96 ±0.74	p<0.001
KM17	9h	YAGuu	426	35.14 ±0.67	p<0.001
TN02A25	12h	mmGlu	365	60.08 ±1.41	-
KM5	12h	mmGlu	406	52.23 ±1.16	p<0.001
KM3	12h	mmGlu	416	44.36 ±0.96	p<0.001
KM17	12h	mmGlu	395	52.75 ±1.17	p<0.001
TN02A25	12h	mmTF	228	40.31 ±1.31	-
KM5	12h	mmTF	352	36.67 ±0.92	p=0.016
KM3	12h	mmTF	354	35.50 ±0.78	p=0.027
KM17	12h	mmTF	349	39.07 ±0.92	p=0.943

[1] Cells were incubated for 9h or 12h in the selected media, then fixed and stained with DAPI and Calcofluor. The germling lengths were measured. The values represent the combination of three separate trials, which gave similar result.
[2] Deletion strains KM13 (Δ*plkA*), KM14 (Δ*plkA*) and negative control KM25 (*plkA*). Regulated strains KM3 (*alcA::plkA*), KM17 (*alcA::plkA*), and negative control KM5(*alcA::*).

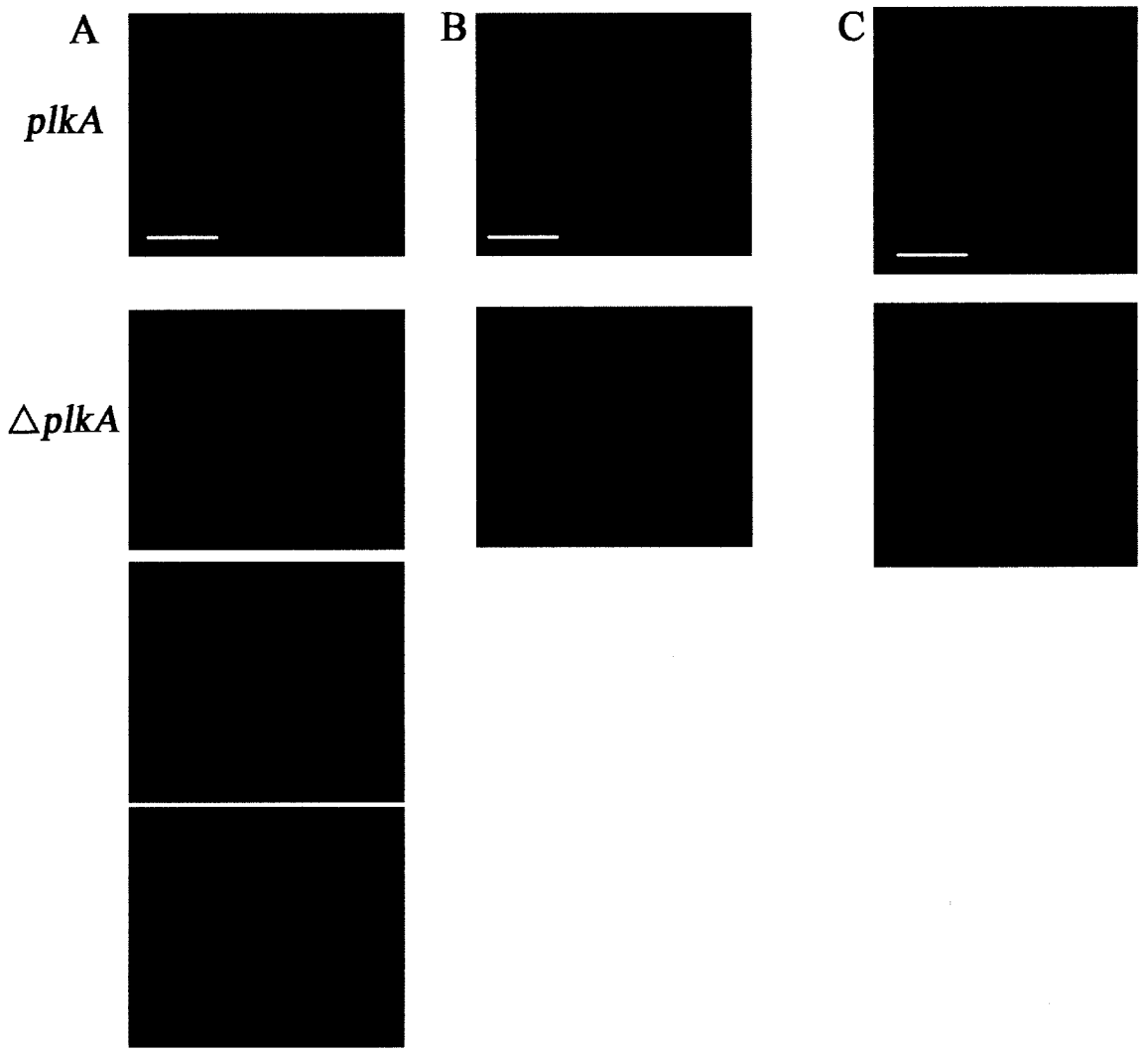

Figure 8: Lengths of hyphae, number of nuclei and septa pattern in cells lacking *plkA*

Strains KM14 (*ΔplkA*) and KM25 (*plkA*) were inoculated at 10^6 conidia/ml in YAG media for 9h (A and B) or 12h (C) at 32°C. The cells were then stained with DAPI and Calcofluor. Bar 10μm.

To validate the results obtained with the deletion strains, conidia from the *alcA::plkA* regulated strains KM3, KM17, and the control strains KM5 and TNO2A25 were inoculated at 32°C for 9 hours in liquid YAG repressing media. While hyphae of KM3 and KM17 were 32.96 μm ± 0.74 (n=362) and 35.14 μm ± 0.67 (n=426), respectively, those of the controls TNO2A25 and KM5 were 50.65 μm ± 1.07 (n=337) and 30.81 μm ± 0.57 (n=385), respectively (Table 4 and Figure 9).

The strains were also tested in minimal inducing and repressing media. A longer incubation time was required since cells grew more slowly in this environment. After 12 hours in minimal repressing media, hyphae of strains KM3 and KM17 were 44.36 μm ± 0.96 (n=416) and 52.75 μm ± 1.17 (n=395), respectively, while control strains TNO2A25 and KM5 were 60.08 μm ± 1.41 (n=365) and 52.23 μm ± 1.16 (n=406), respectively (Table 4 and Figure 9). After 12 hours in inducing media, the control KM5 and the two regulated strains KM3 and KM17 were similar in length, ranging from 35 to 40 μm (Table 4).

Thus, *alcA::plkA* strains were similar in length to control strain KM5 and shorter than strain TN02A25 under repressing conditions, in contrast to results obtained with deletion strains. Thus, it is not clear if PLKA is important for hyphal growth rate, but clearly influences hyphal morphology.

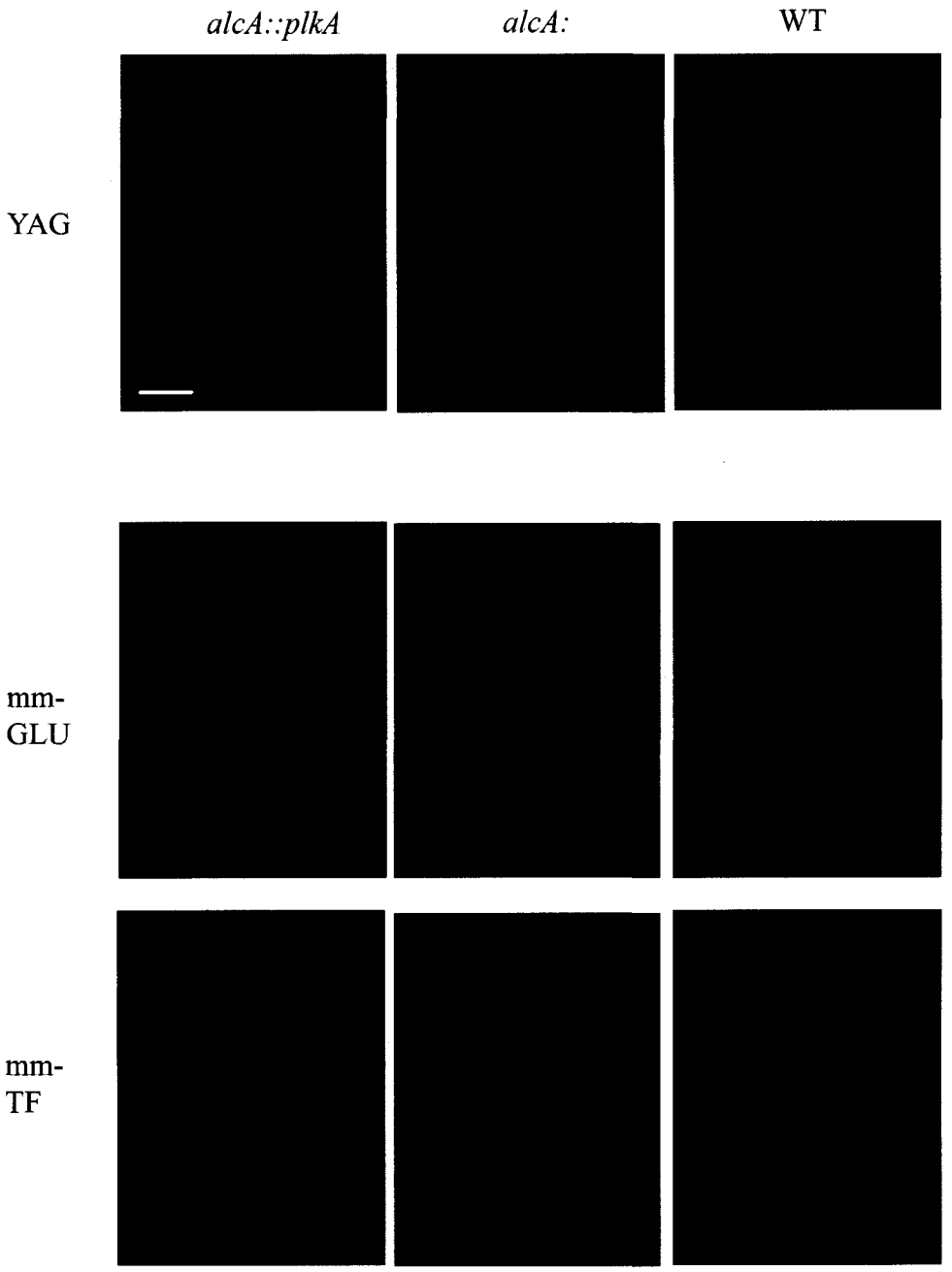

Figure 9: Depletion of PLKA results in normal hyphal length and nuclear division
Strains KM3 (*alcA::plkA*), KM5 (*alcA::*) and wild type TN02A25 were inoculated at 10^6 conidia/ml in YAG (10h), mmGlu (15h) and mmTF (15h) media at 32°C. The cells were then fixed and stained with DAPI and Calcofluor. Bar 10μm.

3.5 PLKA depletion influences the timing and pattern of hyphal germination

While determining length of hyphae, differences in germination patterns were observed. Under normal conditions, after a germ tube emerges and becomes an established hypha, a second germ tube emerges from the conidia at an angle of 180° (Enke et al., 2007). To characterize the germination pattern in cells lacking *plkA*, conidia from the deletion strains KM13 and KM14 and the control strain KM25 were incubated in YAG media for 9 hours and fixed. The proportions of germination patterns, including multi-germinated conidia, as well as angles of emergence, were determined (Table 5). Angles were categorized as being either 180° (hyphae at opposite ends of the conidia), 90° (hyphae emerging at 90° angles of each other) or 0° (hyphae emerging from a similar region on the conidia). In strains KM13 and KM14, the proportion of cells producing a second germ tube was higher compared to the control KM25 at 9 hours (Table 5). Of the cells producing more than one germ tube, many contained angles lower than 180° (Table 5). This was not seen with the control strain KM25, where fewer cells exhibited a second germ tube at either 180° or 90° angles. Even when control cells were inoculated for a longer time to allow for more secondary germination, the proportion of cells that exhibited a second germ tube at a 90° angle was minor compared to those showing an angle of 180 °, unlike that seen with the deletion strain at the shorter incubation time. Similar germination patterns were reported when the microtubule associated proteins *alpA* or *kipA* genes were deleted from *A. nidulans* (Enke et al., 2007). These results support the concept that PLKA may be important for proper establishment of polar axes during hyphal growth.

Table 5: Germination patterns in *alcA::plkA* and in *plkA* deletion cells[1]

Strain[4]	Time	Media	n	Germination Pattern[2]			
					Double		Triple
				180° [3]	90° [3]	0° [3]	
				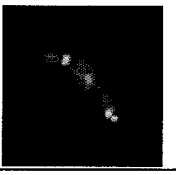	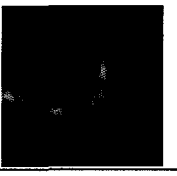	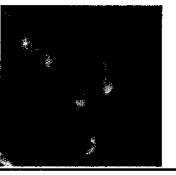	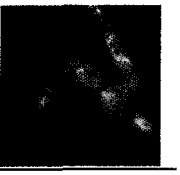
KM25	9h	YAG	326	11.9	2.2	0	0
KM13	9h	YAG	227	17.6	12.3	12.8	4.4
KM14	9h	YAG	250	24.4	8.8	8.8	2.4
KM25	12h	YAG	269	58.7	8.5	0	1.1
TN02A25	10h	YAGuu	597	11.2	4.1	0.2	0.3
KM5	10h	YAGuu	627	8.6	2.9	0.5	0.2
KM3	10h	YAGuu	488	26.2	9.2	2.5	1.0
KM17	10h	YAGuu	487	29.2	12.3	1.6	2.1
TN02A25	12h	mmGlu	497	4.0	1.0	0	0
KM5	12h	mmGlu	520	4.4	1.9	0	0
KM3	12h	mmGlu	501	5.8	3.4	1.4	0.2
KM17	12h	mmGlu	478	8.6	3.3	0	0.2
TN02A25	12h	mmTF	331	2.1	0.9	0	0
KM5	12h	mmTF	524	3.4	0.6	0.2	0
KM3	12h	mmTF	592	2.5	0.7	0.3	0
KM17	12h	mmTF	529	2.8	0.8	0	0
TN02A25	15h	mmGlu	342	11.4	3.2	0	0
KM5	15h	mmGlu	307	28.7	4.9	0	0
KM3	15h	mmGlu	288	45.8	11.5	0.4	0
KM17	15h	mmGlu	288	46.5	6.3	1.7	0
TN02A25	15h	mmTF	329	13.7	3.3	0	0
KM5	15h	mmTF	348	14.9	7.5	0.3	0
KM3	15h	mmTF	357	15.9	2.8	0.3	0
KM17	15h	mmTF	332	17.8	2.4	0	0

1. Cells were incubated for 9h, 10h, 12h or 15h in the selected media, then fixed and stained with DAPI. The number of conidia that contained more than one germ tube was then calculated. The values represent the combination of three separate trials, which gave similar result.
2. Percentage of cells.
3. Angles between germ tubes.
4. Deletion strains KM13 (Δ*plkA*), KM14 (Δ*plkA*) and negative control KM25 (*plkA*). Regulated strains KM3 (*alcA::plkA*), KM17 (*alcA::plkA*), and negative control KM5 (*alcA::*).

To confirm these results, conidia from the *alcA::plkA* regulated strains KM3 and KM17, as well as the control strains KM5 and TN02A25, were incubated in inducing and repressing media. After 9 hours in YAG repressing media, there was no significant increase in the number of conidia that contained two hyphae (data not shown). However, when cells were incubated for 10 hours, a higher proportion of cells demonstrated a double germination pattern in strains KM3 and KM17 compared to control strains KM5 and TN02A25 (Table 5). However, germination angles lower than 180° were not significant. At 12 hours in minimal repressing media, when hyphae were at similar lengths as those grown in rich YAG media for 9 hours (Table 5), no significant difference in angle category was visible between the controls and the regulated strains. However, when cells were grown for 15 hours, more cells with double germination patterns were observed in strains KM3 and KM17 (Table 5) compared to controls, but the frequency of germ tubes emerging at angles less than 180° was not significantly different, in contrast to that seen with the deletions strains. In minimal inducing media, the germination pattern was similar in the *alcA::plkA* regulated and control strains, indicating that the increase in double germination observed in repressing media was due to depletion of PLKA. Thus, the results support the notion that PLKA is required for proper polar axis formation.

3.6 PLKA is not essential for nuclear division but influences nuclear distribution

Since PLKs are major regulators of multiple stages of mitosis in most organisms (Lee et al., 2005) and overexpression of PLKA resulted in an arrest in nuclear division

(Bachewich et al., 2005), we next explored whether mitosis was affected in the absence of PLKA. Conidia from deletion strains KM13, KM14 and the negative control KM25 were inoculated into YAG medium at 32°C for 9 hours, at which point control cells had undergone several rounds of nuclear division. Cells were fixed and stained with DAPI and Calcofluor. Strains KM13 and KM14 contained 6.55±0.12 (n=271) and 6.27±1.82 (n=217) nuclei per germling, respectively, while the negative control KM25 had 6.77±0.11 (n=252) nuclei per germling. Thus nuclear division could occur in the absence of PLKA, but at a slightly slower rate, since the number of nuclei was significantly different from the control (Table 6 and Figure 8). Cells were clearly capable of undergoing mitosis, however, unlike that seen in other systems lacking PLK. In addition, 27% (n=157) and 38% (n=155) of cells from the deletion strains KM13 and KM14, respectively, showed abnormal nuclear distribution, characterized by clustering of nuclei (Figure 8). In contrast, the control strain KM25 demonstrated evenly-spaced nuclei along hyphae.

Table 6: Number of nuclei in *plkA* deletion and *alcA::plkA* regulated cells[1]

Strain[2]	Time	Media	n	# of nuclei±S.E.M.	Mann-Whitney U Test
KM25	9h	YAG	252	6.77±0.11	-
KM13	9h	YAG	271	6.55±0.12	p<0.001
KM14	9h	YAG	217	6.27±1.82	p<0.001
TN02A25	9h	YAGuu	267	7.97±0.19	-
KM5	9h	YAGuu	288	5.33±0.10	p<0.001
KM3	9h	YAGuu	289	5.48±0.11	p<0.001
KM17	9h	YAGuu	288	5.43±0.10	p<0.001
TN02A25	12h	mmGlu	289	6.34±0.17	-
KM5	12h	mmGlu	304	4.15±0.09	p<0.001
KM3	12h	mmGlu	275	4.14±0.10	p<0.001
KM17	12h	mmGlu	299	4.11±0.09	p<0.001
TN02A25	12h	mmTF	193	3.92±0.150	-
KM5	12h	mmTF	320	3.04±0.075	p<0.001
KM3	12h	mmTF	335	3.07±0.060	p<0.001
KM17	12h	mmTF	330	3.18±0.068	p<0.001

[1] Cells were incubated for 9h or 12h in the selected media, then fixed and stained with DAPI and Calcofluor. The number of nuclei per germling was measured. The values represent the combination of three separate trials, which gave similar result.
[2] Deletion strains KM13 (Δ*plkA*), KM14 (Δ*plkA*) and negative control KM25 (*plkA*). Regulated strains KM3 (*alcA::plkA*), KM17 (*alcA::plkA*), and negative control KM5(*alcA::*).

The number of nuclei in germlings was also measured in the *alcA::plkA* regulated strains to validate the deletion strain results. Conidia from the two *alcA::plkA* regulated strains KM3 and KM17 and the controls TN02A25 and KM5 were inoculated for 9 hours in repressing YAG media or 12 hours in mmGlu and mmTF, which produced germlings of approximately equal length (Table 6 and Figure 9). In inducing media, fewer nuclei were present in the germlings in all strains, due to the poor carbon source, but the total number was approximately equal (Table 6 and Figure 9). However, in repressing minimal media, the regulated strains KM3 and KM17 contained a similar number of nuclei as the control strain KM5, while the control strain TN02A25 contained slightly more. This was also observed in repressing YAG media (Table 6 and Figure 9). The slight increase in nuclei in strain TN02A25 is likely due to the fact that the cells were longer. It is possible that the lack of a significant difference between the control KM5 and regulated strains KM3 and KM17 is due to some leakiness of *alcA* promoter. Thus, PLKA is not essential for nuclear division, but may influence the rate in a minor way.

3.7 Absence of PLKA results in a higher mitotic index, a delay in telophase, and defects in spindle assembly and chromosome segregation

Since PLK are required for proper spindle formation in most organisms (Nigg E., 1998), and overexpression of PLKA in *A. nidulans* resulted in several spindle defects (Bachewich et al., 2005), we wanted to determine whether spindle formation and elongation were influenced by the absence of PLKA. Although cells lacking PLKA

contained a similar number of nuclei as control cells, defects in the dynamics of spindle formation could be present. In order to visualize spindles, conidia from the deletion strains KM13 and KM14 and the control strain KM25 were inoculated in YAG media for 9 hours, fixed, and then processed for immunolocalization of α-tubulin. The mitotic index, or proportion of cells in mitosis, was 4.8% (n=852) in strain KM25, which is expected for an asynchronous population of cells (Bergen and Morris, 1983) (Table 7). However, the mitotic indices in deletion strains KM13 and KM14 were 12.9% (n=675) and 11.4% (n=721), respectively (Table 7), suggesting that mitosis might be delayed. Consistent with this, 32.2% (n=87) and 24.4% (n=82) of the total mitotic cells in strains KM13 and KM14, respectively, were in telophase, compared to 4.9% (n=41) of mitotic cells in control strain KM25 (Figure 10A and Table 7). Since telophase cells exhibit fully separated chromosomes connected only by an elongated spindle, a nucleus in telophase would have been scored as two nuclei in the previous section that involved DAPI staining, and the nuclear counts may thus be slightly overestimated. The delay in telophase suggests that PLKA may be important for mitotic exit.

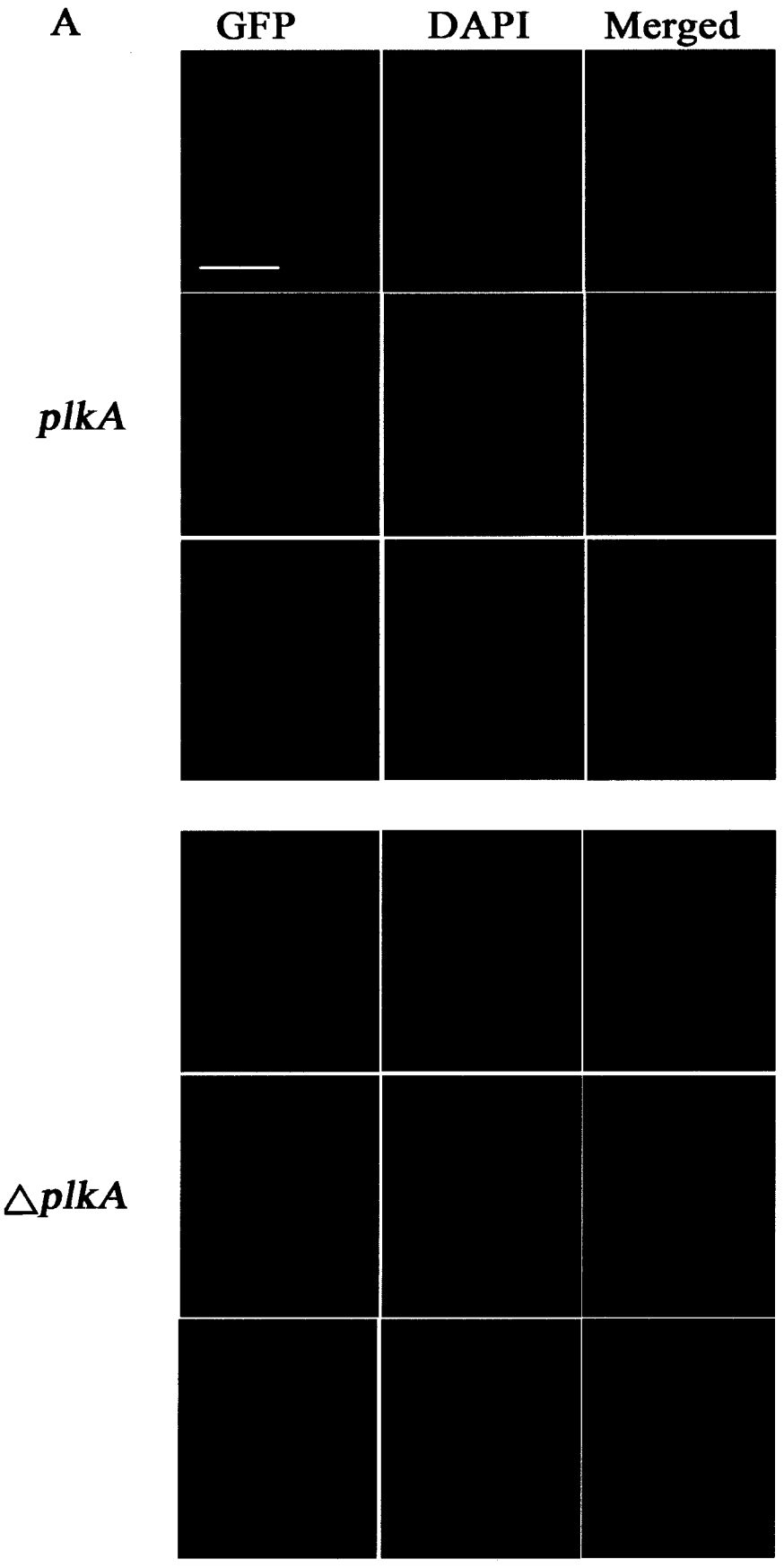
A
GFP
DAPI
Merged
plkA
ΔplkA

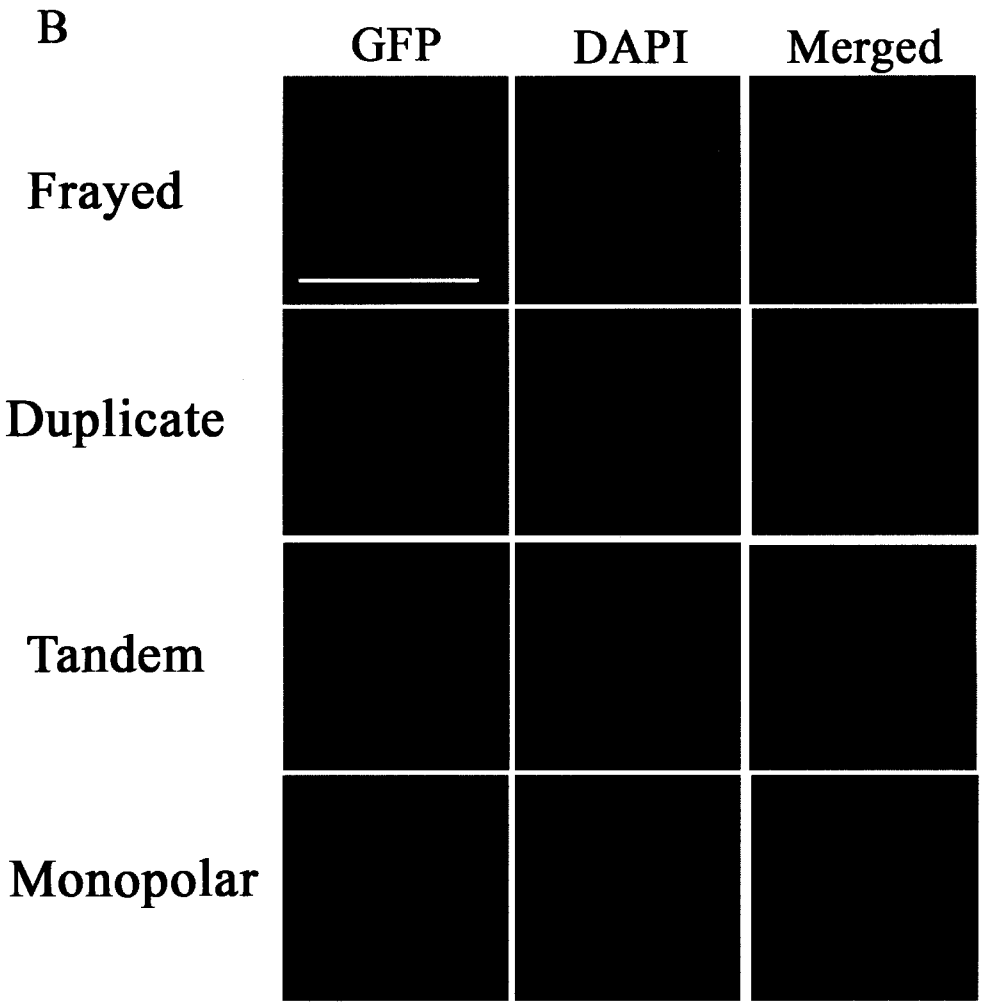

Figure 10: Absence of PLKA results in abnormal spindle assembly
Strains KM14 (*ΔplkA*) and KM25 (*plkA*) were inoculated at 10^6 conidia/ml in YAG media for 9h at 32oC. The cells were then fixed, processed for immunolocalization of α-tubulin and then stained with DAPI. (A) Normal cytoplasmic microtubules and mitotic spindles. First row: cytoplasmic microtubules, second row: early mitosis and third row: late mitosis. (B) Abnormal mitotic spindle pattern. First row: Frayed, second row: duplicate, third row: tandem, forth row: monopolar. Bar 10μm.

Table 7: Mitotic index[2] and spindle patterns in *plkA* deletion cells[1]

Strain[6]	n	Mitotic Index[3]	Normal[4] Spindle	Abnormal[4] Spindle	Spindle Pattern[5]		
					Mishaped/Frayed	Monopolar	Tandem
KM25	852	4.8	100	0	0	0	0
KM13	675	12.9	59.8	40.2	62.8	22.8	14.4
KM14	721	11.4	59.8	40.2	54.5	30.3	15.2

[1.] Cells were incubated for 9h in YAG media, then fixed and processed for immunolocalization of α-tubulin and stained with DAPI.
[2.] The mitotic index was calculated as well as the percentage of cells that had abnormal spindle patterns. The values represent the combination of three separate trials, which gave similar results.
[3.] Percentage of total cells scored
[4.] Percentage of cells with spindles
[5.] Proportion of cells with abnormal spindles
[6.] Strains KM13 (Δ*plkA*), KM14 (Δ*plkA*) and negative control KM25 (*plkA*).

In addition to containing a higher proportion of cells in telophase, approximately 40% of spindles were also abnormal in the deletion strains KM13 and KM14, while none were abnormal in the control strain KM25 (Table 7). Of the abnormal spindles, 54% in strain KM14 and 63% in strain KM13 were misshaped, characterized by being either bent, frayed or in extreme cases, split into two separate bundles, one over top of the other (Figure 10B). None of these spindle patterns were observed in the control strain. Another 23-30% of the abnormal spindles were monopolar in strains KM13 and KM14, compared to 0% for the control strain KM25. The remaining 14%-15% of abnormal spindles were characterized as being "in tandem", where two spindles were immediately side by side or slightly overlapped (Figure 10B). Several of these spindle defects were also observed when PLKA was overexpressed (Bachewich et al., 2005). Cytoplasmic microtules also appeared abnormal in *plkA*-deleted cells, and seemed more frayed than in the control strains, however due to the difficulty of measuring, this was not quantified. Thus, PLKA appears to be important, but not essential, for proper spindle formation in *A. nidulans*.

While analyzing spindle patterns, various defects in chromosome segregation were also observed in 29% to 37% of cells of the deletion strains compared to 0% for the control strain (Table 8). For example, in several telophase cells, uncondensed or fragmented chromatin was wrapped around or distributed along the long spindle, as opposed to being condensed and separated as two compact masses on either ends of the spindle as seen in control cells (Figure 11). Unequal separation of the chromosomes was also observed, where one condensed chromosome mass was larger than the other, or

located in the middle of the spindle, while the other mass was at the end. Finally, some uncondensed chromosomes also appeared to be disassociated from the spindle (Figure 11). Similar deregulation in chromosome segregation was also observed when PLKA was overexpressed (Bachewich et al., 2005). Thus, PLKA might have a novel role in chromosome segregation as well as spindle formation.

Table 8: Chromosome segregation[2] in *plkA* deletion cells[1]

Strain[4]	n	Normal[3]	Abnormal[3]
KM25	852	100	0
KM13	675	71.3	28.7
KM14	721	63.4	36.6

[1] Cells were incubated for 9h in YAG media, then fixed and processed for immunolocalization of α-tubulin and stained with DAPI.
[2] The proportion of cells that contain abnormal chromosome segregation patterns were calculated and compared to the normal chromosome segregation pattern. The values represent the combination of three separate trials.
[3] Percentage of cells with chromosomes segregate patterns in cells with spindles
[4] Strains KM13 (Δ*plkA*), KM14 (Δ*plkA*) and negative control KM25 (*plkA*).

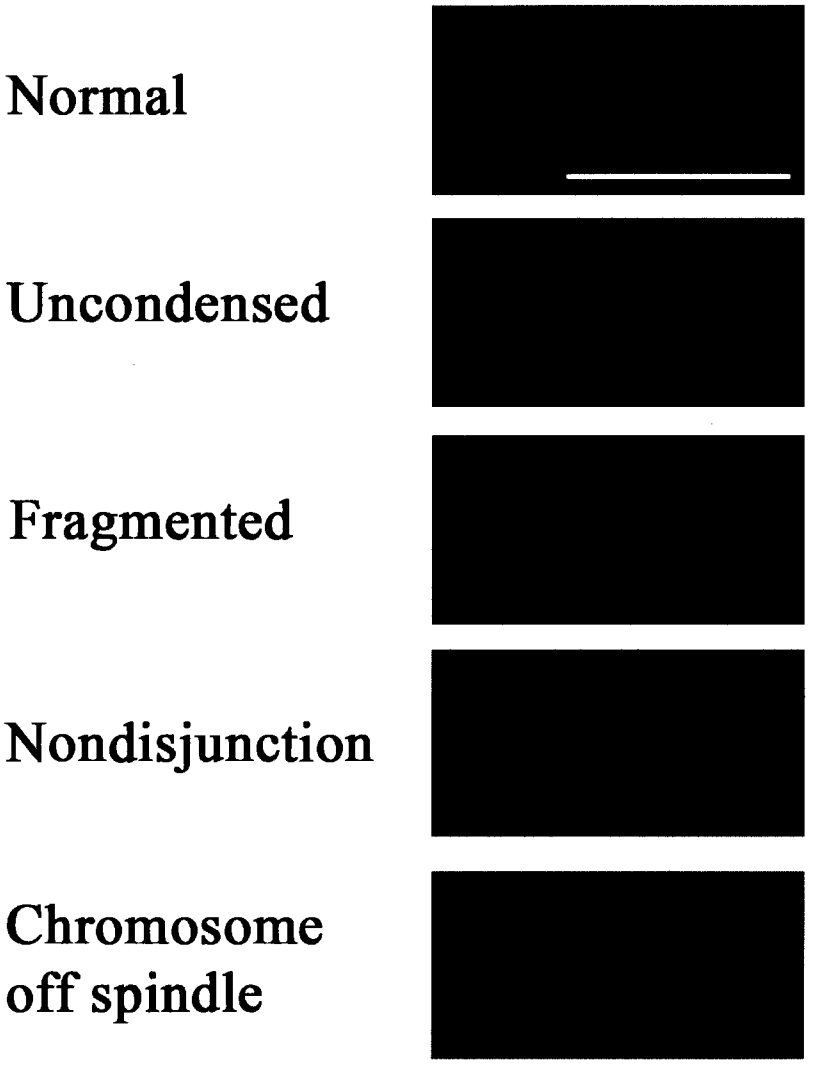

Figure 11: Absence of PLKA results in abnormal chromosome segregation
Strain KM14 (*ΔplkA*) was inoculated at 10^6 conidia/ml in YAG media for 9h at 32°C. The cells were then fixed, processed for immunolocalization of α-tubulin and then stained with DAPI. Bar 10μm.

3.8 Synchronizing *ΔplkA* cells with a *nimT*^{cdc25C} block supports a role for *plkA* in mitotic exit, but also in the G_2/M transition

To determine the rate of mitosis and spindle formation within a synchronous population of cells lacking PLKA, the *plkA* gene was deleted from the *nimT*^{cdc25C} temperature- sensitive strain SO182. This strain is blocked at G_2/M at the restrictive temperature of 43°C. When released into media at the permissive temperature of 32°C, cells enter mitosis in a synchronous fashion (Bergen and Morris, 1983). *plkA* was deleted from the SO182 strain background and replaced with *pyr4*, as previously described. Four transformants with a compact phenotype and two transformants that grew normally were selected, streaked three times to single colonies, and screened for correct integration of the deletion construct. Southern analysis demonstrated the presence of a 2.9kb band in the colonies that grew in a compact manner, including strain KM26, confirming that *plkA* was replaced by *pyr4* (data not shown). The two strains that grew in a normal manner only contained the wild type band at 7.4kb, confirming that they were negative. One strain, KM31, was subsequently used as a negative control.

In order to synchronize the cells, conidia from deletion strain KM26 and control strain KM31 were inoculated onto several coverslips in YAG media at 43°C for 8 hours. Sample coverslips were transferred to media at 32°C for 10 min, 15min or 20min to release the cell cycle block and allow synchronous progression into mitosis. The coverslips were subsequently fixed, processed for immunolocalization of α-tubulin, and stained with DAPI, as previously described. The number of nuclei per germling and spindle mitotic index was quantified at each time point. Cells at time zero were fixed immediately after incubation at 43°C for 8 hours. In the control strain KM31, 100% of

cells were in interphase at time zero, based on the lack of spindles and abundance of cytoplasmic microtubules. In contrast, 5.5% of cells had visible spindles and thus were in mitosis at time zero in strain KM26, suggesting that there was no block (Figure 12). However, after 10min at permissive temperature, 31% of cells in strain KM26 had visible spindles and were in mitosis, indicating that some block and synchronization had occurred at 43°C. In comparison, 29% of cells in the control strain KM31 were in mitosis at this time (Figure 12). The rate of entry into mitosis was therefore similar between the two strains, suggesting that PLKA may not be important for the G_2/M transition. At 15min, 49% of cells demonstrated spindles in the control strain KM31, whereas the mutant remained at approximately 30% (Figure 12A). By 20min, the majority of cells in control strain KM31 had completed mitosis and entered a new cell cycle, based on the spindle mitotic index being back down to 6%. In contrast, 22% of cells still contained spindles in strain KM26, (Figure 12A), suggesting that they maybe delayed in exiting mitosis. Consistent with this, 20% of the spindles were elongated, supporting a telophase arrest. The spindles in strain KM26 also demonstrated many of the defects found with the asynchronous populations. Thus, the data supports the concept that PLKA is required for mitotic exit and proper spindle formation.

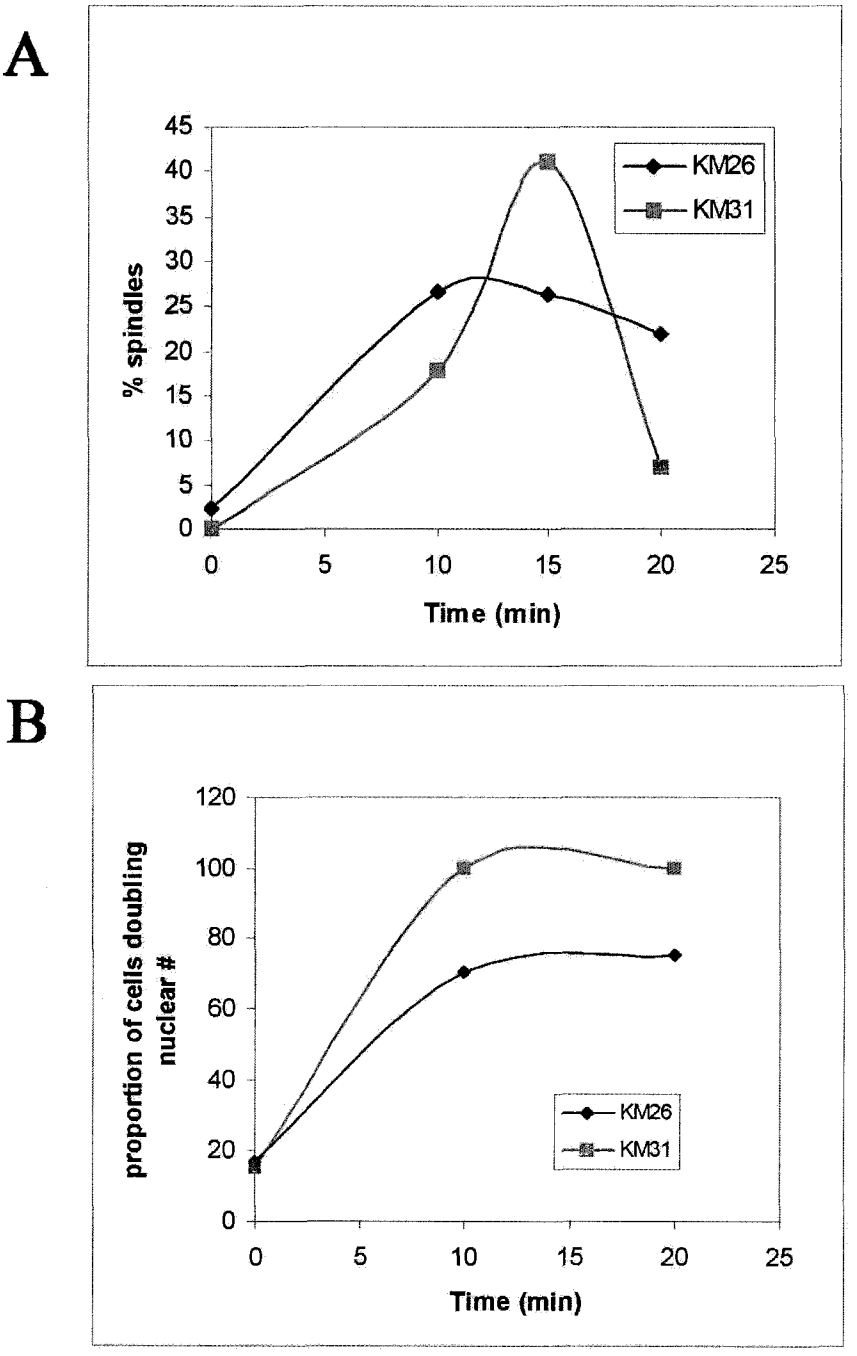

Figure 12: Spindle formation (A) and rate of mitosis (B) upon release release from temperature-sensitive G2 block imposed by *nimT*

Strains KM26 (*ΔplkA*) and KM31 (*plkA*) were inoculated to a 10^6 inoculation density in YAG media for 8h at 43°C to impose block. Samples were then transferred to 32°C to release temperature block, and fixed, processed for immunolocalization of α-tubulin and stained with DAPI at 0, 10, 15 or 20 min.

Note: Since the deletion strains contained more than one nucleus at time "zero", unlike the control strain, the number of nuclei scored at each time point was thus normalized to the mean value observed at time "zero".

Interestingly, when the number of nuclei was scored during the time trial, strain KM26 contained more than one nucleus at time zero, consistent with the presence of spindles at this time. While 70% of cells contained 4 nucleii, (n=83) (Figure 13 and Table 9), 86% of cells in control strain KM31 contained 1 nucleus (n= 109) (Table 9). Since the deletion strains contained more than one nucleus at time "zero", unlike the control strain, the number of nuclei scored at each time point was thus normalized to the mean value observed at time "zero". Once released at permissive temperature, the total number of nuclei almost doubled for each strain (Figure 12B), confirming that mitosis proceeded at a similar rate. The fact that some cells of the *plkA/nimT*^{cdc25C} strain had mitotic spindles and the majority contained at least four nuclei per germling at time zero suggests that the strain was not fully blocked in interphase. The absence of *nimT* was clearly having some effect on mitosis, since we were able to see a large proportion of cells enter mitosis in a synchronous fashion upon release to permissive temperature. However, the block was not as tight as that seen in the control strain, suggesting that absence of PLKA partially suppressed the *nimT*-dependent block. PLKA are reported to interact with and phosphorylate Cdc25C in higher organisms (Lee et al., 2005). If this was happening in *A. nidulans*, we would expect to see an even tighter block in interphase. Our results alternatively suggest that PLKA may have a novel function in negatively regulating the G_2/M transition.

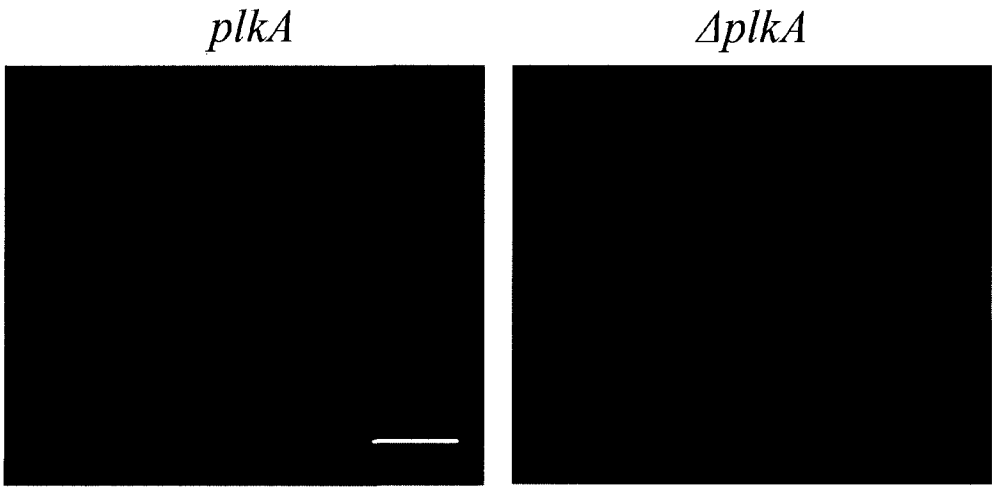

Figure 13: The G2 block in *nimT* cells at restrictive temperature is partially suppressed by absence of *plkA*
Strains KM26 (*ΔplkA, nimT*) and KM31 (*plkA, nimT*) were inoculated to a 10^6 inoculation density in YAG media for 8h at 43°C to impose block. Samples were fixed, processed for immunolocalization of α-tubulin and stained with DAPI.

Table 9: The G2 block in *nimT* cells at restrictive temperature is partially suppressed by absence of *plkA*[1]

Strain[2]	Time (min)	n	Number of nuclei[3]							
			1	2	3	4	5	6	7	>8
KM31	0	109	86	14	0	0	0	0	0	0
KM26	0	83	0	9	9	70	6	6	0	0
KM31	10	98	0	43	11	42	3	0	0	0
KM26	10	101	0	0	0	38	0	58	0	12
KM31	20	170	0	0	0	24	0	10	0	66
KM26	20	118	0	0	0	25	0	17	0	42

[1] Cells were incubated for 8h in YAG media at 43°C to impose the block. Cells were then transferred to permissive temperature of 32°C for 0, 10 or 20min to release the block, fixed and processed for immunolocalization of α-tubulin and stained with DAPI to determine the rate of mitosis.

[2] Strains KM26 (Δ*plkA, nimT*) and negative control KM31 (*plkA, nimT*).

[3] Percentage of cells with specified number of nuclei.

3.9 Septation occurs in the absence of PLKA, but may be deregulated and uncoupled from nuclear division in subapical regions of hyphae

PLK are important for septation in fungi and cytokinesis in higher organisms (Lee et al., 2005). In *A. nidulans,* septa are deposited at the germ tube base after the third round of mitosis when the germling has eight or more nuclei, and along the length of hyphae as they grow (Kaminskyj and Hamer, 1997). Overexpression of PLKA resulted in the absence of septa along the hyphae (Bachewich et al., 2005), suggesting that either PLKA was required for the process, or that septa were lacking due to the primary defect in nuclear division. We further explored the possibility that PLKA was important for septation by incubating cells of strains KM13, KM14 and KM25 in YAG media for 9 hours, fixed and then stained with DAPI and Calcofluor. Septa were observed at the base of hyphae in the deletion strains KM13 and KM14 and in the control strain KM25, and the proportion of cells with septa increased with longer incubation periods (data not shown). Thus, septa can surprisingly form in the absence of PLKA, in contrast to that found in *S. pombe* (Toyoshima-Morimoto et al., 2001) and *S. cerevisiae* (Song et al., 2000).

To identify any possible defects, placement and timing of septa was also examined in older, subapical regions of hyphae. Subapical compartments delimited by septa are approximately 40 μm in hyphae, and contain approximately 4 nuclei (Kaminskyj and Hamer, 1997). Septa lengths were measured in the two deletion strains, KM13 and

KM14, and control strain KM25, which had been incubated for 12 hours in YAG media at 32°C. The compartment lengths for the deletion strains were significantly different, and varied more drastically than those of the control strain. Compartments in stain KM14 (n=292) (Table 10), ranged from 0-63 μm, compared to 8-60 μm for the control KM25 (n=291) (Figure 14). In addition, some compartments did not contain any visible nuclei, (Figure 8 and 14).

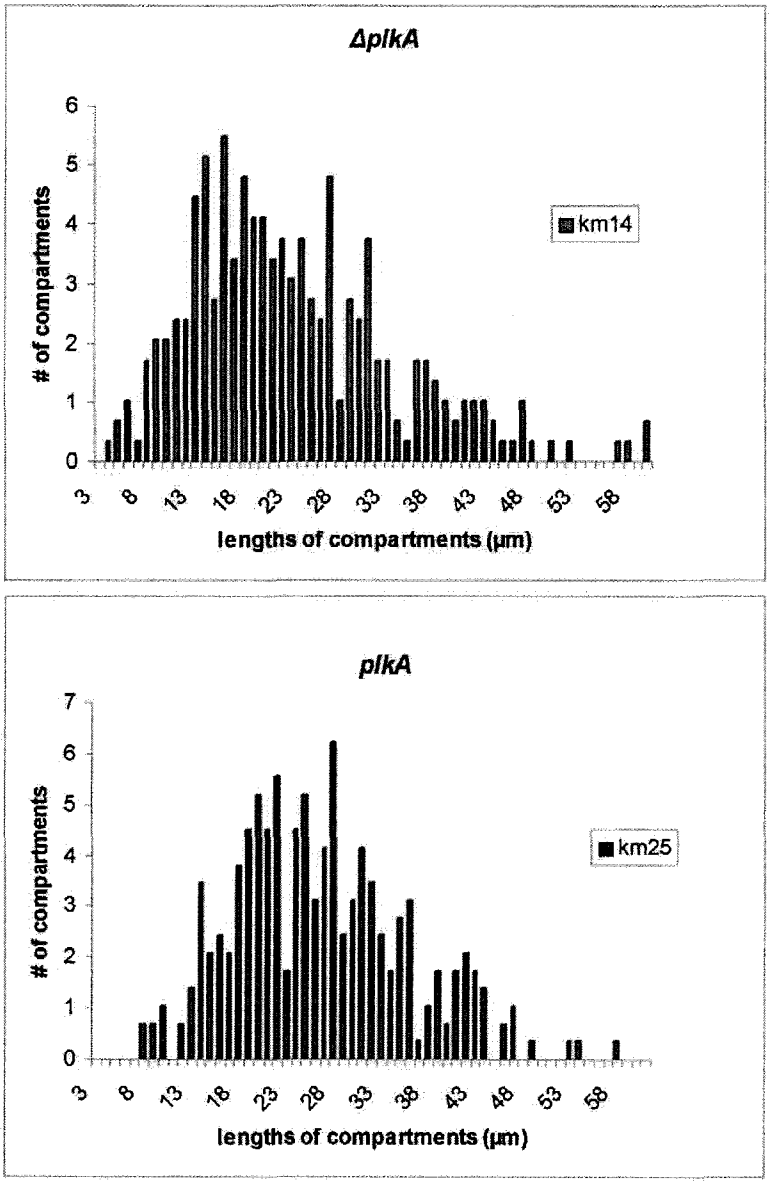

Figure 14: Absence of PLKA results in abnormal lengths of intercalary compartments

Strains KM14 (*ΔplkA*) and KM25 (*plkA*) were incubated for 12h in YAG media, then fixed and stained with DAPI. The compartment lengths were measured. The values represent the combination of three separate trials, which gave similar results.

Table 10: Intercalary lengths[1] in *plkA* deletion and *alcA::plkA* regulated cells[2]

Strain[3]	Time	Media	n	length in μm ±S.E.M.	Mann-Whitney U Test
KM25	12h	YAG	291	26.65 ±0.55	-
KM13	12h	YAG	327	21.57 ±0.51	p<0.001
KM14	12h	YAG	292	23.17 ±0.63	p<0.001
TN02A25	12h	YAGuu	365	29.71 ±0.53	-
KM5	12h	YAGuu	274	20.64 ±0.45	p<0.001
KM3	12h	YAGuu	237	21.23 ±0.65	p<0.001
KM17	12h	YAGuu	302	19.30 ±0.49	p<0.001
TN02A25	15h	mmGlu	371	29.78 ±0.56	-
KM5	15h	mmGlu	367	23.94 ±0.41	p<0.001
KM3	15h	mmGlu	452	21.93 ±0.42	p<0.001
KM17	15h	mmGlu	370	21.69 ±0.48	p<0.001
TN02A25	15h	mmTF	458	34.06 ±0.49	-
KM5	15h	mmTF	462	30.61 ±0.48	p<0.001
KM3	15h	mmTF	402	30.07 ±0.54	p<0.001
KM17	15h	mmTF	344	29.44 ±0.54	p<0.001

[1] Intercalary lengths are compartments that are delimited by septa in subapical regions of hyphae. The values represent the combination of three separate trials, which gave similar result.

[2] Cells were incubated for 12h or 15h in the selected media, then fixed and stained with DAPI and Calcofluor. The intercalary lengths were measured.

[3] Deletion strains KM13 (Δ*plkA*), KM14 (Δ*plkA*) and negative control KM25 (*plkA*). Regulated strains KM3 (*alcA::plkA*), KM17 (*alcA::plkA*), and negative control KM5 (*alcA::*).

Table 11: Number of nuclei in intercalary compartments[1] in *plkA* deletion and *alcA::plkA*[2] regulated cells

Strain[3]	Time	Media	n	Nuclei±S.E.M.	Mann-Whitney U Test
KM25	12h	YAG	221	2.63±0.07	-
KM13	12h	YAG	260	2.35±0.07	p = 0.018
KM14	12h	YAG	211	2.59±0.10	p = 0.29
TN02A25	12h	YAGuu	288	3.01±0.060	-
KM5	12h	YAGuu	222	2.17±0.055	p<0.001
KM3	12h	YAGuu	183	2.00±0.069	p<0.001
KM17	12h	YAGuu	222	1.94±0.061	p<0.001
TN02A25	15h	mmGlu	270	2.44±0.059	-
KM5	15h	mmGlu	192	1.94±0.056	p<0.001
KM3	15h	mmGlu	300	1.83±0.050	p<0.001
KM17	15h	mmGlu	244	1.77±0.054	p<0.001
TN02A25	15h	mmTF	310	2.23±0.045	-
KM5	15h	mmTF	310	1.92±0.037	p<0.001
KM3	15h	mmTF	263	1.88±0.041	p<0.001
KM17	15h	mmTF	330	1.77±0.034	p<0.001

[1.] Intercalary lengths are compartments that are delimited by septa in subapical regions of hyphae. The number of nuclei in the intercalary lengths was measured. The values represent the combination of three separate trials, which gave similar result.
[2.] Cells were incubated for 12h or 15h in the selected media, then fixed and stained with DAPI and Calcofluor.
[3.] Deletion strains KM13 (Δ*plkA*), KM14 (Δ*plkA*) and negative control KM25 (*plkA*). Regulated strains KM3 (*alcA::plkA*), KM17 (*alcA::plkA*), and negative control KM5 (*alcA::*).

To confirm that these effects were due to absence of PLKA, septa were also analyzed in the regulated strains. Strains KM3, KM17 and control strains TN02A25 and KM5 grown in minimal inducing media did not demonstrate any difference in compartment length or number of nuclei (Tables 10, 11; Figure 15). In repressing media, however, the *alcA::plkA* regulated strains demonstrated a decrease in subapical lengths related to the control TN02A25 (Table 10 and Figure 15), but not compared to the control KM5. This result was surprising given the similarity between strains KM5 and TN02A25 with respect to growth rate and other parameters, and differences compared to strains KM3 and KM17. Although additional measurements will have to be taken to clarify the relationship in the regulated strains, the results demonstrated that PLKA is not essential for septation, but may be required for proper timing and placement of septa.

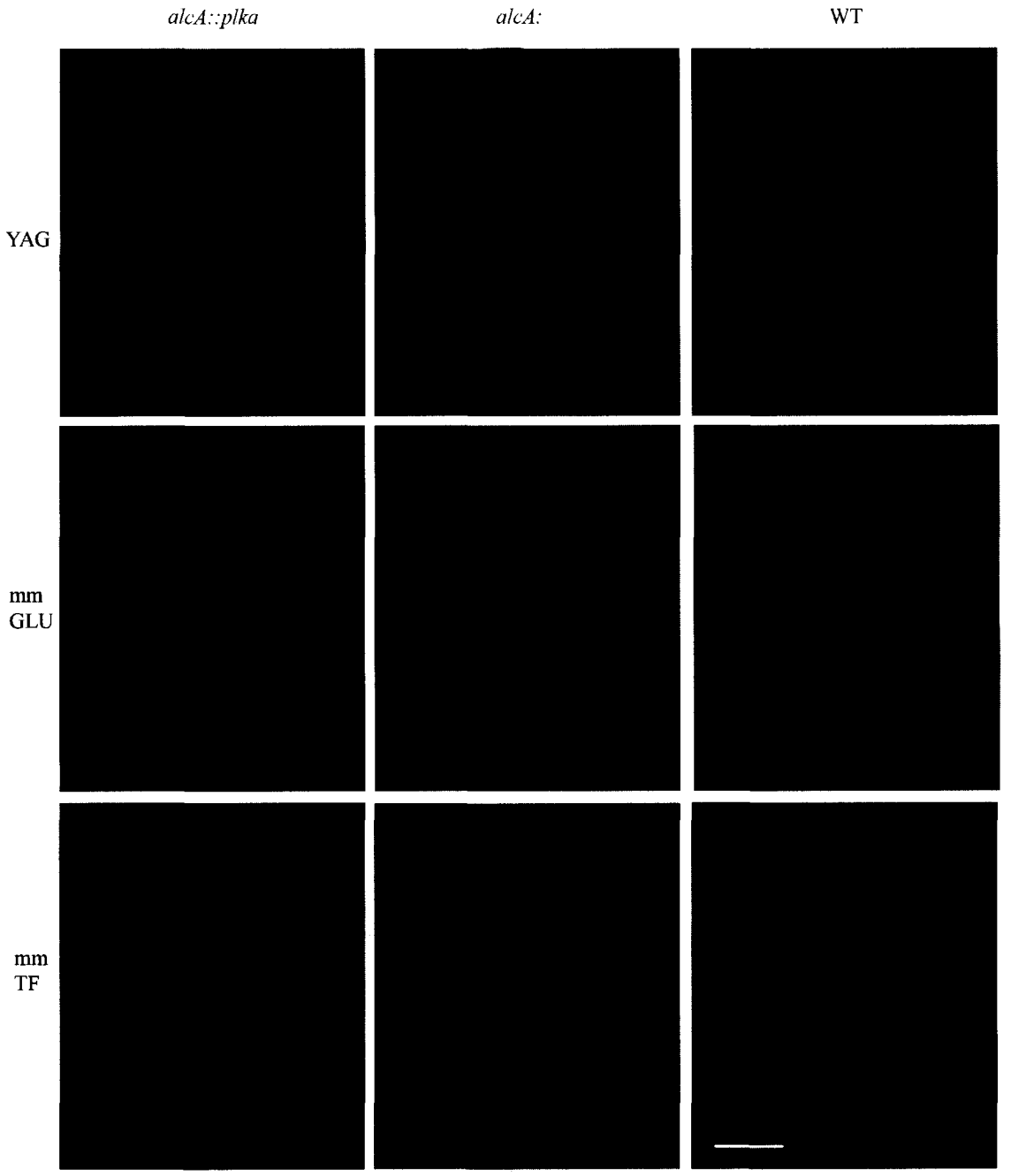

Figure 15: Intercalary compartments in cells lacking *plkA*
Strains KM3 (*alcA::plkA*), KM5 (*alcA::*) and wild type TN02A25 were inoculated at 10^6 conidia/ml in YAG (12h) , mmGlu (19h) and mmTF (19h) media at 32°C. The cells were then fixed and stained with DAPI and Calcofluor. Bar 10μm.

3.10 The *plkA* growth phenotype is cold sensitive and suppressed by benomyl

Based on defects in spindle formation, hyphal polarity, and nuclear distribution, PLKA may be important for microtubule structure/dynamics. Since cells containing defects in microtubule function are often cold sensitive (Jung et al., 2001), we tested the temperature sensitivity of the *plkA* deletion strains. Conidia from strains KM13 and KM14 and the control strains KM25 and TN02A25 were point inoculated onto YAGuu plates and incubated at 32°C, 37°C and 42°C for three days (Figure 3). At 32°C, strains KM13 and KM14 demonstrated compact growth, while the control strains KM25 and TN02A25 grew normally, as previously described. At 37°C, growth of KM13 and KM14 was less compact than at 32°C, and colony diameters resembled those of the controls. At 42°C, all four strains grew in a similar manner with a diameter slightly less than at the optimal temperature of 37°C. When conidia from all four strains were incubated for a week at 21°C, strains KM13 and KM14 demonstrated compact growth similar to that at 32°C, whereas the control strains, KM25 and TN02A25 grew normally (data not shown). To demonstrate that this growth sensitivity was due to absence of PLKA, the *alcA::plkA* strains were also tested. Conidia from strains KM3, KM17 and control strain KM5 were inoculated onto minimal inducing and repressing media, and YAG repressing media (Figure 3). Strain TN02A25 was only included on YAGuu media because of the auxotrophy for *pyrG*. While KM3 and KM17 demonstrated the compact growth phenotype at 32°C on repressing media only, this defect was no longer visible at 37°C or 42°C, where the strains grew to the same diameter as the controls. On inducing minimal media, when *plkA* is expressed, strains KM3 and KM17 grew normally and in a similar

manner as the control strain KM5 at all three temperatures (Figure 3). Thus, the compact growth defect was suppressed by higher temperature, suggesting that the *plkA* deletion/depletion is cold sensitive, and that *plkA* may be important for microtubule function.

To obtain more evidence for this possibility, we tested the sensitivity of the cells lacking *plkA* to benomyl, a microtubule destabilizing agent. YAG plates were prepared with 0, 0.2, 0.4, 0.6, 0.8, and 1.0μg/ml concentrations of benomyl and 2000 spores from strains KM13, KM14 and KM25 were spot inoculated on each plate. After incubation at 32°C for three days, strains KM13 and KM14 grew in a compact manner, as previously described, while the control strain KM25 grew normally on plates lacking benomyl. In the presence of 0.2-0.4μg/ml of benomyl however, the diameter of colonies from strains KM13 and KM14 doubled, no longer appeared compact, and resembled that of control strain KM25. On 0.6μg/ml of benomyl, growth of the deletion strains was decreased, but not to the same extent as that seen with the control strain KM25. At 0.8-1.0μg/ml, growth was completely inhibited in the deletion strains KM13 and KM14, while the control strain KM25 demonstrated some residual growth (Figure 16). Thus, at the low concentrations of benomyl, the *plkA* phenotype is suppressed, but at higher concentrations, the *plkA* strain is slightly more sensitive than the control strain. These results suggest that PLKA is important for microtubule dynamics in a complex fashion.

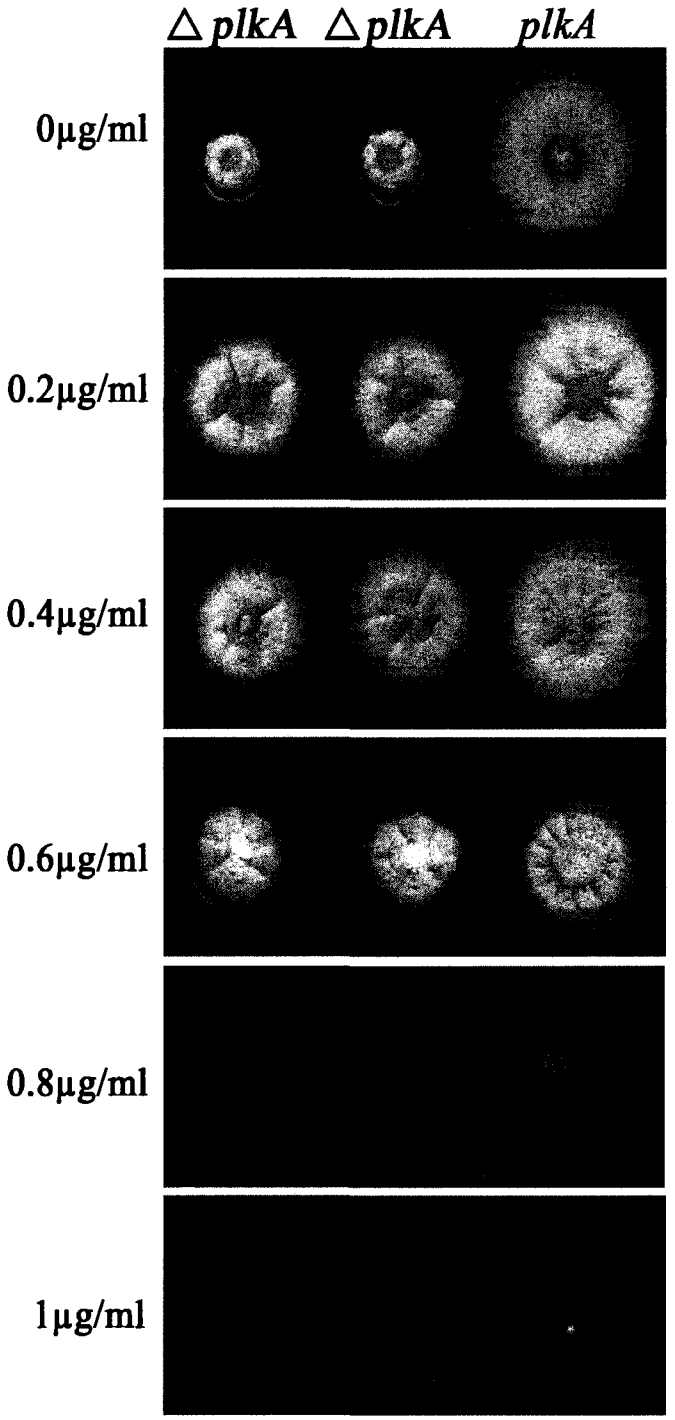

Figure 16: How concentration of Benomyl suppresses the compact growth phenotype of *ΔplkA* strains

Strains KM13 (*ΔplkA*), KM14 (*ΔplkA*) and KM25 (*plkA*) were spot inoculated for three days in YAG with 0, 0.2, 0.4, 0.6, 0.8 and 1.0μg/ml of Benomyl at 32oC.

Note: ΔplkA is more sensitive to high concentration of Benomyl than the wild type strain.

3.11 Absence of PLKA results in abnormal asexual development

In *Aspergillus nidulans*, asexual development commences approximately 20 hours after vegetative growth has started. At the center of a colony, aerial hyphae differentiate and produce aerial stalks, the apical tips of which swell and produce vesicles that contain multiple nuclei. Budding then causes a primary metullae layer to appear on the surface of the vesicle and a single nucleus enters each cell. A single division follows and produces a secondary phialide layer, where nuclear division proceeds. One daughter cell remains at the tip of the phialide, whereas the other one buds off to form a conidium, or asexual spore. The process continues, producing a long chain of conidia at various stages of maturity (Boylan et al., 1987). The color observed on plates is due to spore-specific pigments. While many genes contribute to variations in spore color, the genes *wA* and *yA* are central to the process, where mutants produce white or yellow conidia colors, respectively. When both genes are wild type, green conidia are produced (Adams et al., 1998). After three days of growth on YAG media at 32°C, conidia from deletion strains KM13 and KM14 had an abnormal grey-white color. In contrast, conidia of control strain KM25 and the wild type strain TN02A25 were yellow, which was most likely due to the media and not a mutation (Figure 17). The difference in colony color suggested that asexual development was affected in the absence of PLKA. To investigate this further, conidia were inoculated into top agar media, which was used to increase synchronous growth across the plate. After three days at 32°C, the plates were analyzed using a dissection microscope. In control strain KM25, abundant conidiophore heads were present. In contrast, conidiophore heads were less frequent and of aerial hyphae

were detected, in strains KM13 and KM14, suggesting that asexual development was affected (Figure 18A).

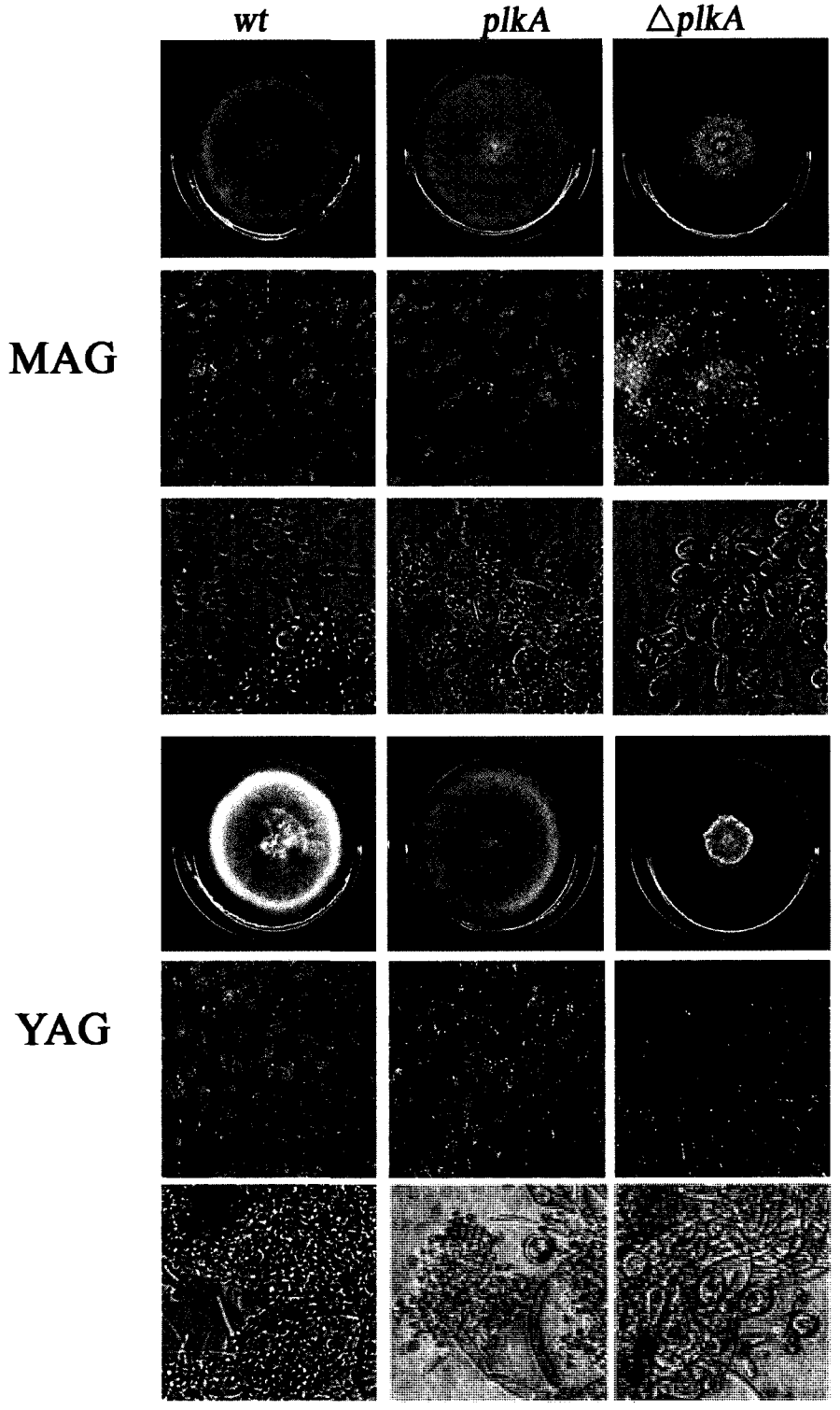

Figure 17: Absence of PLKA results in early sexual development
Strains KM14 (*ΔplkA*), KM25 (*plkA*) and wild type TN02A25 were spot inoculated on YAG and MAG plates and incubated for seven days at 32°C. Plates were examined under at 11.25X and 40X objective.

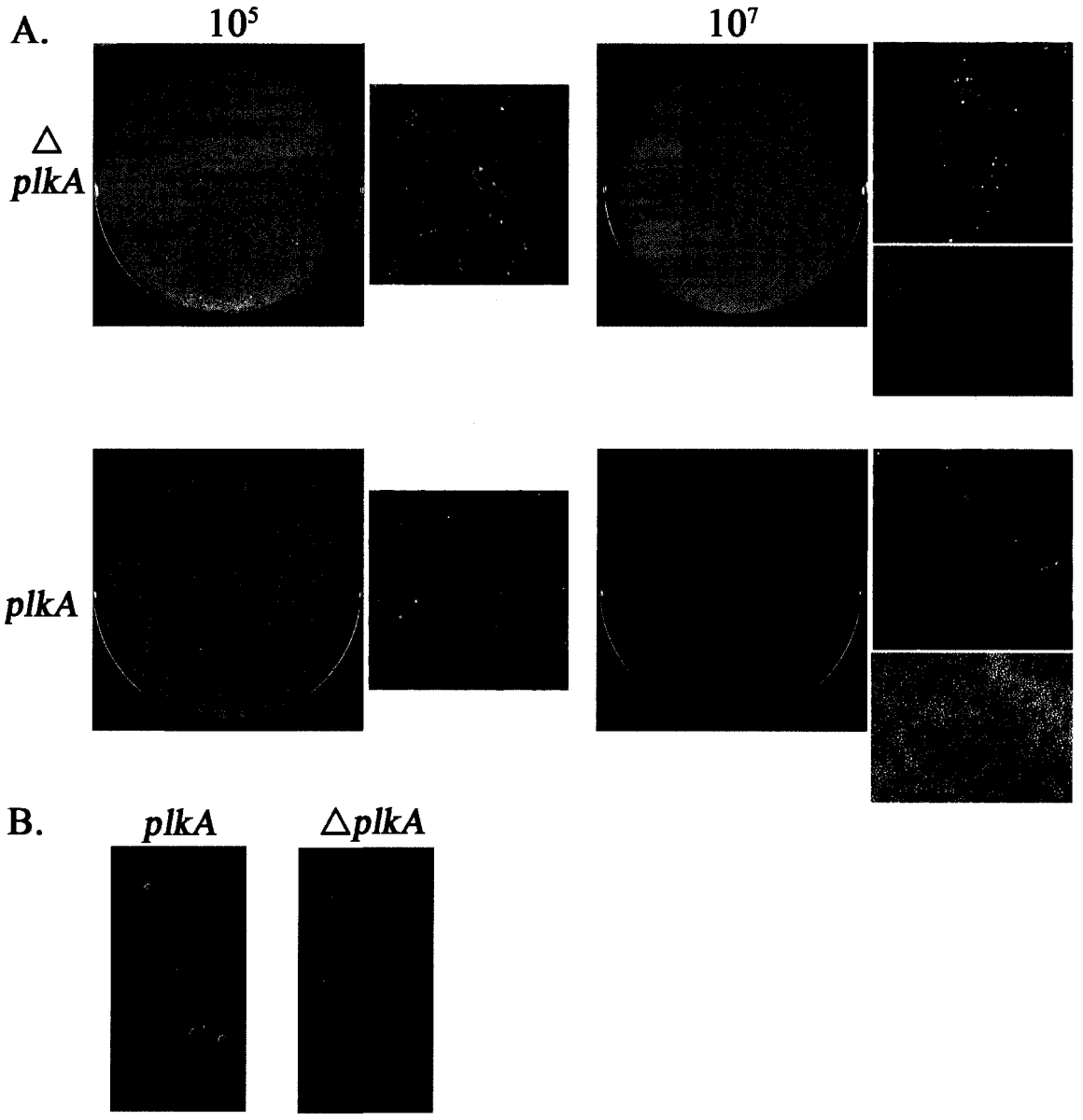

Figure 18(A,B): Absence of PLKA results in abnormal asexual development and de-represses sexual development
(A) Strains KM14 (*ΔplkA*), and KM25 (*plkA*) were inoculated at 10^5 or 10^7 conidia/ml in top agar, which was then poured onto YAG plates. Plates were incubated for three days at 32°C. (B) Sample Conidiophores head.

When sections of plates were examined at higher magnification, abnormal conidiophore heads were observed in strains KM13 and KM14. Many appeared to have only the primary phialide structure, whereas others produced the secondary metullae structure. Several conidiophore heads contained a mixture of structures at different stages of development (Figure 18B). In addition, conidia size varied, and in general few mature conidia could be seen attached to the head. In contrast, the control strain KM25 appeared to be normal with synchronous development within a conidiophore head, and contained numerous chains of conidia (Figure 18B). Although conidia were clearly being produced and could be isolated from the deletion strains, the abundance was diminished compared to controls. These results suggest that PLKA might have a function in conidiophore development.

In order to demonstrate that the effect was due to absence of PLKA, asexual development was also examined in the *alcA::plkA* regulated strains. Conidia from strains KM3, KM17 and KM5 were inoculated into top agar repressing and inducing minimal media for three days at 32°C. Conidia from strains KM3 and KM17 had an abnormal grey-white color, while control strain KM5 was green (Figure 19), supporting a conidiation defect in the absence of PLKA. When *alcA::plkA* regulated strains were analyzed under the dissection microscope, many aerial hyphae were present and mature conidiophores were less frequent under repressing conditions. In contrast, the control strain KM25 had an abundance of conidiophore heads. In minimal inducing media, conidia from all strains were green, suggesting that the grey-white color was due to repression of *plkA*. KM5 was yellow in repressing YAG media, like strains mentioned previously. When examined under the dissection microscope, the *alcA::plkA* regulated

strains grew in a similar manner as the control strain, demonstrating the presence of conidiophore heads. Undifferentiated aerial hyphae were present in all strains in inducing media, but this was likely due to the poor carbon source since the severity was less than that seen with strains KM3 and KM17 under repressing conditions. Regardless, the results clearly support the notion that asexual development is reduced in strains lacking PLKA.

The defects in conidiation were not suppressed by higher temperature as seen with the compact growth phenotype. For example, deletion strains KM13 and KM14 and regulated strains KM3 and KM17 were still white-grey compared to the yellow color of the controls KM25, KM5 and TN02A25 at 37°C and 42°C (Figures 3,6). This suggests that different mechanisms underline PLKA's role in regulating growth vs asexual development.

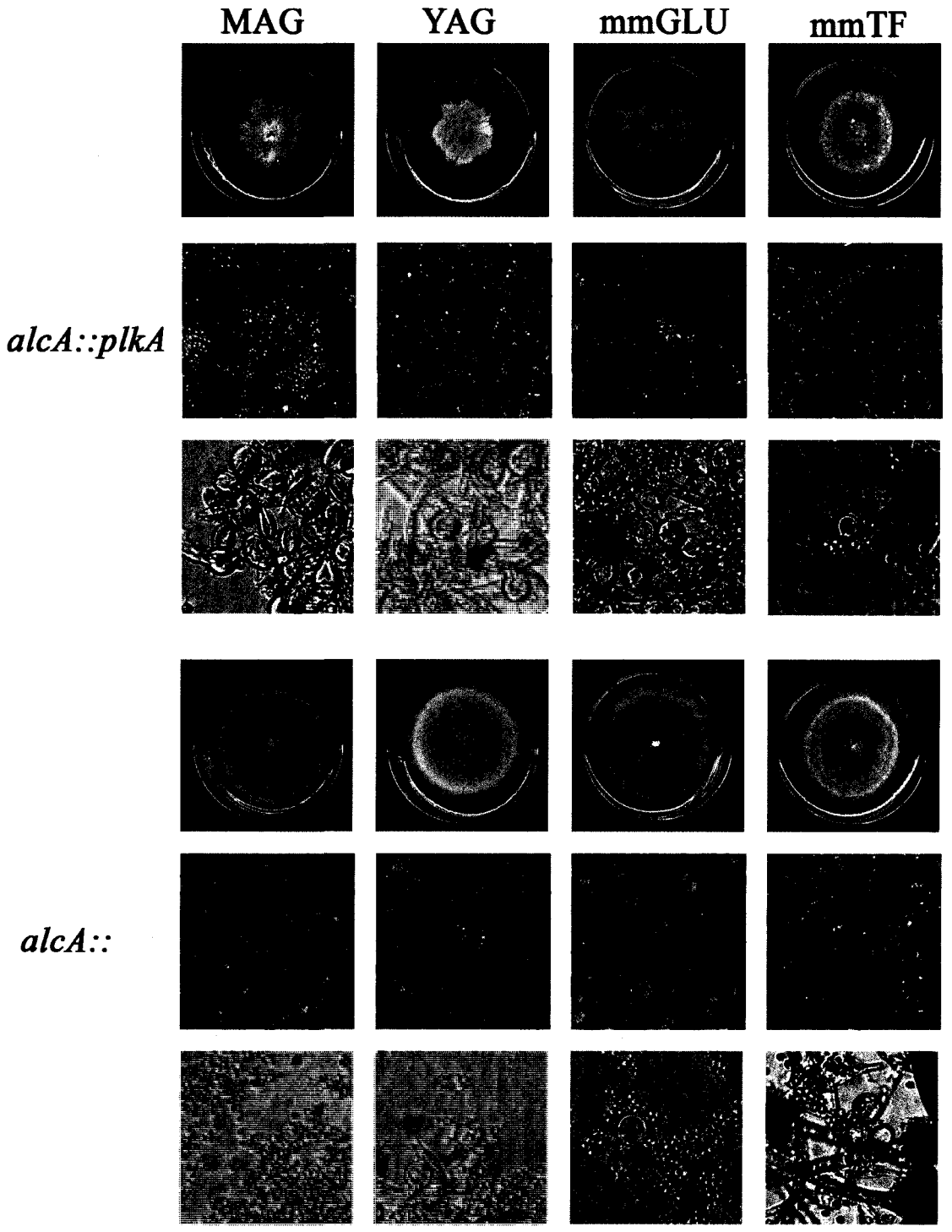

Figure 19: Depletion of PLKA results in early sexual development
Strains KM3 (*alcA::plkA*) and KM5 (*alcA::*) were spot inoculated on MAG, YAG, mmGlu and mmTF plates, and incubated for seven days at 32°C. Plates were examined under at 11.25X and 40X objective.

3.12 Absence of PLKA results in early sexual development

A. nidulans undergoes sexual development after approximately one week of growth and when the carbon source has been depleted. Sexual structures are obtained in the older regions, at the center of the colony. Cleistothecia are the fruiting bodies seen during sexual development and are filled with asci, each containing eight binucleated ascospores (Adams et al., 1998). Specialized Hülle cells surround the cleistothecia. Since Hülle cells were observed upon collection of conidia from deletion strains KM13 and KM14, we investigated whether the absence of *plkA* affected sexual development. Conidia from *plkA* deletion strains KM13 and KM14 and from control strains KM25 and TN02A25 were spot inoculated on MAG and YAG media at 32°C, and growth was examined on a daily basis. By the third day, the control strains on MAG were green, and full of conidiophore heads. When cells were scraped from the center of the colony and examined at a higher magnification, conidia and asexual structures were abundant. Similar results were found on YAG, except some Hülle cells were visible. In contrast, deletion strains KM13 and KM14 were grey-white on both MAG and YAG media, and when material was scraped and analyzed at high magnification, an abundance of Hülle cells was seen. By day seven, some sexual structures such as young cleistotheciae and Hülle cells were visible in strains KM25 and TN02A25, but conidia and asexual structures predominated. In contrast, young cleitothecial structures and Hülle cells were more abundant than conidiophore heads in the deletion strains KM13 and KM14 (Figure 17). Thus, abundant sexual structures were observed as early as three days in the *plkA* deletion strain, suggesting that PLKA may play a role in repressing sexual development.

Since sexual development normally occurs in the older regions of the colonies after seven days, and the *ΔplkA* strains grew in a compact manner, it was possible that the sexual structures observed were due to a mixing of older regions of the colony with the growing edge. To address this issue, we analyzed sexual development in cells grown in top agar, which allows for synchronous growth and development (Bussink and Osmani, 1998). Conidia from strains KM13, KM14 and KM25 were inoculated at either 10^5 spores/ml or 10^7 spores/ml inoculation density in YAG media, since it was previously shown that inoculation density can influence sexual development, although under conditions of limiting phosphate availability (Bussink and Osmani, 1998). After three days at 32°C, young cleistotheciae were visible in the *plkA* deletion strains inoculated at 10^7 spores/ml, but not in the control strain at the same conidia density (Figure 18). In contrast, the control strain only contained asexual structures. When cells were examined at a higher magnification, abundant Hülle cells were observed in the deletion strains, but few Hülle cells were recovered in the control strain. At the lower inoculation density of 10^5 spores/ml, young cleistothecia and Hülle cells were observed in the *plkA* deletion and the control strains, but were much less abundant in the control strain (Figure 18). Although low inoculation density can contribute to sexual development, the results clearly demonstrated a higher abundance of sexual structures in the absence of PLKA, supporting the concept that PLKA may have a function in suppressing sexual development.

To validate the results obtained with deletion strains, sexual development was also analyzed in the *alcA::plkA* regulated strains under repressing and inducing conditions. Strains KM3, KM17 and KM5 were spot inoculated on repressing MAG, YAG and

minimal repressing media as well as minimal inducing media at 32°C. By seven days, sexual structures were visible in the control strains in repressing media, but they were much less abundant than the asexual structures. In contrast, sexual structures like cleistothecia and Hülle cells were much more abundant in the *alcA::plkA* regulated strains in all three repressing media. While some sexual structures were visible in all strains under inducing conditions, this was likely due to poor carbon source, and, they were less abundant than that observed in repressing media and in comparison to the asexual structures.

The strains were also tested at different inoculation densities and using the top agar method to ensure synchronous development. 10^5 or 10^7 spores/ml of strains KM3 and KM17 and the control strain KM5 were inoculated onto YAG repressing, minimal repressing and minimal inducing media for three days at 32°C. At 10^7 spores/ml, cleistothecial structures and Hülle cells were visible in strains KM3 and KM17 in both YAG and repressing minimal media, while control strain KM5 had fewer cleistothecial structures and Hülle cells, and more abundant asexual structures (Figure 20). In minimal inducing media, all strains grew in a similar fashion, producing some Hülle cells, but they were less than that observed in *plkA* deletion strains under repressing conditions. At the lower concentration of 10^5 spores/ml, Hülle cells and cleistothecial structures were observed in all strains in all media, but were most abundant in *plkA*-regulated strains KM3 and KM17 under repressing conditions. Thus, earlier sexual development is associated with the absence of PLKA.

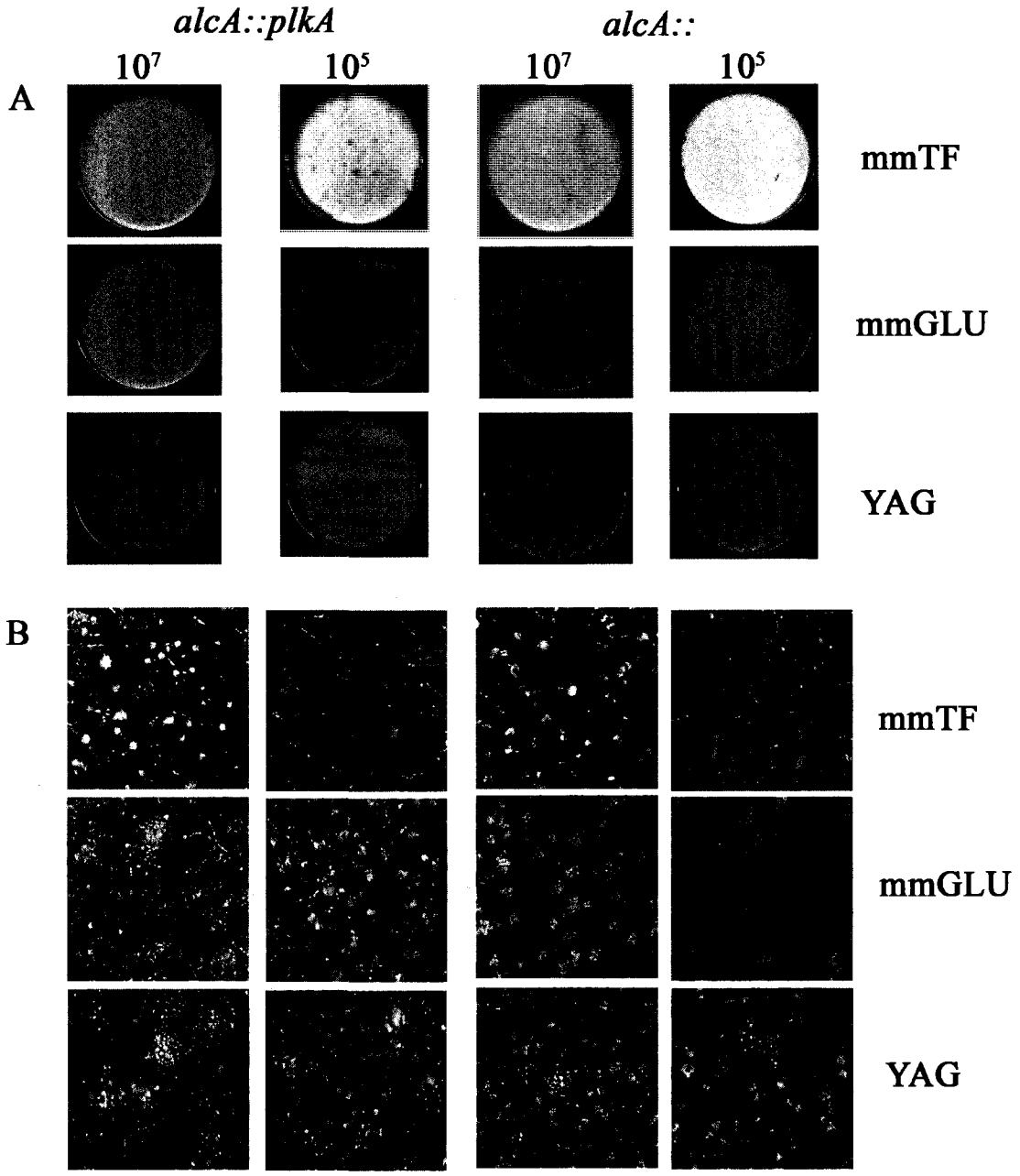

Figure 20 (A,B): Depletion of PLKA results in abnormal asexual development and de-represses sexual development

(A) Strains KM3 (*alcA::plkA*), and KM5 (*alcA::*) were inoculated to 10^5 and 10^7 conidia/ml in top agar, which was then poured onto YAG, mmGlu and mmTF plates. Plates were incubated for three days at 32°C. (B) Plates were examined under at 11.25X objective.

3.13 Localization of PLKA does not require NIMT or BIME

A previous investigation demonstrated novel aspects of PLKA localization and determined that the major cell cycle regulating factor NIMA was not required (Bachewich et al., 2005). To determine whether other major cell cycle factors contribute to PLKA localization, $NIMT^{Cdc25C}$ and $BIME^{APC27}$ were selected. PLKA was tagged with GFP using two-step fusion PCR to create a 7kb product, which was subsequently transformed in the temperature-sensitive strains SO182 (*nimT*) and ASH262 (*bimE*), respectively. Transformants from each strain were selected and streaked three times to single colony. Transformants were confirmed by Southern and visualization of the GFP signal under the microscope (Figure 21).

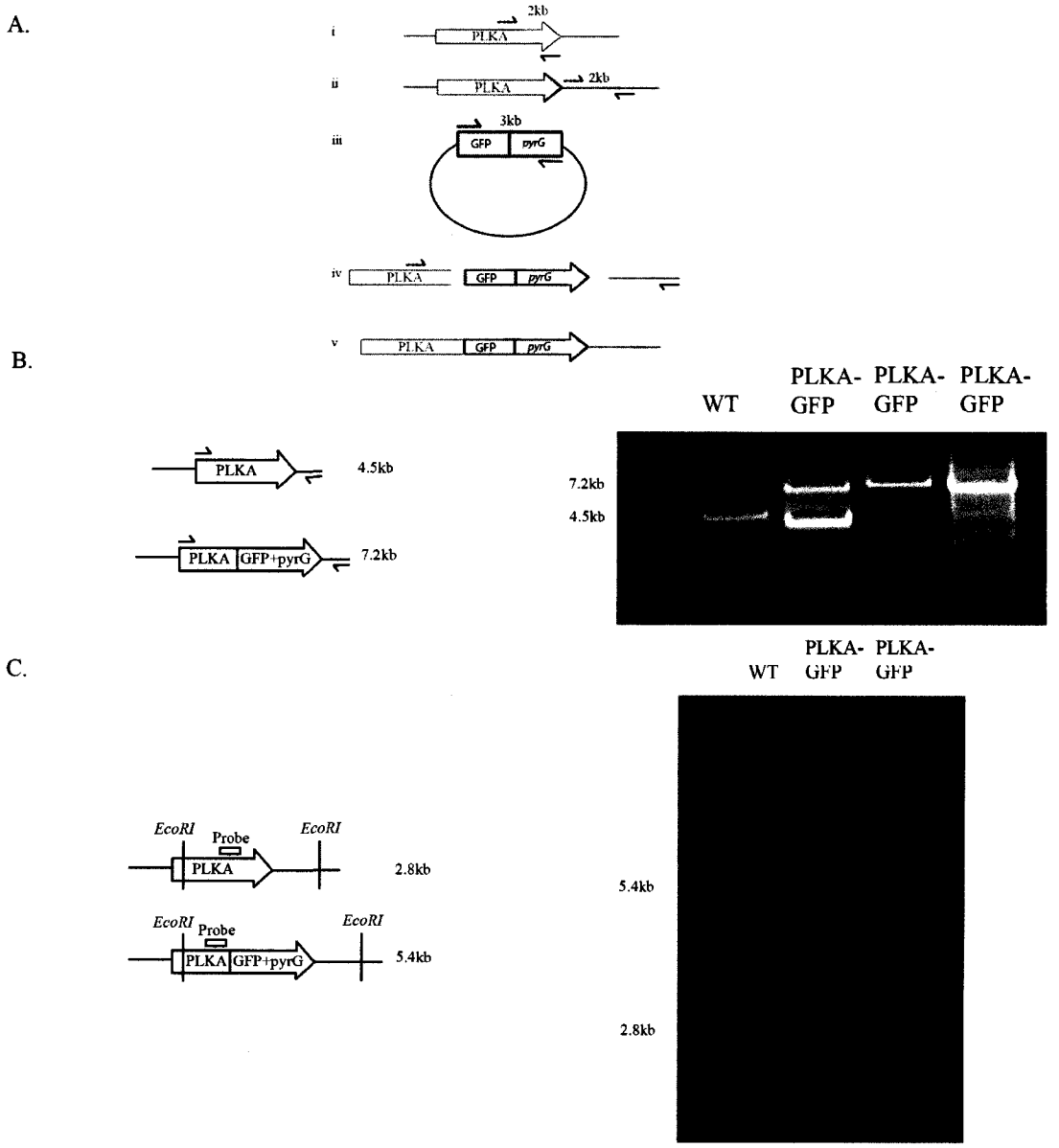

Figure 21: Tagging PLKA with GFP in strains ASH262 and SO182
(A) Strategy to construct a PLKA-GFP strain. (i) a 2kb fragment was PCR amplified upstream of the stop site. (ii) a 2kb fragment including and downstream of the stop site. (iii) a 3kb fragment PCR amplified the GFP tag and *pyrG* marker from plasmid pFN03. (iv-v) three fragments were used as a template in a fusion PCR reaction to create a 7kb final product that was transformed into SO182 and ASH262 strains. (B) PCR screening demonstrating that strains KM1 and KM2 are positive (7.2kb) and a third was removed due to a band close to 4.5kb. (C) Southern analysis demonstrating that strains KM10 and KM11 are positive (5.4kb) whereas the wild-type only contained the 2.8kb band.

To determine whether NIMT and BIME were required for PLKA localization, conidia from strains KM1 (PLKA::GFP in *nimT* background) and KM10 (PLKA::GFP in *bimE* background) were inoculated into liquid YAG medium for 12 hours at 32°C. Cells were then fixed and stained with DAPI. PLKA-GFP signal was observed as a single spot on the nucleus, which corresponds to the spindle pole body, in both strains. Conidia from strains KM1 and KM10 were then inoculated into liquid medium at 42°C to repress *nimT* or *bimE* and therefore block cells at the respective cell cycle stage. Strain KM1 was incubated for 9 hours, whereas strain KM10, which grew slower, was incubated for 15 hours. Cells were then fixed and strained with DAPI. In strain KM1 and KM10, PLKA-GFP signal was observed at the spindle pole body (Figure 22). Thus, NIMT and BIME are not required for PLKA localization to the spindle pole body.

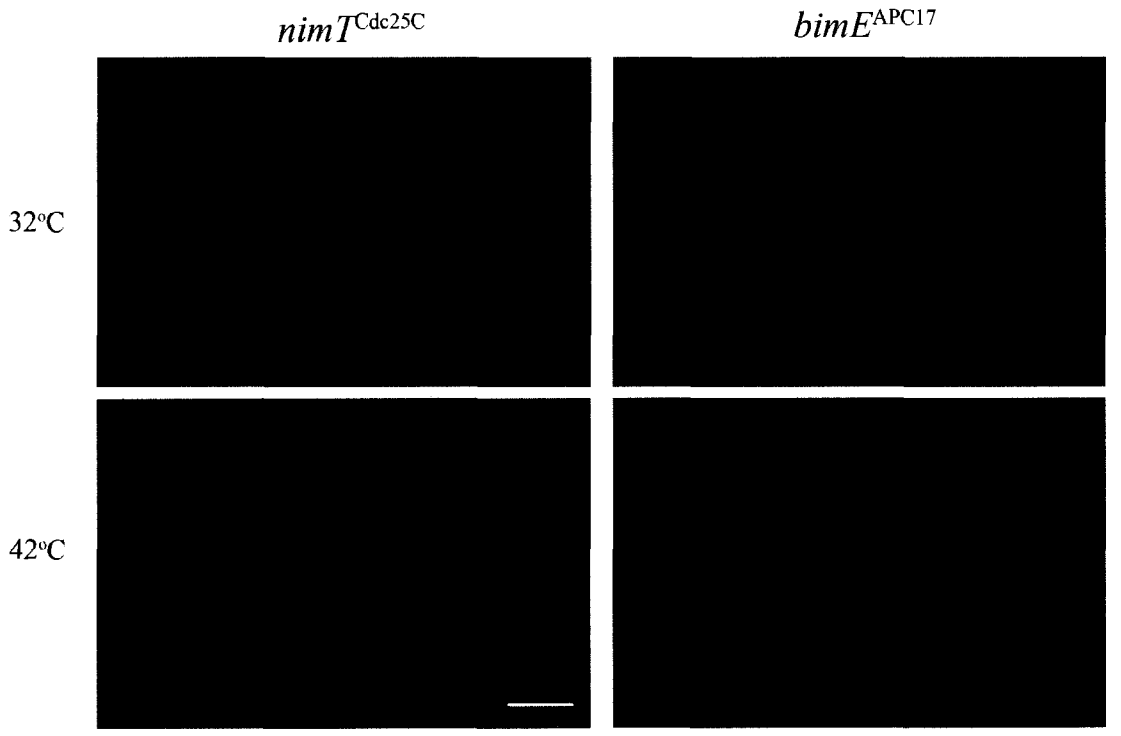

Figure 22: Localization of PLKA does not require NIMT or BIME
Strains KM1 (PLKA-GFP) and KM10 (PLKA-GFP) were inoculated to a 10^6 inoculation density in YAG media for 12h at 32°C or 9h at 42°C. PLKA-GFP signal is indicated by the arrow.
Note Strain KM10 was inoculated for 15h at 42°C. The cells were then fixed and stained with DAPI. Bars 10μm.

4. Discussion

Polo-like kinases are conserved cell cycle regulators with multiple functions (Lee et al., 2005). PLKA from *A. nidulans* was previously identified as the first PLK in a filamentous fungus, but the functions were not clear (Bachewich et al., 2005). We have constructed strains deleted for *plkA* or carrying a single copy under the control of the *alcA* promoter to address function, and discovered both conserved and novel roles. Hallmark functions in spindle formation and mitotic exit, possibly through regulating microtubule dynamics, were identified, as well as a role in chromosome segregation. However, we also found that, despite being the single PLK in *A. nidulans*, *plkA* was not essential. PLKA was required for normal growth and hyphal morphogenesis, since colonies lacking the gene were compact and hyphae had aberrant tips and germination patterns. PLKA was not essential for nuclear division, but its absence partially suppressed the G2/M block of *nimT* cells at restrictive temperature, suggesting that PLKA plays some role in negatively regulating the G2/M transition. Surprisingly, we found that PLKA is not required for septation, and may play novel roles in regulating asexual and sexual development. Thus, our work demonstrates that PLKA has conserved as well as novel functions, which sets the stage for fruitful future investigations of this important, multi-functional cell cycle factor.

4.1 Successful creation of deletion and regulated *plkA* strains

Despite previous unsuccessful attempts to create a strain that lacked *plkA* or one that contained a single copy of the gene under control of the *alcA* promoter (Bachewich et al., 2005), we were able to create the strains using different strategies. The Δ*nku* strain

allowed an increase in transformation efficiency, and decrease in heterologous integration, which contributed to the success in making deletion and regulated strains. However, this was not the sole reason for the success, since transforming strain backgrounds LO879 and SO182, which were not Δ*nku,* also resulted in positive transformants. The following reasons provide a rationale for why we were successful. First, the *alcA::plkA* regulated strains were selected by plating transformants on 0.6% threonine/0.9% fructose (Romero et al., 2003; James et al 1999), whereas previous attempts to create a regulated strain grew the potential transformants on 0.2% fructose (Bachewich et al., 2005). We found that our *alcA::plkA* regulated strains grew vegetatively but did not conidiate on media containing fructose alone (data not shown). Since threonine is a stronger inducer of the *alcA* promoter (Bussink and Osmani, 1999), our inclusion of it in the selection plates could have contributed to the production of more healthy, transformed colonies. Secondly, the regulated *plkA* strains in the current study were created by transforming a linear DNA fragment to replace the promoter, whereas previous attempts utilized a circular plasmid that contained a 3' truncated copy of *plkA* cloned after the *alcA* promoter. A linear DNA fragment with 2kb sequence homology at either end has a better chance to integrate at the correct site, compared to a circular plasmid. In addition, integration of the plasmid would result in one full length copy of *plkA* under the control of the *alcA* promoter, and a 3' truncated copy, the latter of which could be expressed and complicate the phenotype. A different strategy was also used for the deletion of *plkA*. In the previous study, *plkA* was assumed to be essential. Thus, a diploid strain that was heterozygous for *plkA* was created, and then haploidized to isolate cells that lacked *plkA*. However, the only cells that subsequently grew were wild-type for

plkA, suggesting that conidia that acquired the deleted allele during haploidization were unable to survive or germinate. Haploidization required the use of benomyl at a concentration of 1.2μg/ml (Bachewich et al., 2005), yet we now know that at this concentration *ΔplkA* strains are more sensitive than wild-type strains. Therefore benomyl might have contributed to the lack of isolation of *ΔplkA* cells (Bachewich et al., 2005). Thus, with the use of a different DNA manipulation technique and a more direct deletion strategy, we were able to successfully create the *alcA::plkA* regulated and *ΔplkA* deletion strains. The *alcA::plkA* strain was subsequently used as a control to confirm the deletion strain phenotype. In most cases, there was agreement between the deletion and regulated strain under repressing conditions, indicating that the results were due to absence of PLKA.

4.2 PLKA has two start sites that could constitute valid start signals

Two start sites were reported for the *plkA* gene, utilizing two different experimental approaches. Start site A was determined by RACE PCR (Bachewich et al., 2005), while Start site B was reported when the entire *Aspergillus nidulans* genome was sequenced (Galagan et al., 2005). The Kozak consensus sequence ((gcc)gccRccAUGG), is used to determine a strong start site. The R must be a purine (either adenine or guanine), and there must be a G after the start codon (Kozak M., 1986). The strength of the sequence is calculated by the combination at the start site; the G at +4 and a purine at -3 (Kozak M., 1986). The sequence for start site A is ACT [redacted]TA ATG GAG, where two

of the criteria are met, whereas the sequence for start site B is CCA ACA ATG GAA, which meets all three criteria. However, both sites constitute valid start signals. In the first report on PLKA, which was done before the whole *Aspergillus nidulans* genome was sequenced, start site A was used, since it was the most valid upstream start site (Bachewich et al., 2005). However, we decided to test both sites in separate promoter-replacement constructs. The *alcA::plkA* regulated strains KM3 (start site B) and KM17 (start site A) were tested against a control strain KM5. In minimal inducing media, when *plkA* expression was turned on, all three strains grew in a similar manner. In contrast, in minimal repressing media, when expression was turned off, KM3 and KM17 grew in a similar compact phenotype, while KM5 grew normally. Therefore, no visible phenotypic difference was observed between the two *alcA::plkA* regulated strains, implying either start site was valid.

4.3 PLKA is not essential in *Aspergillus nidulans*

The results from shutting off *plkA* expression or deleting the gene revealed that *plkA* was not essential, which was surprising considering that PLKs are essential in other organisms that only have one copy of the gene, including Cdc5p (Cheng et al., 1998) and Plo1p (Reynolds and Ohkura, 2002), in *S. cerevisiae* and *S. pombe,* respectively. On the other hand, in higher organisms such as vertebrates, multiple copies exist with some functional redundancy (Johnson et al., 2007). Mammals, for example, contain PLK1, PLK2, PLK3 and PLK4, of which PLK1 and PLK3 have numerous important functions throughout mitosis and in the DNA damage/repair pathway, whereas the functions of the other two members are mainly unknown (Johnson et al., 2007). PLK4 is the most

structurally divergent member of the PLK family. Whereas all other PLKs have two polo box domains that interact with each other, PLK4's second polo box has a very divergent sequence that does not interact with the first polo box and is referred to as a cryptic polo box (Bettencour-Dias et al., 2005). PLK4's function is largely unknown, other than its role in regulating centriole duplication (Habedanck et al., 2005). Interestingly, when we created a clustal alignment tree, PLKA appeared closest in sequence to PLK4 compared to the other PLKs (Figure 23). This suggests that the initial divergence created two members, one of which was the ancestor of PLK1, PLK2, PLK3, Plo1, Cdc5 and POLO while the other was the ancestor of PLK4 and PLKA. When the full PLKA sequence was compared to the other organisms, it demonstrated 43% identity and 64% similarity to *CDC5* in *S. cerevisiae*, 44% identity and 63% similarity to plo1 in *S. pombe*, 42% identity and 61% similarity to Plk1 in *Homo sapiens* and 42% identity and 60% similarity to Plk4 in *Homo sapiens.*

Since PLKA was not essential, we looked for other sequence homologues. PLKA's sequence is the longest of the PLK family and other than the N terminal kinase domain and the C terminal polo box, the middle portion does not have homology with any known motifs. Even though sequence homology confirms that PLKA is a member of the PLK family, based on the presence of the polo box and PLK-specific kinase domain, the fact that it is not essential suggests that other factors may help carry out conserved PLK functions, some of which may interact with PLKA Affinity capture coupled to Mass spectrometry could help elucidate the nature of this factor(s). To this end, we have tagged PLKA with the S-tag (Kim and Raines, 1993).

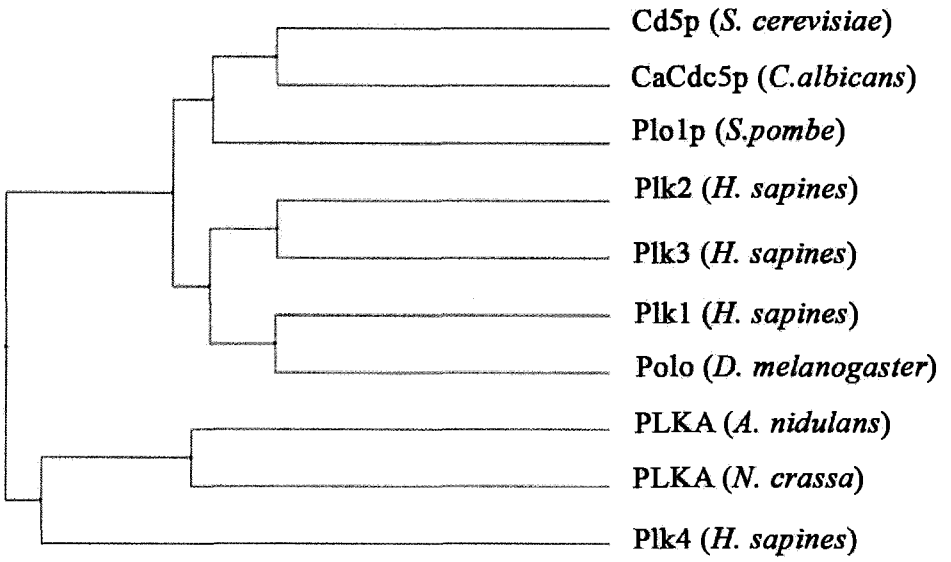

Figure 23: PLKA protein sequence is closer to Plk4, than to other homologues
Phylogenetic analysis of polo-like kinase homologues. Tree was constructed with ClustalW.

4.4 PLKA is required for normal colony growth and polar axis formation in hyphae

Deletion or repression of *plkA* resulted in a compact colony, indicating that the gene was required for normal growth. Since hyphae of the colonies were multi-branched and contained split tips, this suggested that *plkA* is required for proper polar growth of hyphae and polar axis formation. Consistent with this, we found that hyphae in liquid media had abnormal germination patterns; a higher proportion of cells had a second germ tube at 180°compared to the control. In addition, more cells produced a second germ tube at an axis less than the normal 180°. Similar results were obtained with the regulated strain under repressing conditions, except there were not a significant number of cells showing germination axis less than 180°. This difference could be due to different composition of the growth medium (YAG in the deletion strains, and YAGuu in the regulated strains), or perhaps some leakiness from the *alcA* promoter. A Northern would be required to determine whether promoter expression had an influence on the results. Regardless, the data support the fact that PLKA is required for proper axis formation. Such a role has not been described for other PLKs. A similar phenotype was observed in *A. nidulans* strains lacking *alpA*, a microtubule associated protein (MAP), or *kipA*, a conventional kinesin (Enke, 2007). Deletion of either gene resulted in a second germ tube emerging at angles lower than 180° (Enke 2007). Interestingly, *alpA* and *kipA* deletion strains also demonstrated compact growth, and *alpA* localized to the complete spindle and spindle pole bodies like PLKA during mitosis (Enke, 2007). The apices of hyphae in the *ΔalpA* and *ΔkipA* strains did not contain a Spitzenkörper, a vesicle-rich organelle that directs growth of the hyphal apex (Enke 2007). The similar phenotype between mutants in these

genes and *ΔplkA* suggest that *plkA* may also play a role in maintaining polarity, perhaps through interaction with these MAPs and/or regulating microtubule dynamics This hypothesis is further supported by the fact that the mammalian homologue Plk1 interacts with several MAPs such as NIp (ninein-like protein) (Casenghi et al., 2003), TCTp (microtubule-stablizing protein) (microtubule stabilizing protein), MKLP-1 and -2 (mitotic kinesis like protein) (Budde et al., 2001) and stathmin (microtubule destabilizing protein (Budde et al., 2001). In addition, a recent study has demonstrated that the *alpA* homolog Stu2p interacts with and is phosphorylated by the PLK Cdc5p in *S. cerevisiae* (Park et al., 2008). However the exact phosphorylation sites on the protein are still unknown. Therefore, *plkA* is important for proper hyphal growth and polar axis formation. The mechanism underlying this function may involve regulation of the Spitzenkörper and/or microtubule dynamics.

4.5 PLKA is not essential for nuclear division

In *A. nidulans*, *plkA* is not essential for nuclear division, since nuclei could still divide in cells lacking the gene. This was surprising, since PLK in other organisms are major regulators of mitosis. There was only a minor decrease in the total number of nuclei compared to control cells of a similar length. Fewer nuclei per germling were also seen in the regulated strains compared to the wild-type strain in repressing media, but not when compared to the prototrophic control (Table 6). Although it is not clear why the wild-type strain grew better, the fact that it was longer could account for it having a higher number of nuclei. Although not essential for nuclear division, PLKA may play some role in regulating the G_2/M transition, since *nimT*^{Cdc25C}cells lacking *plkA*

leaked through the interphase block and entered mitosis. This is intriguing given the current knowledge of the relationship between PLK and Cdc25C phosphatase. PLK can phosphorylate and activate Cdc25 (Lee et al., 2005), suggesting that PLK may play some role in the G_2/M transition. If this were the case in *A. nidulans*, we would expect an even stronger block in interphase in *nimT/plkA* cells. The fact that we get the opposite suggests a potential different function for PLKA. The genetic interaction suggests that PLKA may function downstream of Cdc25 and negatively regulate MPF by an unknown mechanism. In previous work, cells overexpressing *plkA* did not enter mitosis at the same rate as the controls following release from a *nimA* or *nimT* induced block in G2 (Bachewich et al., 2005). In fact, the cells predominately remained in G_2 for sometime. These results are consistent with the hypothesis that PLKA has some regulatory influence on G_2/M. PLKA may also have a role in mitotic exit, suggested by the high mitotic index and significant number of telophase spindles in cells lacking PLKA. These cells were likely only delayed in mitotic exit, since the total number of nuclei in *ΔplkA* vs control cells was somewhat similar (Table 6). Thus, even though PLKA is not essential for nuclear division, it may have a role in negatively regulating entry into mitosis, which has not been described for any other PLK, and a positive role in mitotic exit.

Although nuclear division was not dramatically affected in the absence of PLKA, nuclear distribution defects were observed, where 27-38% of cells appeared to have nuclei clustered in one region of the hypha. This was somewhat similar to the "*nud*" mutants. The *nud* genes were initially discovered in *A. nidulans* and function in moving nuclei into the hyphae (Morris and Enos, 1992). NUDC associates with the cytoplasmic dynein/dynactin complex and has a role in nuclear movement in both fungi and higher

organisms, as well as a role in mitosis and cytokinesis (Morris, 2000). Intriguingly, Plk1 was shown to interact with NudC in mammals and depletion of NudC decreased microtubule attachment at the kinetochore and resulted in defects in chromosome congression (Nishino et al., 2006). The similarities between mammals and *A. nidulans* in their respective cell cycles suggest that PLKA might interact with NUDC, and improper activation of NUDC may in turn give rise to the nuclear distribution defects in *ΔplkA* cells. Overexpressing NUDC in *ΔplkA* cells, for example, could help resolve any relationship between the factors. Thus PLKA is not essential for mitosis but plays conserved as well as novel roles in the process.

4.6 PLKA may be important for septa positioning, but not septa formation

Since PLK are required for septation in all organisms studied (Lee et al., 2005), it was surprising that septa could form in the absence of PLKA. In young hyphae lacking PLKA, the first septa appeared in a normal location and with normal kinetics at the conidia/hypha junction. Although we do not know if the septa are complete, they do form, suggesting that PLKA does not play the central role in septa formation found with PLK in other fungi. However, results from the intercalary compartment lengths of older hyphae showed some defects in placement of septa. Compartments delimited by septa in subapical regions of hyphae are approximately 40 μm, and contain on average 4 nuclei (Kaminskyj and Hamer, 1997). The compartment lengths for the *ΔplkA* strains varied more drastically than those of the control strain, ranging from 0-63 μm, compared to 8-60 μm for the control. In addition, some compartments did not contain any visible nuclei.

This suggests that septation was deregulated and uncoupled from nuclear division. However, while compartment lengths of the *alcA::plkA* strains under repressing conditions were different from the wild-type strain, in agreement with the deletion strain results, they were similar to the isogenic control. This was surprising given the similarity between the isogenic control strain and the wild type strain with respect to growth rate and other parameters. Thus, we can only conclude that PLKA does not have a significant role in regulating septa formation, unlike PLK in yeast, but may contribute to the timing/placement of septation. It will be informative to look at the interaction between PLKA and septa-regulating factors, and utilize septa mutants to help resolve the nature of the relationship. The ability to form septa in the absence of PLKA has profound implications for the regulation of septation in this organism, and compared to others that require PLK to form septa.

4.7 PLKA is important for proper spindle formation

PLKA has a role in spindle formation, since cells lacking *plkA* had a significant number of abnormal spindles. This was highlighted when cells were synchronized using a *nimT* temperature-sensitive block. When released into permissive temperature to allow synchronous entry into mitosis, a higher proportion of cells with spindles were visualized, and the majority were abnormal, like those seen in cells overexpressing *plkA* (Bachewich et al., 2005) and in PLK mutations in other organisms (Xie et al., 2005). In a recent study, a temperature-sensitive *CDC5* mutant demonstrated similar abnormal spindle defects that we observed in the *plkA* deletion, such as the bent and "discontinuous" spindle (Park et al., 2008). The study reported that only 25% of cells exhibited these

defects, which is very close to our value of 30%. The low proportion may be due to stochastic events during mitosis. Thus, PLKA is important, but not essential, for proper spindle formation in *A. nidulans.*

4.8 PLKA is important for microtubule dynamics

The defects in hyphal polarity, nuclear distribution and spindle formation collectively suggest that PLKA has some role in regulating microtubule dynamics. In support of this, cells lacking PLKA were cold sensitive in that the compact growth phenotype was suppressed at higher temperature. When cells contain defects in microtubule function, cold sensitivity is often a result (Jung et al., 2001). Therefore, the cold sensitivity suggests that a different gene might compensate for PLKA function at higher temperatures. Nonetheless, PLKA still has a regulating function at the G2/M transition at higher temperature, as seen with the suppression of the *nimT* phenotype at restrictive temperature by the absence of PLKA

Consistent with PLKA's role in regulating microtubule dynamics, is that the compact growth phenotype was suppressed in the presence of low amounts of the anti-microtubule agent benomyl. However, at higher concentrations, the deletion strain was more sensitive than the control. Similar responses were found with two alleles of the γ-tubulin gene, *mip*AK284 and *mip*AR338, which were cold sensitive and suppressed with either benomyl or nocodazole (Jung et al., 2001). These mutants resembled the *ΔplkA* cells with respect to having abnormal spindles, including monopolar and frayed spindles (Jung et al., 2001). Since the Δ*plkA* and *mipA* mutant strains behaved similarly with respect to cold sensitivity and suppression by the addition of benomyl, the two genes might interact

with each other or lay in separate pathways leading to the microtubule nucleation process. Mutants of *CDC5*, the PLKA homologue in *S. cerevisiae*, also demonstrated suppression of the temperature-sensitive growth defect when plated on low concentrations of benomyl (Lee et al., 2005). Thus, PLKA may have a role in microtubule dynamics and in microtubule nucleation, as suggested for other PLK.

4.9 NIMT and BIME are not required for PLKA localization

Previous work has demonstrated that PLKA localizes to the spindle pole body, and that NIMA is not required for this localization (Bachewich et al., 2005). Two more cell cycle genes were chosen to determine whether they were required for PLKA localization to the spindle pole body, $NIMT^{Cdc25C}$ (required in G_2/M transition) and $BIME^{APC27}$ (required in the APC complex). These two cell cycle genes were chosen for their known interacting roles with PLK in other organisms. After tagging PLKA with GFP in *bimE* and *nimT* temperature-sensitive strains, and incubating at restrictive temperature, PLKA-GFP signal was localized to the nucleus in both strain backgrounds. Thus, NIMT and BIME are not required for PLKA localization to the nucleus.

4.10 PLKA plays a role in asexual and sexual development

In addition to expected roles in regulating the cell cycle, we found unexpected roles for PLKA in development. The compact colonies that were observed in cells lacking *plkA* had an unusual grey-white color that was not observed in the control or wild type strains, suggesting poor asexual development, since conidia pigment give rise to the

green color. Consistent with this, both conidia and the conidiaphore heads had abnormal morphologies, conidia varied in size, and the conidiaphore heads appeared to be missing structures. In addition, the frequency conidiophore heads was less than in the control strains and an abundance of aerial hyphae were detected in the *ΔplkA* strains. No other PLK's have been reported to have roles in activating developmental pathways. However, *A. nidulans* is the first filamentous fungi to have PLKA characterized, and thus a link between asexual development and PLK might be found in other filamentous fungi as well.

Although benomyl suppressed the compact growth phenotype of the *plkA* deletion, it did not suppress the conidiation defect, where the colony color remained grey-white. Since microtubules are important for vegetative growth and conidiation development, one might assume that these processes would be affected equally upon exposure to the anti-microtubule depolymerization agent benomyl. However, low concentrations of benomyl only suppressed the vegetative growth defect, and not conidiation, suggesting that microtubule dynamics are different during conidiation, rendering the process more sensitive to benomyl. Alternatively, PLKA might function during vegetative growth and asexual development using different benomyl-sensitive and insensitive mechanisms.

In addition to be required for asexual development, the results suggest that PLKA plays some role in negatively regulating sexual development. The emergence of sexual structures when *plkA* was absent in *A. nidulans* is novel, since no other organism has shown a relationship between PLKs and activation of the sexual development pathway. PLKs have been shown to function in initiation of meiosis in yeast and mammals at the level of regulating the meiotic spindle. For example, in *S. cerevisiae*, *CDC5* mutants

cause a delay in meiosis I, demonstrating that Cdc5p has a function in chiasmata resolution and co-orientation of sister kinetochores (Clyne et al., 2003). In *Drosophilia*, Mtrm (matrimony) is a regulator that binds to POLO and physically inactivates it. When Mtrm is destroyed, POLO is released and reactivates meiosis by phosphorylation of Cdc25 (G_2/M transition) (Xiang et al., 2007). In *Xenopus*, XErp1, a meiosis-specific gene, is an inhibitor of APC/C and subsequently meiosis; when Plx1 phosphorylates XErp1, the block on APC/C and meiosis is released (Schmidt et al., 2005). Neither Mtrm nor XErp1 have homologues to any genes in *A. nidulans*. We have shown that the absence of PLKA turns on sexual development, suggesting that *plkA* has a role in suppressing the pathway leading to sexual development. This is also supported by the *alcA::plkA* regulated strains under repressing conditions, especially in rich media. In minimal inducing media, sexual structures were seen in both the regulated and control strains, which was likely due to the threonine carbon source. In repressing media, more sexual structures were seen in the *alcA::plkA* strains. Little is known about Hülle cell development, and how PLKA may be influencing sexual development is not clear. Future studies will include producing double knockouts of *plkA* and important sexual suppressing genes such as *veA* and *rcoA*, and investigating the expression of sexual pathway genes in cells lacking PLKA. Overall, the results suggest that PLKA plays separate roles during growth and development.

4.11 Conclusion

In summary we have shown that PLKA, the first PLK to be characterized in a filamentous fungus, is not essential. Nevertheless, it has important functions throughout the cell cycle and in vegetative growth, including roles in spindle formation, chromosome segregation, mitotic exit and microtubule dynamics. As well, our work has also uncovered several novel functions of PLKA, such as the potential negative regulation of the G_2/M transition, control of hyphal morphogenesis, and regulation of asexual and development. These results set the stage for exciting future experiments, which will help identify the mechanisms of PLKA action during the cell cycle and define its novel and unexpected role in regulating morphogenesis and development.

5. References

Adams T.H., Wieser J.K., and Yu J.H. (1998) Asexual sporulation in *Aspergillus nidulans*. *Microbiol Mol Biol Rev* **62:** 35-54.

Al-Bassam J., van Breugel M., Harrison S.C., and Hyman A. (2006) Stu2p binds tubulin and undergoes an open-to-closed conformational change. *J Cell Biol* **172:** 1009-1022.

Alexandru G., Uhlmann F., Mechtler K., Poupart M.A., and Nasmyth K. (2001) Phosphorylation of the cohesin subunit Scc1 by Polo/Cdc5 kinase regulates sister chromatid separation in yeast. *Cell* **105:** 459-472.

Bachewich C., Masker K., and Osmani S. (2005) The polo-like kinase PLKA is required for initiation and progression through mitosis in the filamentous fungus aspergillus nidulans. *Mol Microbiol* **55:** 572-587.

Bachewich C., Thomas D.Y., and Whiteway M. (2003) Depletion of a polo-like kinase in *Candida albicans* activates cyclase-dependent hyphal-like growth. *Mol Biol Cell* **14:** 2163-2180.

Barrowman J., Sacher M., and Ferro-Novick S. (2000) TRAPP stably associates with the golgi and is required for vesicle docking. *EMBO J* **19:** 862-869.

Bergen L.G., and Morris N.R. (1983) Kinetics of the nuclear division cycle of *Aspergillus nidulans*. *J Bacteriol* **156:** 155-160.

Berman J., and Sudbery P.E. (2002) *Candida albicans*: A molecular revolution built on lessons from budding yeast. *Nat Rev Genet* **3:** 918-930.

Bettencourt-Dias M., Rodrigues-Martins A., Carpenter L., Riparbelli M., Lehmann L., Gatt M.K., *et al.* (2005) SAK/PLK4 is required for centriole duplication and flagella development. *Curr Biol* **15:** 2199-2207.

Bonifacino J.S., and Glick B.S. (2004) The mechanisms of vesicle budding and fusion. *Cell* **116:** 153-166.

Boylan M.T., Mirabito P.M., Willett C.E., Zimmerman C.R., and Timberlake W.E. (1987) Isolation and physical characterization of three essential conidiation genes from *Aspergillus nidulans*. *Mol Cell Biol* **7:** 3113-3118.

Budde P.P., Kumagai A., Dunphy W.G., and Heald R. (2001) Regulation of Op18 during spindle assembly in xenopus egg extracts. *J Cell Biol* **153:** 149-158.

Bussink H.J., and Osmani S.A. (1999) A mitogen-activated protein kinase (MPKA) is involved in polarized growth in the filamentous fungus, *Aspergillus nidulans. FEMS Microbiol Lett* **173:** 117-125.

Bussink H.J., and Osmani S.A. (1998) A cyclin-dependent kinase family member (PHOA) is required to link developmental fate to environmental conditions in *Aspergillus nidulans. EMBO J* **17:** 3990-4003.

Cai H., Zhang Y., Pypaert M., Walker L., and Ferro-Novick S. (2005) Mutants in trs120 disrupt traffic from the early endosome to the late golgi. *J Cell Biol* **171:** 823-833.

Care R.S., Trevethick J., Binley K.M., and Sudbery P.E. (1999) The MET3 promoter: A new tool for candida albicans molecular genetics. *Mol Microbiol* **34:** 792-798.

Casenghi M., Meraldi P., Weinhart U., Duncan P.I., Korner R., and Nigg E.A. (2003) Polo-like kinase 1 regulates nlp, a centrosome protein involved in microtubule nucleation. *Dev Cell* **5:** 113-125.

Casselton L., and Zolan M. (2002) The art and design of genetic screens: Filamentous fungi. *Nat Rev Genet* **3:** 683-697.

Chen D.C., Yang B.C., and Kuo T.T. (1992) One-step transformation of yeast in stationary phase. *Curr Genet* **21:** 83-84.

Cheng K.Y., Lowe E.D., Sinclair J., Nigg E.A., and Johnson L.N. (2003) The crystal structure of the human polo-like kinase-1 polo box domain and its phospho-peptide complex. *EMBO J* **22:** 5757-5768.

Cheng L., Hunke L., and Hardy C.F. (1998) Cell cycle regulation of the *Saccharomyces cerevisiae* polo-like kinase cdc5p. *Mol Cell Biol* **18:** 7360-7370.

Chow T.Y.K., and Kafer E. (1993) A rapid method for isolation of total nucleic acids from *Aspergillus nidulans. Fungal Genet Newsletter* **40:** 25.

Clement M., Fournier H., de Repentigny L., and Belhumeur P. (1998) Isolation and characterization of the *Candida albicans* SEC4 gene. *Yeast* **14:** 675-680.

Clyne R.K., Katis V.L., Jessop L., Benjamin K.R., Herskowitz I., Lichten M., and Nasmyth K. (2003) Polo-like kinase Cdc5 promotes chiasmata formation and cosegregation of sister centromeres at meiosis I. *Nat Cell Biol* **5:** 480-485.

Davies J.R., Osmani A.H., De Souza C.P., Bachewich C., and Osmani S.A. (2004) Potential link between the NIMA mitotic kinase and nuclear membrane fission during mitotic exit in *Aspergillus nidulans*. *Eukaryot Cell* **3:** 1433-1444.

De Souza C.P., Osmani A.H., Hashmi S.B., and Osmani S.A. (2004) Partial nuclear pore complex disassembly during closed mitosis in *Aspergillus nidulans*. *Curr Biol* **14:** 1973-1984.

Elia A.E., Rellos P., Haire L.F., Chao J.W., Ivins F.J., Hoepker K., *et al.* (2003) The molecular basis for phosphodependent substrate targeting and regulation of plks by the polo-box domain. *Cell* **115:** 83-95.

el-Maghrabi E.A., Dixon D.M., and Burnett J.W. (1990) Characterization of *Candida albicans* epidermolytic proteases and their role in yeast-cell adherence to keratinocytes. *Clin Exp Dermatol* **15:** 183-191.

Enke C., Zekert N., Veith D., Schaaf C., Konzack S., and Fischer R. (2007) *Aspergillus nidulans* Dis1/XMAP215 protein AlpA localizes to spindle pole bodies and microtubule plus ends and contributes to growth directionality. *Eukaryot Cell* **6:** 555-562.

Ernst J.F. (2000) Transcription factors in *Candida albicans* - environmental control of morphogenesis. *Microbiology* **146 (Pt 8):** 1763-1774.

Funabiki H., Kumada K., and Yanagida M. (1996) Fission yeast Cut1 and Cut2 are essential for sister chromatid separation, concentrate along the metaphase spindle and form large complexes. *EMBO J* **15:** 6617-6628.

Galagan J.E., Calvo S.E., Cuomo C., Ma L.J., Wortman J., Batzoglou S., *et al.* (2005) Sequencing of *Aspergillus nidulans* and comparative analysis with *A. fumigatus* and *A. oryzae*. *Nature* **438:** 1105.

Glover D.M., Hagan I.M., and Tavares A.A. (1998) Polo-like kinases: A team that plays throughout mitosis. *Genes Dev* **12:** 3777-3787.

Gola S., Martin R., Walther A., Dunkler A., and Wendland J. (2003) New modules for PCR-based gene targeting in *Candida albicans*: Rapid and efficient gene targeting using 100 bp of flanking homology region. *Yeast* **20:** 1339-1347.

Golsteyn R.M., Schultz S.J., Bartek J., Ziemiecki A., Ried T., and Nigg E.A. (1994) Cell cycle analysis and chromosomal localization of human Plk1, a putative homologue of the mitotic kinases drosophila polo and *Saccharomyces cerevisiae* Cdc5. *J Cell Sci* **107 (Pt 6):** 1509-1517.

Grallert A., and Hagan I.M. (2002) *Schizosaccharomyces pombe* NIMA-related kinase, Fin1, regulates spindle formation and an affinity of polo for the SPB. *EMBO J* **21:** 3096-3107.

Habedanck R., Stierhof Y.D., Wilkinson C.J., and Nigg E.A. (2005) The polo kinase Plk4 functions in centriole duplication. *Nat Cell Biol* **7:** 1140-1146.

Harris S.D. (2006) Cell polarity in filamentous fungi: Shaping the mold. *Int Rev Cytol* **251:** 41-77.

Harris S.D. (2001) Septum formation in *Aspergillus nidulans*. *Curr Opin Microbiol* **4:** 736-739.

Harris S.D., and Momany M. (2004) Polarity in filamentous fungi: Moving beyond the yeast paradigm. *Fungal Genet Biol* **41:** 391-400.

Hazan I., Sepulveda-Becerra M., and Liu H. (2002) Hyphal elongation is regulated independently of cell cycle in *Candida albicans*. *Mol Biol Cell* **13:** 134-145.

Hubbard M., and Kaminskyj S. (2007) Growth rate of *Aspergillus nidulans* hyphae is independent of a prominent array of microtubules. *Mycol Process* **6:** 179.

Hube B., Sanglard D., Odds F.C., Hess D., Monod M., Schafer W., *et al.* (1997) Disruption of each of the secreted aspartyl proteinase genes SAP1, SAP2, and SAP3 of candida albicans attenuates virulence. *Infect Immun* **65:** 3529-3538.

Ichinomiya M., Yamada E., Yamashita S., Ohta A., and Horiuchi H. (2005) Class I and class II chitin synthases are involved in septum formation in the filamentous fungus *Aspergillus nidulans*. *Eukaryot Cell* **4:** 1125-1136.

Inoue S., Turgeon B.G., Yoder O.C., and Aist J.R. (1998) Role of fungal dynein in hyphal growth, microtubule organization, spindle pole body motility and nuclear migration. *J Cell Sci* **111 (Pt 11):** 1555-1566.

James S.W., Bullock K.A., Gygax S.E., Kraynack B.A., Matura R.A., MacLeod J.A., *et al.* (1999) nimO, an *Aspergillus* gene related to budding yeast Dbf4, is required for DNA synthesis and mitotic checkpoint control. *J Cell Sci* **112 (Pt 9):** 1313-1324.

Johnson E.F., Stewart K.D., Woods K.W., Giranda V.L., and Luo Y. (2007) Pharmacological and functional comparison of the polo-like kinase family: Insight into inhibitor and substrate specificity. *Biochemistry* **46:** 9551-9563.

Jung M.K., Prigozhina N., Oakley C.E., Nogales E., and Oakley B.R. (2001) Alanine-scanning mutagenesis of aspergillus gamma-tubulin yields diverse and novel phenotypes. *Mol Biol Cell* **12:** 2119-2136.

Kaminskyj S.G. (2000) Septum position is marked at the tip of *Aspergillus nidulans* hyphae. *Fungal Genet Biol* **31:** 105-113.

Kaminskyj S.G., and Hamer J.E. (1998) Hyp loci control cell pattern formation in the vegetative mycelium of *Aspergillus nidulans*. *Genetics* **148:** 669-680.

Kim D.W., Sacher M., Scarpa A., Quinn A.M., and Ferro-Novick S. (1999) High-copy suppressor analysis reveals a physical interaction between Sec34p and Sec35p, a protein implicated in vesicle docking. *Mol Biol Cell* **10:** 3317-3329.

KIM J., and RAINES R.T. (1993) Ribonuclease S-peptide as a carrier in fusion proteins. *Protein Sci* **2:** 348-356.

Kim J.M., Lu L., Shao R., Chin J., and Liu B. (2006) Isolation of mutations that bypass the requirement of the septation initiation network for septum formation and conidiation in *Aspergillus nidulans*. *Genetics* **173:** 685-696.

Kitada K., Johnson A.L., Johnston L.H., and Sugino A. (1993) A multicopy suppressor gene of the *Saccharomyces cerevisiae* G1 cell cycle mutant gene dbf4 encodes a protein kinase and is identified as CDC5. *Mol Cell Biol* **13:** 4445-4457.

Kozak M. (1986) Point mutations define a sequence flanking the AUG initiator codon that modulates translation by eukaryotic ribosomes. *Cell* **44:** 283-292.

Krappmann S., Jung N., Medic B., Busch S., Prade R.A., and Braus G.H. (2006) The *Aspergillus nidulans* F-box protein GrrA links SCF activity to meiosis. *Mol Microbiol* **61:** 76-88.

Kubler E., Mosch H.U., Rupp S., and Lisanti M.P. (1997) Gpa2p, a G-protein alpha-subunit, regulates growth and pseudohyphal development in Saccharomyces cerevisiae via a cAMP-dependent mechanism. *J Biol Chem* **272:** 20321-20323.

Kumagai A., and Dunphy W.G. (1996) Purification and molecular cloning of Plx1, a Cdc25-regulatory kinase from xenopus egg extracts. *Science* **273:** 1377-1380.

Lane H.A., and Nigg E.A. (1996) Antibody microinjection reveals an essential role for human polo-like kinase 1 (Plk1) in the functional maturation of mitotic centrosomes. *J Cell Biol* **135:** 1701-1713.

Leberer E., Harcus D., Dignard D., Johnson L., Ushinsky S., Thomas D.Y., and Schroppel K. (2001) Ras links cellular morphogenesis to virulence by regulation of the MAP kinase and cAMP signalling pathways in the pathogenic fungus *Candida albicans*. *Mol Microbiol* **42:** 673-687.

Lee K.S., Park J.E., Asano S., and Park C.J. (2005) Yeast polo-like kinases: Functionally conserved multitask mitotic regulators. *Oncogene* **24:** 217-229.

Li J.J., and Li S.A. (2006) Mitotic kinases: The key to duplication, segregation, and cytokinesis errors, chromosomal instability, and oncogenesis. *Pharmacol Ther* **111:** 974-984.

Li S., Bao D., Yuen G., Harris S.D., and Calvo A.M. (2007) basA regulates cell wall organization and asexual/sexual sporulation ratio in *Aspergillus nidulans*. *Genetics* **176:** 243-253.

Lindon C., and Pines J. (2004) Ordered proteolysis in anaphase inactivates Plk1 to contribute to proper mitotic exit in human cells. *J Cell Biol* **164:** 233-241.

Lo W.S., and Dranginis A.M. (1996) FLO11, a yeast gene related to the STA genes, encodes a novel cell surface flocculin. *J Bacteriol* **178:** 7144-7151.

Mao Y., Kalb V.F., and Wong B. (1999) Overexpression of a dominant-negative allele of SEC4 inhibits growth and protein secretion in *Candida albicans*. *J Bacteriol* **181:** 7235-7242.

Miller E., Antonny B., Hamamoto S., and Schekman R. (2002) Cargo selection into COPII vesicles is driven by the Sec24p subunit. *EMBO J* **21:** 6105-6113.

Momany M. (2002) Polarity in filamentous fungi: Establishment, maintenance and new axes. *Curr Opin Microbiol* **5:** 580-585.

Momany M., and Hamer J.E. (1997) Relationship of actin, microtubules, and crosswall synthesis during septation in aspergillus nidulans. *Cell Motil Cytoskeleton* **38:** 373-384.

Morris N.R. (2000) Nuclear migration. from fungi to the mammalian brain. *J Cell Biol* **148:** 1097-1101.

Morris N.R. (1975) Mitotic mutants of aspergillus nidulans. *Genet Res* **26:** 237-254.

Morris N.R., and Enos A.P. (1992) Mitotic gold in a mold: *Aspergillus* genetics and the biology of mitosis. *Trends Genet* **8:** 32-37.

Mulvihill D.P., Petersen J., Ohkura H., Glover D.M., and Hagan I.M. (1999) Plo1 kinase recruitment to the spindle pole body and its role in cell division in *Schizosaccharomyces pombe*. *Mol Biol Cell* **10:** 2771-2785.

Murray, A and Hunt, T. (1993) The cell cycle an introduction. New York: Oxford University Press.

Nayak T., Szewczyk E., Oakley C.E., Osmani A., Ukil L., Murray S.L., *et al.* (2006) A versatile and efficient gene-targeting system for *Aspergillus nidulans*. *Genetics* **172:** 1557-1566.

Neef R., Preisinger C., Sutcliffe J., Kopajtich R., Nigg E.A., Mayer T.U., and Barr F.A. (2003) Phosphorylation of mitotic kinesin-like protein 2 by polo-like kinase 1 is required for cytokinesis. *J Cell Biol* **162:** 863-875.

Nigg E.A. (1998) Polo-like kinases: Positive regulators of cell division from start to finish. *Curr Opin Cell Biol* **10:** 776-783.

Nishino M., Kurasawa Y., Evans R., Lin S.H., Brinkley B.R., and Yu-Lee L.Y. (2006) NudC is required for Plk1 targeting to the kinetochore and chromosome congression. *Curr Biol* **16:** 1414-1421.

Noble S.M., and Johnson A.D. (2005) Strains and strategies for large-scale gene deletion studies of the diploid human fungal pathogen *Candida albicans*. *Eukaryot Cell* **4:** 298-309.

Oakley B.R., and Osmani S.A. (1993) Cell-cycle analysis using the filamentous fungus *Aspergillus nidulans*. In The Cell Cycle: A Practical Approach. Fantes, P., and Brooks, R. (eds). New York: IRL Press, pp. 127-142.

Ohkura H., Hagan I.M., and Glover D.M. (1995) The conserved *Schizosaccharomyces pombe* kinase plo1, required to form a bipolar spindle, the actin ring, and septum, can drive septum formation in G1 and G2 cells. *Genes Dev* **9:** 1059-1073.

OSHEROV N., and MAY G.S. (1998) Optimization of protein extraction from *Aspergillus nidulans* for gel electrophoresis. *Fungal Genet Newslett* **45:** 38.

Osmani S.A., and Mirabito P.M. (2004) The early impact of genetics on our understanding of cell cycle regulation in *Aspergillus nidulans*. *Fungal Genet Biol* **41:** 401-410.

Osmani S.A., May G.S., and Morris N.R. (1987) Regulation of the mRNA levels of nimA, a gene required for the G2-M transition in *Aspergillus nidulans*. *J Cell Biol* **104:** 1495-1504.

Park C.J., Song S., Lee P.R., Shou W., Deshaies R.J., and Lee K.S. (2003) Loss of CDC5 function in *Saccharomyces cerevisiae* leads to defects in Swe1p regulation and Bfa1p/Bub2p-independent cytokinesis. *Genetics* **163:** 21-33.

Park C.J., Park J.E., Karpova T.S., Soung N.K., Yu L.R., Song S., *et al.* (2008) Requirement of the budding yeast polo kinase Cdc5 in proper microtubule growth and dynamics. *Eukaryot Cell* .

Park J.E., Park C.J., Sakchaisri K., Karpova T., Asano S., McNally J., *et al.* (2004) Novel functional dissection of the localization-specific roles of budding yeast polo kinase Cdc5p. *Mol Cell Biol* **24:** 9873-9886.

Park Y.N., and Morschhauser J. (2005) Tetracycline-inducible gene expression and gene deletion in *Candida albicans*. *Eukaryot Cell* **4:** 1328-1342.

Phillips A.J., Crowe J.D., and Ramsdale M. (2006) Ras pathway signaling accelerates programmed cell death in the pathogenic fungus *Candida albicans*. *Proc Natl Acad Sci U S A* **103:** 726-731.

PONTECORVO G., ROPER J.A., HEMMONS L.M., MACDONALD K.D., and BUFTON A.W. (1953) The genetics of *Aspergillus nidulans*. *Adv Genet* **5:** 141-238.

Rasband W.S. Image J, U.S. National Institutes of Health, Bethesda, Maryland, USA, http://rsb.info.nih.gov/ij/,1997-2007.

Reagan-Shaw S., and Ahmad N. (2005) Silencing of polo-like kinase (plk) 1 via siRNA causes induction of apoptosis and impairment of mitosis machinery in human prostate cancer cells: Implications for the treatment of prostate cancer. *FASEB J* **19:** 611-613.

Reynolds N., and Ohkura H. (2003) Polo boxes form a single functional domain that mediates interactions with multiple proteins in fission yeast polo kinase. *J Cell Sci* **116:** 1377-1387.

Romero B., Turner G., Olivas I., Laborda F., and De Lucas J.R. (2003) The *Aspergillus nidulans* alcA promoter drives tightly regulated conditional gene expression in *Aspergillus fumigatus* permitting validation of essential genes in this human pathogen. *Fungal Genet Biol* **40:** 103-114.

Rose F., and Winston F.a.H.,P. (1990) Yeast smash and grab gDNA extraction. Yeast smash and grab gDNA extraction. Cold Spring Harbor, New York: Cold Spring harbor Laboratory Press, pp. 10-11.

Sacher M., Barrowman J., Wang W., Horecka J., Zhang Y., Pypaert M., and Ferro-Novick S. (2001) TRAPP I implicated in the specificity of tethering in ER-to-golgi transport. *Mol Cell* **7:** 433-442.

Sacher M., Jiang Y., Barrowman J., Scarpa A., Burston J., Zhang L., *et al.* (1998) TRAPP, a highly conserved novel complex on the cis-golgi that mediates vesicle docking and fusion. *EMBO J* **17:** 2494-2503.

Schmidt A., Duncan P.I., Rauh N.R., Sauer G., Fry A.M., Nigg E.A., and Mayer T.U. (2005) Xenopus polo-like kinase Plx1 regulates XErp1, a novel inhibitor of APC/C activity. *Genes Dev* **19:** 502-513.

Sherr C.J., and Roberts J.M. (2004) Living with or without cyclins and cyclin-dependent kinases. *Genes Dev* **18:** 2699-2711.

Shi X., Sha Y., and Kaminskyj S. (2004) *Aspergillus nidulans* hypA regulates morphogenesis through the secretion pathway. *Fungal Genet Biol* **41:** 75-88.

Smits V.A., Klompmaker R., Arnaud L., Rijksen G., Nigg E.A., and Medema R.H. (2000) Polo-like kinase-1 is a target of the DNA damage checkpoint. *Nat Cell Biol* **2:** 672-676.

Snead J.L., Sullivan M., Lowery D.M., Cohen M.S., Zhang C., Randle D.H., *et al.* (2007) A coupled chemical-genetic and bioinformatic approach to polo-like kinase pathway exploration. *Chem Biol* **14:** 1261-1272.

Song S., Grenfell T.Z., Garfield S., Erikson R.L., and Lee K.S. (2000) Essential function of the polo box of Cdc5 in subcellular localization and induction of cytokinetic structures. *Mol Cell Biol* **20:** 286-298.

Sonneborn A., Bockmuhl D.P., and Ernst J.F. (1999) Chlamydospore formation in *Candida albicans* requires the Efg1p morphogenetic regulator. *Infect Immun* **67:** 5514-5517.

Staab J.F., and Sundstrom P. (2003) URA3 as a selectable marker for disruption and virulence assessment of *Candida albicans* genes. *Trends Microbiol* **11:** 69-73.

Strebhardt K., and Ullrich A. (2006) Targeting polo-like kinase 1 for cancer therapy. *Nat Rev Cancer* **6:** 321-330.

Sunkel C.E., and Glover D.M. (1988) Polo, a mitotic mutant of drosophila displaying abnormal spindle poles. *J Cell Sci* **89 (Pt 1):** 25-38.

Toyoshima-Morimoto F., Taniguchi E., Shinya N., Iwamatsu A., and Nishida E. (2001) Polo-like kinase 1 phosphorylates cyclin B1 and targets it to the nucleus during prophase. *Nature* **410:** 215-220.

Ushinsky S.C., Harcus D., Ash J., Dignard D., Marcil A., Morchhauser J., *et al.* (2002) CDC42 is required for polarized growth in human pathogen candida albicans. *Eukaryot Cell* **1:** 95-104.

van Vugt M.A., Smits V.A., Klompmaker R., and Medema R.H. (2001) Inhibition of polo-like kinase-1 by DNA damage occurs in an ATM- or ATR-dependent fashion. *J Biol Chem* **276:** 41656-41660.

van Vugt M.A., van de Weerdt B.C., Vader G., Janssen H., Calafat J., Klompmaker R., *et al.* (2004) Polo-like kinase-1 is required for bipolar spindle formation but is dispensable for anaphase promoting complex/Cdc20 activation and initiation of cytokinesis. *J Biol Chem* **279:** 36841-36854.

Walker G.M., and White N.A. (2005) Introduction to fungal physiology. In Fungi. Kavanagh, K. (ed). England: Wiley, .

Wang I.C., Chen Y.J., Hughes D., Petrovic V., Major M.L., Park H.J., *et al.* (2005) Forkhead box M1 regulates the transcriptional network of genes essential for mitotic progression and genes encoding the SCF (Skp2-Cks1) ubiquitin ligase. *Mol Cell Biol* **25:** 10875-10894.

Wang Q., Xie S., Chen J., Fukasawa K., Naik U., Traganos F., *et al.* (2002) Cell cycle arrest and apoptosis induced by human polo-like kinase 3 is mediated through perturbation of microtubule integrity. *Mol Cell Biol* **22:** 3450-3459.

Waring R.B., May G.S., and Morris N.R. (1989) Characterization of an inducible expression system in *Aspergillus nidulans* using alcA and tubulin-coding genes. *Gene* **79:** 119-130.

Weber Y., Santore U.J., Ernst J.F., and Swoboda R.K. (2001) Divergence of eukaryotic secretory components: The *Candida albicans* homolog of the *Saccharomyces cerevisiae* ++Sec20 protein is N terminally truncated, and its levels determine antifungal drug resistance and growth. *J Bacteriol* **183:** 46-54.

Wolkow T.D., Harris S.D., and Hamer J.E. (1996) Cytokinesis in *Aspergillus nidulans* is controlled by cell size, nuclear positioning and mitosis. *J Cell Sci* **109 (Pt 8):** 2179-2188.

Xiang Y., Takeo S., Florens L., Hughes S.E., Huo L.J., Gilliland W.D., *et al.* (2007) The inhibition of polo kinase by matrimony maintains G2 arrest in the meiotic cell cycle. *PLoS Biol* **5:** e323.

Xie S., Xie B., Lee M.Y., and Dai W. (2005) Regulation of cell cycle checkpoints by polo-like kinases. *Oncogene* **24:** 277-286.

Yang L., Ukil L., Osmani A., Nahm F., Davies J., De Souza C.P., *et al.* (2004) Rapid production of gene replacement constructs and generation of a green fluorescent protein-tagged centromeric marker in *Aspergillus nidulans*. *Eukaryot Cell* **3:** 1359-1362.

Yarm F.R. (2002) Plk phosphorylation regulates the microtubule-stabilizing protein TCTP. *Mol Cell Biol* **22:** 6209-6221.

Yuan J.H., Feng Y., Fisher R.H., Maloid S., Longo D.L., and Ferris D.K. (2004) Polo-like kinase 1 inactivation following mitotic DNA damaging treatments is independent of ataxia telangiectasia mutated kinase. *Mol Cancer Res* **2:** 417-426.

Zachariae W., and Nasmyth K. (1999) Whose end is destruction: Cell division and the anaphase-promoting complex. *Genes Dev* **13:** 2039-2058.

Appendix 1

Determination of PLKA interactive partners

In order to identify interacting factors, *plkA* was tagged with the S-tag using the same two-step PCR method previously described, with the exception that the STAG sequence was amplified instead of the GFP sequence (Appendix Figure 1). After fusion PCR, the 7kb product was transformed into the ASH262 strain. Four transformants were selected and streaked to single colony, screened by PCR and confirmed by Southern. Strains KM8 and KM9 only had the 4.7kb band, whereas the wild type had the 2.8kb (Appendix Figure 1). Therefore, after confirmation that the S-tag is being expressed, affinity purification followed by mass spectrometry will be utilized to determine the interactive partners of this novel PLK.

A.

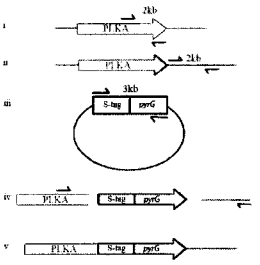

B.

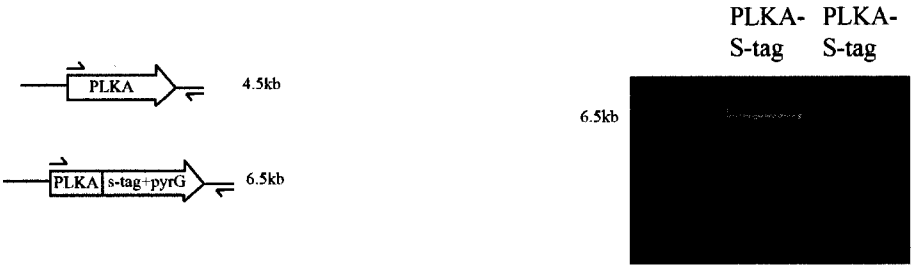

C.

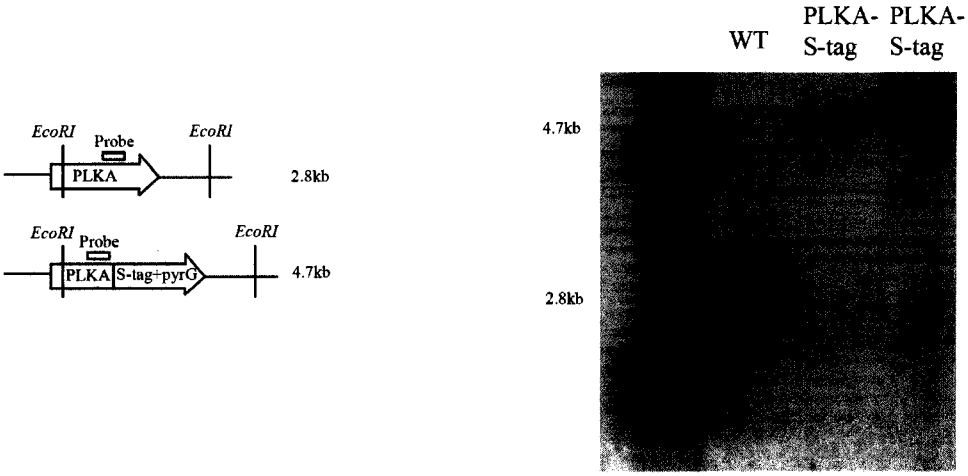

Appendix Figure 1: Tagging PLKA with S-tag in strain ASH262
(A) Strategy to construct a PLKA-S-tag strain. (i) a 2kb fragment was PCR amplified upstream of the stop site. (ii) a 2kb fragment including and downstream of the stop site. (iii) a 3kb fragment PCR amplified the GFP tag and *pyrG* marker from plasmid pAO81. (iv-v) three fragments were used as a template in a fusion PCR reaction to create a 7kb final product that was transformed into ASH262 strain. (B) PCR screening demonstrating that strains KM8 and KM9 are positive (6.5kb). (C) Southern analysis confirming that strains KM8 and KM9.are positive (4.7kb).

Appendix 2

Abstract

The Role of *TRS120* in the Cell Cycle in *Candida albicans*

Klarita Mogilevsky

The TRAPP complexes regulate membrane traffic in the cell, where they help to control transport to and from the Golgi network. *TRS120* is a subunit of the TRAPPII complex, and mutations in this essential factor in *Saccharomyces cerevisiae* lead to the accumulation of abnormal membrane structures, and prevent normal vesicle trafficking from endosomes to late Golgi. In the filamentous fungus *Aspergillus nidulans*, the *TRS120* homologue HYPA is also required for endomembrane organization and proper secretion, but HYPA is not essential, and mutations also drastically influence hyphal morphogenesis. At restrictive temperature, the apical hyphal cells of the *hypA1* strain stopped growing and died, but the previously quiescent, subapical hyphal compartments resumed growth in an abnormal, depolarized manner, which was also accompanied by uncontrolled nuclear division. We have investigated the role of the Trs120p/HYPA homologue in growth and morphogenesis of *C. albicans.* TRS120 in *C. albicans* is 25% identical to Trs120p in *S. cerevisiae*, and 24% to HYPA in *A. nidulans.* To determine the phenotype of cells lacking *TRS120*, a strain containing a single copy of *TRS120* under control of the *MET3* promoter was constructed. When the strain was placed on solid inducing medium, yeast growth continued and colonies appeared normal in morphology. In contrast, growth was inhibited when cells were plated on solid repressing medium that contained methionine and cysteine, suggesting that *TRS120* is essential. In liquid

inducing medium, yeast cells demonstrated a near normal doubling rate, and cell morphology was normal, although a small proportion of cells were enlarged. In liquid repressing medium, growth was inhibited by 5-6 h, and cell morphology increasingly became abnormal. The arrested cells were highly enlarged, consistent with isometric expansion, while others were various abnormal shapes and often lacked clear buds. Nuclear division was also abnormal and uncoupled from septation and cell division. Thus, Trs120p is essential for growth, proper morphogenesis and associated nuclear division in yeast cells of *C. albicans*. In exploring the role of Trs120p during the hyphal growth stage of *C. albicans*, the *MET3p*-regulated strain was found to be sensitive to the higher temperature of 37°C, even when *TRS120* was expressed. Cells stopped growing and demonstrated isotropic expansion, similar to when the strain was incubated under repressing conditions at 30°C. The temperature sensitivity was partially suppressed by the addition of 1M sorbitol. However, sorbitol did not suppress the growth defect associated with shutting off *TRS120* at 30°C. The results suggest that the levels of *TRS120* expression that are sufficient for growth at 30°C are not sufficient for growth at 37°C, and that Trs120p may be critical for proper secretion and cell wall structure under normal and stress-inducing conditions, including higher temperature.

Introduction

Candida albicans is an opportunistic fungal pathogen that is found in the human gastrointestinal and genitourinary tracts (Berman and Sudbery, 2002). *C. albicans* is harmless in healthy individuals, but it can cause death if a person becomes immunocompromised. A common infection found in HIV pathients is Candidiasis (Berman and Sudbery, 2002), where *C. albicans* has multiplied exponentially to cause symptoms and local infections in the mouth and vagina. A more deadly infection is Candidaemia, where the organism invades the blood stream and causes fungal growth masses in the kidney, heart or brain (Berman and Sudbery, 2002). *C. albicans* can grow in three different forms which are yeast, pseudohyphae and true hyphal cells. Yeast cells are round and grow by budding, while pseudohyphal cells are more elongated yeast cells that remain attached while continuing to grow. True hyphal cells are long and polarized, and elongate at the apical tips (Berman and Sudbery, 2002). All three forms contain a single nucleus prior to mitosis. The main differences between the three forms are the position of the septa, the movement of the nucleus and the degree of separation of the daughter cell (Berman and Sudbery, 2002).

Secretion is an important virulence-determining trait, since many of the virulence factors produced in response to changes in the environment are secretory proteins. For example, the secreted aspartyl proteinases (SAP) play a role in the adhesion of the organism to the human mucosal or epidermal cells (El-Maghrabi et al., 1990). There are nine members in the *SAP* family, which are activated by various environmental

conditions, and contribute to virulence by playing different roles during the infection process. For example, *SAP1* and *SAP3* are regulated during the switch between yeast and hyphae, whereas *SAP2* is regulated during the yeast form. *SAP4* to *SAP6* are expressed during the phenotypic switch at neutral pH (Hube et al., 1997). When the *SAP1*, *SAP2* and *SAP3* genes were deleted independently, the null mutants were less virulent (Hube et al., 1997). Thus, the process of secretion is critical not only for cell growth, but also virulence in *C. albicans*.

Pathogenesis of *C. albicans* also requires the ability of the organism to switch between different cell types. Therefore there exists a link between the morphological form and the virulence of *C. albicans*. There are numerous signally pathways that play a role in the switching between hyphal and yeast forms. For example, the mitogen-activated protein (MAP) kinase cascade pathway has been shown to be involved in the morphological switching between the yeast and hyphal form (Leberer et al., 2001). This pathway is well conserved and is found in most organisms from yeast to mammals. It is required for example, in responding to stress and changes in osmolarity. In *S. cerevisiae*, it is involved in the morphological change from yeast to pseudohyphal growth (Kübler et al., 1997). In *C. albicans*, environmental factors stimulate the passage through the cascade and interactions with the transcription factor Efg1p causes the transition from yeast to hyphal form (Leberer et al., 2001). A second pathway involved in the morphological switch is the cAMP pathway. Both pathways are activated by an upstream regulator, CaRAS1p. This GTP-binding protein is not required for vegetative growth, yet is essential for hyphae formation (Leberer et al., 2001). Recent work in *C. albicans* has demonstrated that blocking the Ras-cAMP pathway *(ras1Δ)* causes a delay in apoptosis,

while mutations in RAS that stimulate the pathway (*RAS1*^{val13}) cause acceleration into apoptosis (Phillips et al., 2006). Therefore RAS might have a direct role in turning on apoptosis.

The signaling pathways are stimulated by many environmental factors, including temperature, pH and carbon source. For example, at 30°C the organism is mostly in a yeast form, whereas at the higher temperature of 37°C, the hyphal form is more prevalent. Other factors such as oxidative stress or the medium source will trigger different genes, including virulence factors, to be transcribed and expressed. However, it is not clear exactly how pathways converge to produce cell switching and expression of virulence factors.

Secretion is a fundamental cellular process that shuttles proteins from the ER to the Golgi and finally out of the cell (Bonifacino and Glick, 2004). The pathway is well conserved from yeast to humans, containing many of the same orthologs. The current hypothesis for the secretory pathway is that as the proteins are made, they are moved by "vesicle budding", where the protein surrounded by a membrane buds from the ER. The enclosed protein is transported to its destination, where the vesicle fuses with the target membrane and liberates the cargo (Bonifacino and Glick, 2004).

As proteins are translated from mRNA, an export signal is added to the cytosolic domain of the proteins (Bonifacino and Glick, 2004). There are various export signals and each helps to determine the final destination of the proteins. The signal can be of various lengths, some are di-actic motifs, whereas others are short hydrophobic motifs, such as FF, YYM, FY, LL or IL (Bonifacio and Glick, 2004). COPII, a non-clathrin coat that encloses the desired protein, is responsible for both the recognition of these export

signals and the sorting of proteins to the correct destination COPII is composed of various secretory proteins, including Sec24p, which is in charge of binding to the export signal (Miller et al., 2002).

An important complex in the eukaryotic secretory pathway is the transport protein particle (TRAPP) complex. It is involved in trafficking proteins from the ER to the Golgi equivalent (Sacher et al., 2001). The TRAPP complex is composed of two forms, TRAPP I and TRAPP II. TRAPPI is composed of seven subunits, including: Bet5p, Bet3p, Trs20p, Trs31p, Trs33p and Trs85p. TRAPPII has three additional subunits: Trs120p, Trs130p and Trs65p. TRAPP I functions as the receptor on the Golgi for the ER derived, COPII vesicle. Once the COPII binds to the complex, Yptp, a Ras-like small GTPase, is activated by the conversion of the GDP form to the GTP form (Sacher et al., 2001). Once Ypt1p is activated, other tethering factors are recruited. TRAPP II has a later function in the Golgi transport pathway. The exact role is unknown, yet preliminary results have shown that *trs130* mutants accumulate carboxypeptidase Y and invertase in the Golgi (Sacher et al., 2001). Since both of these proteins are made in the ER, yet final processing occurs in the Golgi, this indicates that Trs130p might have a role after the transport to the Golgi.

Trs120p is a subunit of the TRAPP II complex. The gene is essential in the model yeast *S. cerevisiae*, and *trs120* mutants were found to have an accumulated amount of irregular membranes structures called Berkeley bodies (Cai et al., 2005). A *TRS120* homologue, HYPA, has also been investigated in the filamentous fungus *A. nidulans*. Unlike that seen in *S. cerevisiae*, HYPA is not essential and is required for hyphal morphogenesis. In normal cells, conidia germinate to give rise to polar growing hyphae.

The subapical compartments, created through septation, become dormant, while the apical section of the hyphae grows and is mitotically active (Kaminskyj et al., 2000). Branching from the subapical compartments stimulates growth and resumes the cell cycle in these compartments. In *hypA* mutants, conidia inoculated at restrictive temperature form abnormal cells, which were multinucleated, multi-septated, and aberrant in shape. When established hyphae were switched to restrictive temperature, the apical cell would die and the subapical compartment would restart nuclear division and growth (Shi et al., 2004). As well, a loss of size control was found to occur in the mutant, since conidia appeared larger than normal and some were also anucleated (Shi et al., 2004).

The secretory pathway is not well understood in *C. albicans*. Some homologues of the defined pathway in *S. cerevisiae* have been found in *C. albicans*. For example, *SEC18*, *SEC14* and *SEC4* are genes that are required in the various stages of transport from the ER to the plasma membrane (Bonifacino and Glick, 2004). Other genes in the pathway have not yet been characterized, such as *SEC26*, *SEC13,* and many of the genes involved in the TRAPP complex. Since secretion is critical for growth, morphogenesis and virulence in *C. albicans*, but the regulation of this process is not well understood in the pathogen, we wanted to investigate the role of the TRAPP complex, with a focus on the *TRS120* homologue, in *C. albicans.* Since *C. albicans* is dimorphic, these studies would allow us to investigate the functions of Trs120p in both yeast and hyphal cells for comparison with studies in *S. cerevisiae* and *A. nidulans*.

Materials and Methods

Strains, oligos, plasmid and media

Strains and plasmids are listed in Appendix 2 Table 1 and Table 2 respectively. Oligos are listed in Appendix 2 Table 3. Cells were grown in either YPD containing 1% yeast extract, 2% peptone and 2% glucose or SD media containing 0.67% yeast nitrogen base without amino acids, 2% glucose and 0.15% of amino acid drop-out mixture. Expression from the *MET3* promoter was regulated with SD media containing 2.5mM methione and 0.5mM cysteine (repressing; +MC) or lacking methione and cysteine (inducing; -MC) (Care et al., 1999). 1M sorbitol was added to SD media to test cell wall viability. 2% agar was used for solid media.

DNA manipulation

In order to create a strain carrying one copy of *TRS120* under control of the *MET3* promoter, one copy of *TRS120* was replaced using a deletion construct prepared by amplifying the *URA3* marker in plasmid pBS-cURA3 (Gola et al., 2003) with oligos CBSK1F and CBSK1RB, which contain 80bp homology to the 5' and 3' flanks of *TRS120*, respectively, and 20bp homology to pBS-cURA3. The running conditions for the PCR reaction consisted of: 1 cycle of 94°C for 4 min, 25 cycles of 94°C for 1 min, 46°C for 1 min, and 68°C for 3 min, and 1 cycle of 68°C for 7 min. 30μM oligos, 20mM of dNTP's, and 40ng of plasmid was used in the reaction. Expand Long Template Polymerase with Buffer 3 (Roche) was used for the reaction. The second copy of the gene was placed under the control of the *MET3* promoter. This replacement construct was prepared by PCR amplifying the *MET3p* and *HIS1* marker from plasmid pFA-HIS1-

MET3p (Gola et., 2003) with oligos CB114F and CB114R, which contain 80bp of homology to sequences immediately up and down stream from the start codon and 20bp homology to pFA-HIS1-Met3p. The running conditions for the PCR reaction consisted of: 1 cycle of 94°C for 4 min, 25 cycles of 94°C for 1 min, 41°C for 1 min, and 68°C for 3 min, and 1 cycle of 68°C for 7 min. 30μM oligos, 20mM of dNTP's, and 40ng of plasmid was used in the reaction. Expand Long Template Polymerase with Buffer 3 (Roche) was used for the reaction.

Transformation

Strains were transformed according to Chen et al., (1992). Briefly, wild type BWP17 cells were inoculated overnight in YPD, whereas the second round heterozygote for *TRS120* cells were inoculated in SD (-HIS) media, such that the next day the cells were in late stationary phase. 200μl of cells were placed into a one step buffer (15mg/ml DTT, 2.5% ssDNA, 0.2M LiAC and 40% PEG) and vortexed with the transforming DNA. The Eppendorf tube was then placed at 30°C overnight. The following day, the cells were given a heat shock at 43°C for 15min, plated on selective media, and allowed to grow for three days at 30°C.

Screening and Southern analysis

Once transformants were streaked to single colony three times, cells were incubated in zymolase solution (2.5mg/ml, 1.2M sorbitol and 0.1M $NaPO_4$) for 1 hour at 37°C. These cells were subsequently used in the PCR screen for proper integration. Oligos KM1F and KM1R, which are located outside the ORF, were used to PCR screen the

strains for correct integration. This was done twice, once for the deletion of the first copy, and a second time for the *MET3* promoter replacement. The running conditions for the PCR screening reaction consisted of: 1 cycle of 94°C for 3 min, 30 cycles of 94°C for 30 sec, 42°C for 30 sec, and 68°C for 4 min, and 1 cycle of 68°C for 7 min. 75μM oligos, 10mM of dNTP's, and 2μl of zymolased cells was used in the reaction. Expand Long Template Polymerase with Buffer 1 (Roche) was used for the reaction.

Southern analysis was performed on four positive and two negative transformants using the DIG Hybridization System (Roche Diagnostics, Mannheim, Germany). Briefly, cells were inoculated overnight in SD media, so that the next day they were in late stationary phase. Cells were then collected and genomic DNA was extracted using the method of Rose et al., 1990. 4μg of DNA was cut with 35U of *SphI* overnight. The following day, 4μl of 5M NaCl and 400μl of 95% EtOH was added to the gDNA, which was precipitated overnight at -20°C. The following day, the gDNA was centrifuged at 4°C for 10min, washed with 70% EtOH, then air dried. DNA was dissolved in 20μl of TE and run overnight on a 0.7% agarose gel at 25V. The following day, the gel was denatured, neutralized and then allowed to transfer for a minimum of 5 hours onto a positive charged nylon membrane (Roche). Probe construction and hybridization were performed according to the DIG Hybridization System (Roche Diagnostics, Mannheim, Germany). Oligos KM8F and KM8RR were used to amplify a product homologous to a sequence downstream of the stop codon and used as the probe. For probe construction, 500ng of PCR product was boiled for 5min, placed on ice for 5min and mixed with 10μl of 10X hexanucleotide mix, 10μl of 10X dNTP labeling reaction and 5μl of Klenow polymerase enzyme (Roche). The microcentrifuge tube was gently mixed and incubated

at 37°C overnight. The next day, 4µl of 0.5M EDTA, 1µl of 20mg/ml glycogen (Roche), 7.62µl of 5M LiCl and 300µl of cold 95% EtOH were added, and the contents were incubated overnight at -20°C. The following day, the tube was centrifuged at 14,000 x g for 10min (4°C), and the supernatant was removed. The pellet was washed with cold 70% EtOH and centrifuged at 14,000 x g for 5min (4°C). The pellet was allowed to air dry for 15 min, and then dissolved in 50µl of TE buffer. To quantify the probe, 1µl of probe DNA was diluted in 10µl of solution I (0.1M Maleic acid, 0.15M NaCl, 0.175M NaOH and additional NaOH up to pH 7.5), and serial diluted 1/10, 1/100, 1/1000, 1/10 000 and 1/100 000 times in 50µl of solution I. A control probe of known concentration (5ng/ml) was diluted to the same concentrations. 1µl of each sample was spotted on a positive charged membrane (Roche). The membrane was UV-cross linked in a UV linker (Stratagene) and then washed with solution I for 1 min. The membrane was then incubated in 50ml of solution II (1% blocking agent (Roche) diluted in solution I) for 30 min and then washed briefly with solution I. After 30 min incubation with 1:5000 dilution of anti-DIG antibody conjugated with alkaline phosphatase (Roche) in solution I, the membrane was washed twice for 15 min in solution I. The membrane was then equilibrated for 2 min in 20 ml of solution III (0.1M NaCl and 0.1M Tris-HCl pH9.5), and incubated in a dark container with 40µl of NBT/BCIP (Roche) and 2ml of solution III for up to 20 min. When the desired intensity of coloration was achieved, the membrane was washed with 5ml of solution IV (0.01M Tris-HCl pH8.0 and 0.001M EDTA) for 5 min to stop the reaction. Since the control concentration was known, the probe concentration could be estimated. The probe was estimated to be 50ng/µl and 50ng was used for the Southern.

Phenotypic analysis, Cell Staining and Microscopy

To determine the effects of Trs120p depletion, cells were incubated overnight at 30°C to mid-exponential phase in SD inducing media. An aliquot was diluted to an $O.D._{600nm}$ of 0.15 in either inducing (-MC) or repressing (+MC) media. Samples were read at $O.D._{600nm}$ every two hours up to 10 hours and then a final reading at 24 hours. These readings were used to create the growth curves.

To examine the nuclei and septa pattern in Trs120p depleted cells, cells were grown in a similar manner as previously described, except they were collected at 8 hours and 24 hours only. Cells were then spun down, transferred to an Eppendorff tube, fixed with 70% ethanol and incubated overnight at 4°C. The following day, cells were spun down, rinsed with ddH_2O, and stained with 1μg/ml DAPI (4',6'-Diamidino-2-phenylindole, Sigma) for 20min. Cells were subsequently spun down, rinsed with ddH_2O, and stained 1μg/ml Calcofluor (Sigma) for 10min. After a final spin and rinse with ddH_2O, cells were placed on a microscope slide, covered with a coverslip and sealed with nail polish. Cells were then examined under a Carl Zeiss microscope (Carl Zeiss, Axioplan) using a 100X immersion oil EC Plan-Neofluar objective.

To observe microtubules, immunolocalization of α-tubulin was performed (Bachewich et al., 2003). Cells were incubated overnight at 30°C and grown in a similar manner as previously described. Samples were collected at 8 hours and 24 hours. Cells were spun down, transferred to an Eppendorff tube and then fixed with 8% fixative for 20 min. Fix consisted of 8% paraformaldehyde, 50mM PIPES pH6.8, 50mM EGTA, 10mM $MgSO_4$, 10μg/ml of leupeptin (MP Bio), 3μg/ml of aproptinin (MP Bio) and 200μM

AEBSF (4-(2-aminoethyl) benzenesulfonyl fluoride, MP Bio). To dissolve paraformaldehyde in ddH_2O, the addition of 10µl of NaOH was required, prior to the addition of the remaining components. Cells were then spun down at 6000rpm for 3 min at room temperature, the supernatant was removed and 500µl of PEM buffer (50mM PIPES pH6.8, 25mM EGTA, 5mM $MgSO_4$) at 4°C, was used to rinse the cells. 100µl of pre-warmed digestive solution (PEM buffer, 180mg/µl Sorbitol, 200mg/µl BSA, 25µg/ml Zymolase, 0.2µg/ml of leupeptin, and 8µM AEBSF) was subsequently added and incubated at 37°C for 30 min. Cells were then spun down at 5000rpm for 2 min at room temperature, and rinsed with 500µl of chilled PEM buffer. 100µl of permeabilizer solution (PEM buffer with 0.1% Nonidet P40 Substitute (Fluka)) was subsequently added and incubated at room temperature for 5min. After cells were spun down and rinsed with PEM buffer, cells were incubated overnight at 4°C in primary antibody solution (PEM buffer, 0.05% sodium azide, 2% BSA and 1:100 dilution monoclonal anti-α-tubulin (DM1A, Sigma)). The next day cells were spun down, rinsed with 500µl of chilled PEM buffer and then incubated for 2 hours in secondary antibody solution (PE buffer, 0.05% sodium azide, 2% BSA and 1:100 dilution of anti-mouse IgG $F(ab')_2$ fragment-FITC, Sigma). Cells were then spun down, rinsed with 500µl of chilled PEM buffer and stained with 1µg/ml of DAPI for 20min. After a final spin and rinse with chilled PEM buffer followed, cells were placed on a microscope slide that contained a drop of SlowFade gold antifade reagent (Invitrogen), covered with a coverslip and sealed with nail polish. The slides were then examined on a Leica microscope (DM6000B) using a 100X immersion oil objective and the DAPI (460nm) and FITC (520nm) filters.

Appendix 2 Table 1: *Candida albicans* strains used in this study

Strain	Genotype	Source
SC5314	*CaCDC5/CaCDC5 URA3/URA3 HIS1/HIS1*	Fonzi and Irwin 1993
BWP17	*ura3::**imm434/ura3::** *imm434his1::hisG/his1::hisG arg4::hisG/arg::hisG*	Wilson et al., 1999
KMCa5a	*TRS120/MET3::TRS120-HIS1* in BWP17	This study
KMCa6a	*trs120::URA3/MET3::TRS120-HIS1* in BWP17	This study
KMCa6e	*trs120::URA3/TRS120, HIS1* in BWP17	This study

Appendix 2 Table 2: Oligos used in this study

Oligonucleotides	Nucleotide Sequence (5' to 3')
CBSK1F	CTA AAT TAT AGA CAA CGC TGT CAT TTT ACA AAG CCA CAC CGC CAC CAA GAA GAT CAT TTG AAA GTG CAC TTG TAC ATA GTT ATA GGG CGA ATT GGA GCT C
CBSK1RB	CCA TTG CCA TTC AAG ATT GAA GGG GTT AAG AAA TAG TGA ATT AAC AAA CAC ACA CAT ATA TTT GTA TAT AAG CCA TGA AAG ACG GTA TCG ATA AGC TTG A
CB114F	CAT TTA CAC GAC TAC TGG TTT CAT GTA CAT AAA GTT ATT GAC GCG ATT ATA CAA TTT GAT TTC TCG AGT TGG CAC TAT GGA TCC TGG AGG ATG AGG AGA C
CB114R	GAA ATT GGA CGG AGT GCA ATC ATT TAT TGG AAC CAA CAA CAC TCG AAC TTT TGC TGG AGT GAT AAA ATT ATA TTT GTC CCA CAT GTT TTC TGG GGA GGG T
KM1F	CTT GGA GGT CAA GAA TGC AT
KM1R	AAT TGG AAT CCG AAG GTG CC
KM8F	GAT CTA TAG ATC CAG ATG CC
KM8RR	TCG TGG TGA TCA TGA CTT GG

Appendix 2 Table 3: Plasmids used in this study

Plasmid	Genotype	Source
pBS-cURA3	*C. albicans URA3*	Gola et al., 2003
pBS-HIS1-MET3p	*C. albicans MET3* promoter and *HIS1*	Gola et al., 2003

Results

TRS120 is placed under the control of the *MET3* promoter

The *TRS120* gene (orf19.7694) in *C. albicans* is 28% identical and 50% similar to *TRS120* in *S. cerevisiae* and is 20% identical and 40% similar to *hypA* in *A. nidulans.* To address the function of *TRS120*, we attempted to knockout both copies, but were unsuccessful, suggesting that the gene was essential. Thus, we created a regulated strain, where one copy was replaced by *URA3* (Appendix 2 Figure 1a), while the second copy was placed under the control of the *MET3* promoter (Appendix 2 Figure 1b) in the wild type strain BWP17. After streaking to single colony, strains were screened by PCR using flanking oligos KM1F and KM1R, which lie outside the transforming DNA sequence. Strain KMCa5a was positive for the *MET3* promoter replacement, since it contained a 7.2kb band as opposed to a 4.4kb band as seen in wild type BWP17 strain (data not shown). A second PCR screening was performed for the second copy, which was replaced by *URA3*. Strain KMCa6a was positive, since it contained a 1.9kb band as opposed to a 4.4kb band seen in control KMCa6e strain (data not shown). Southern analysis demonstrated the presence of the 5.8kb and 11kb bands in KMCa6a, but a 8.3kb band in the wild-type strain, confirming replacement of one copy and promoter replacement in the other (Appendix 2 Figure 2). KMCa6e strain was also analyzed by Southern, and demonstrated that one copy had the promoter replaced (7.2kb), while the second copy remained wild-type (4.4kb) (Appendix 2 Figure 2). Thus, KMCa6a and KMCa6e were used for all further analyses.

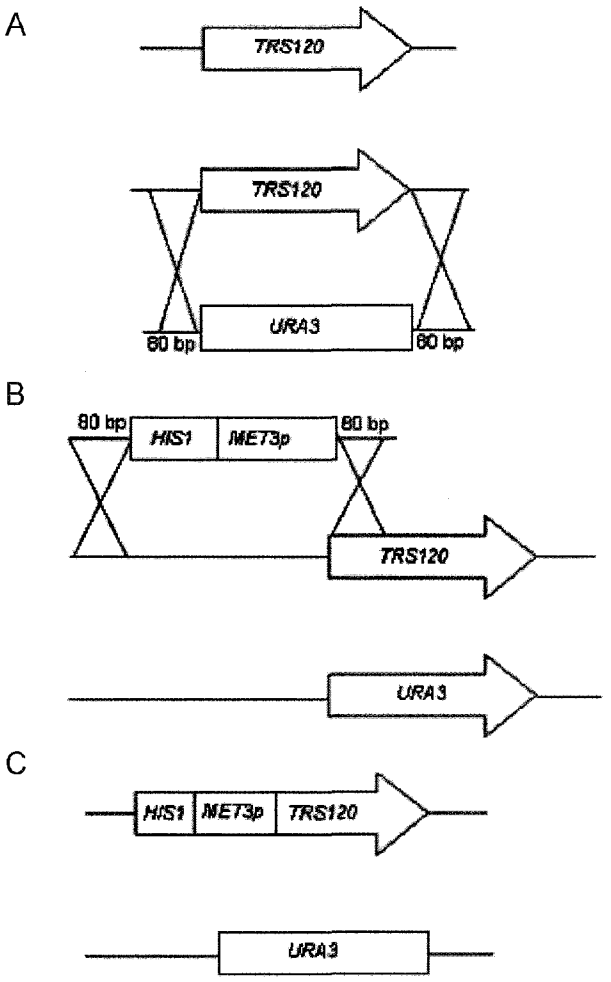

Appendix 2 Figure 1: Strategy for construction of a *MET3p*-regulated strain of *TRS120*.

(A) One copy of *TRS120* (orf19.7604) was replaced using a deletion construct prepared by amplifying the *URA3* marker in plasmid pBS-c*URA3* (kindly provided by J. Douglas, I.D. Broadbent, and A.J.P. Brown) with oligos containing 80 bp homology to the 5'and 3' flanks of *TRS120*. **(B, C)** The second copy of the gene was placed under control of the *MET3* promoter. This replacement construct was prepared by PCR amplifying the *MET3* promoter and *HIS1* marker from plasmid pFA-HIS1-MET3p (3) with oligos containing 80 bp of homology to sequences immediately up and down stream from the START codon.

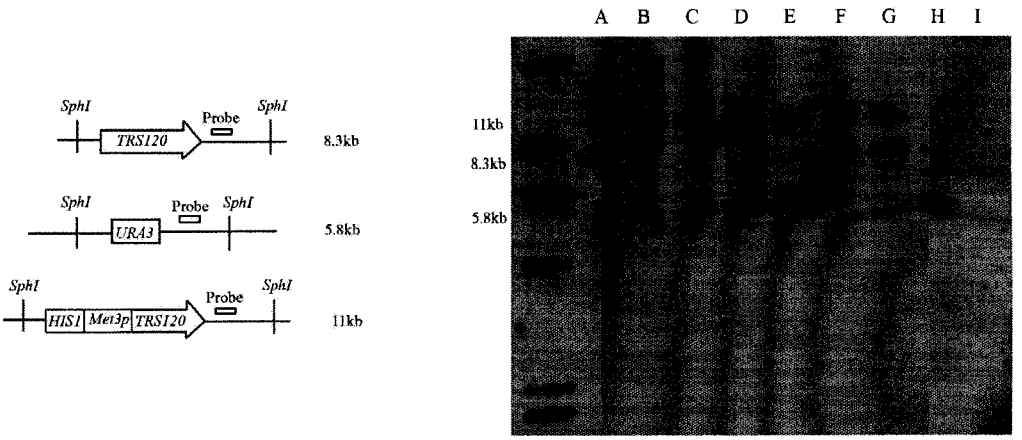

Appendix 2 Figure 2: Southern analysis for *MET3p*-regulated strains of *TRS120*. Southern analysis confirming that strain KMCa6a is positive (11 and 5.8kb), and KMCa6e is negative (11 and 8.3kb). Note: A: Wild type, B-E: *trs120::URA3/MET3::TRS120-HIS1*, F-G: *trs120::URA3/TRS120, HIS1* and H-I (*TRS120/MET3::TRS120-HIS1* in BWP17)

Shutting off TRS120 under yeast growth conditions inhibits growth

To determine the effects of depleting Trs120p, cells from strain KMCa6a and control strain KMCa6e were plated on solid inducing and repressing media for two days at 30°C. Under inducing conditions, strains KMCa6a and KMCa6e demonstrated normal growth. In contrast, under repressing conditions, strain KMCa6a was unable to grow, while KMCa6e grew to the same extent as on inducing media (Appendix 2 Figure 3).

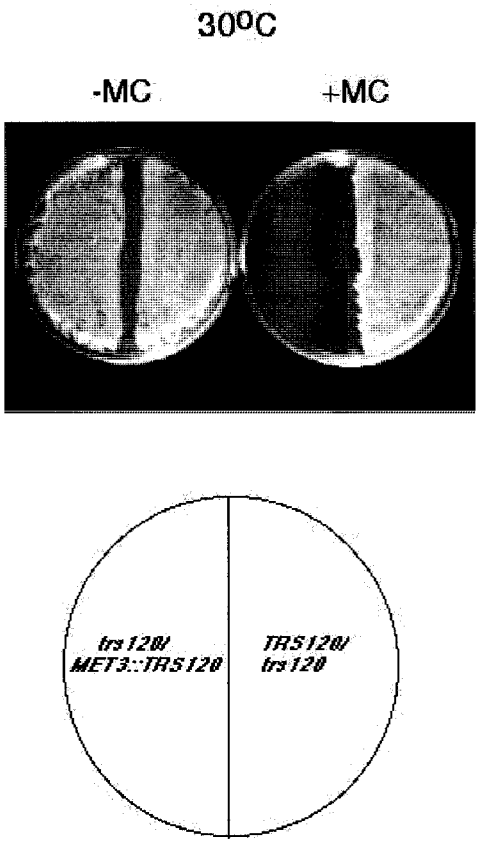

Appendix 2 Figure 3: Shutting off *TRS120* under solid yeast growth conditions (30°) inhibits growth.
Strains KMCa6A *(trs120::URA3/MET3::TRS120-HIS1)* and KMCa6E *(trs120::URA3/TRS120, HIS1)* were plated on SD media with (+MC) or without (-MC) 2.5 mM methionine and 0.5 mM cysteine, and incubated at 30°C for 48 h.

In order to confirm that growth was arrested, cells were quantified over time in repressing and inducing media. Cells from strain KMCa6a and control strain KMCa6e were inoculated overnight in liquid inducing media at 30°C. The next day, cells in exponential phase were diluted to an $0.D._{600nm}$ of 0.15 in either inducing or repressing media. Cells were collected in exponential phase, because at this time they are growing without any restrictions, whereas cells in stationary phase take some time to resume growth. The $0.D._{600nm}$ was then recorded every two hours for a 10 hour period and a final reading was taken at 26 hours (Appendix 2 Figure 4). In inducing (-MC) media, strain KMCa6a was able to grow, but with a slight decrease in the doubling rate compared to the control strain KMCa6e (Appendix 2 Figure 4). In contrast, in repressing (+MC) media, growth of strain KMCa6a was significantly inhibited by 10 hours, after which a slight increase was observed at 24 hours. In contrast, the control strain KMCa6e grew to a similar extent as in inducing media (Appendix 2 Figure 4). Thus, when cells are depleted of *TRS120*, growth is inhibited.

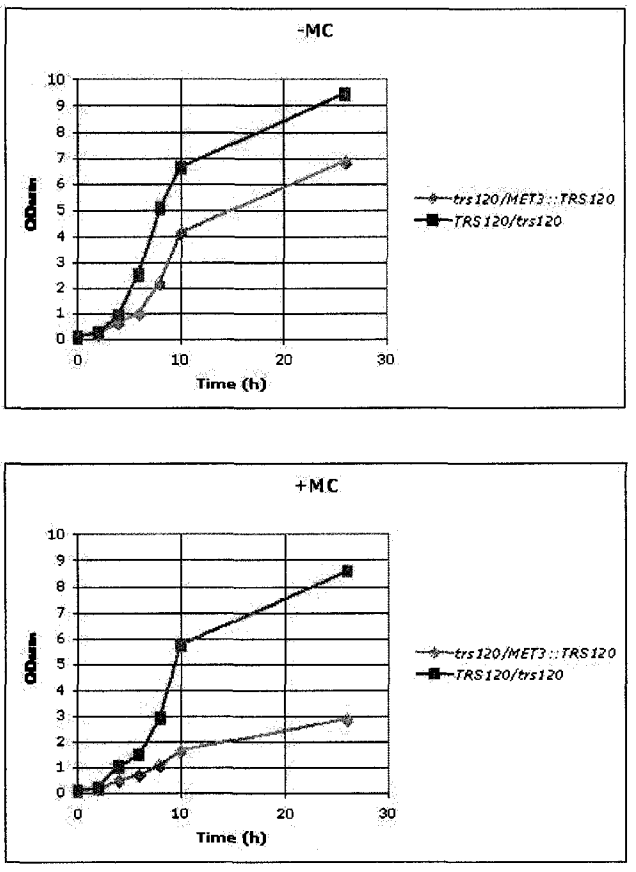

Appendix 2 Figure 4: Yeast cell growth is inhibited after shutting off *TRS120*. Strains KMCa6A and KMCa6E were grown overnight in liquid –MC SD media, and exponential-phase cells were diluted to an $O.D._{600nm}$ of 0.15 in +MC and –MC SD media. The $O.D._{600nm}$ was recorded every 2h for 10h, and again at 26h.

Shutting off TRS120 under yeast growth conditions results in isometric cell expansion, and abnormal cell morphology

In order to determine how Trs120p maybe influencing cell growth, strain KMCa6a and control strain KMCa6e were grown overnight in inducing media. The next day, cells in exponential phase were inoculated in inducing and repressing liquid media at an $O.D._{600nm}$ of 0.15 and collected after 10 and 24 hours. Both strains grew in inducing media and appeared as normal exponential cells (Appendix 2 Figure 5). After 10h in repressing media, however, strain KMCa6a had a swollen shape, and cells were extremely enlarged by 24 hours (Appendix 2 Figure 5). In contrast, the control strain KMCa6e had a normal morphology at 10 and 24 hours (Appendix Figure 5).

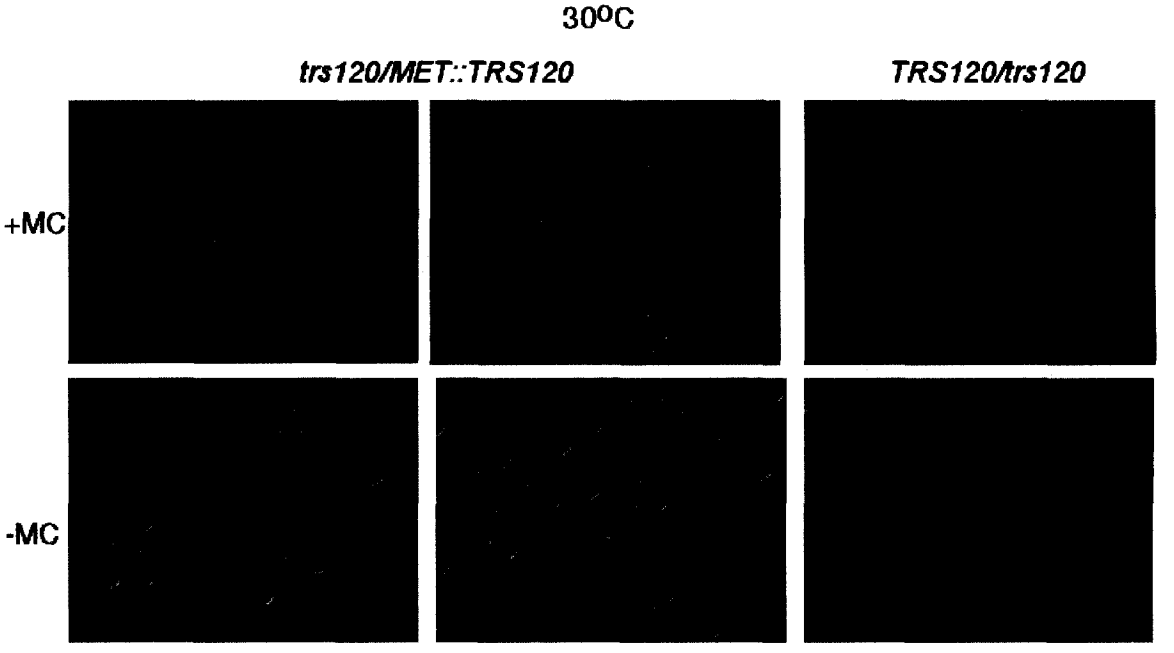

Appendix 2 Figure 5: Shutting off *TRS120* under liquid yeast growth conditions (30°) results in isometric cell expansion and abnormal cell morphology
(A) Strains KMCa6A *(trs120::URA3/MET3::TRS120-HIS1)* and KMCa6E *(trs120::URA3/TRS120, HIS1)* were grown overnight in –MC SD liquid media, diluted to an $O.D._{600nm}$ of 0.15 in +MC and –MC SD media, and incubated for 10 and 24 h. Bar: 10 μm.

In order to determine if nuclear division occurred or was arrested in the enlarged cells, cells were strained with DAPI. In inducing media, both strains demonstrated one nucleus per cell. However, in repressing conditions at 10 hours, KMCa6a often had separated chromatin within an enlarged mother cell that contained a small bud (Appendix 2 Figure 6). By 24 hours, the abnormally large cells contained several nuclei (Appendix 2 Figure 6). When abnormal cells and the nuclear patterns were quantified at 8h in repressing media, 5.4% of cells in strain KMCa6a had separated chromatin within an enlarged mother cell, 28.5% had separated chromatin within an enlarged mother cell that contained a small bud, and 10.5% had two separated chromatin masses in two enlarged cells that were still connected (Appendix 2 Table 4). By 24 hours, KMCa6a demonstrated, 29.3% of cells with separated chromatin within an enlarged mother cell, 23.8% with separated chromatin within an enlarged mother cell that contained a small bud and 11.1% with two separated chromatin masses in two enlarged cells that were still connected (Appendix 2 Table 4). On the other hand, enlarged cells with separated chromatin were only seen in less than 2% of the population at both 8 and 24 hours in strain KMCa6a in inducing media (Appendix 2 Table 4). In contrast, the control strain KMCa6e had normal growing cells at both time points and resembled the cells in inducing media. Enlarged cells with separated chromatin were not observed in the in either repressing or inducing media (Appendix 2 Table 4). Thus shutting off *TRS120* results in isometric cell expansion and uncoupling of nuclear and cell division.

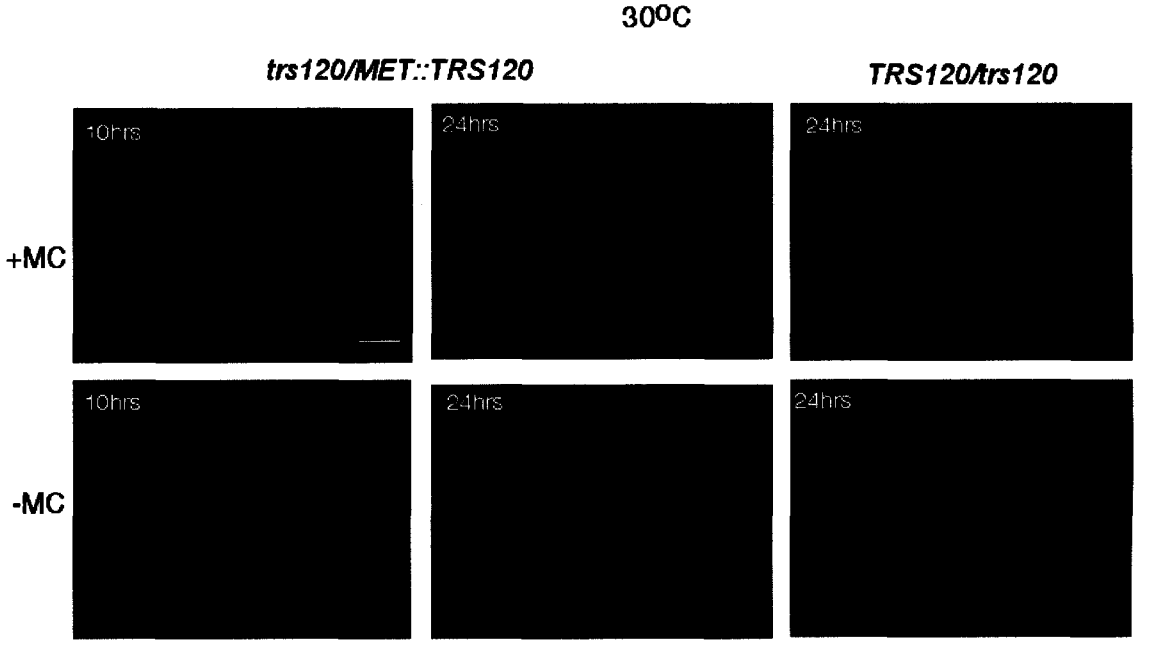

Appendix 2 Figure 6: Shutting off *TRS120* expression under liquid yeast growth conditions (30°) results in abnormal nuclear division, and uncouples nuclear division from septation.
Strains KMCa6A *(trs120::URA3/MET3::TRS120-HIS1)* and KM Ca6E *(trs120::URA3/TRS120, HIS1)* were grown overnight in –MC SD liquid media, diluted to an $O.D._{600nm}$ of 0.15 in +MC and –MC SD media, and incubated for 10 h and 24 h. Cells were fixed, and nuclei and septa were stained with DAPI and Calcofluor, respectively. Bar: 10 μm.

Appendix 2 Table 4. Cell morphology and nuclear division pattern in *trs120* depleted cells

Strain/ Media[1]	hours	Cell morphology and nuclear division pattern					
		Single	with small bud	with large bud	Single **enlarged**[2] bud	**enlarged**[2] bud with small bud	Two **enlarged**[2] buds
		1 nucleus	1 nucleus	1 nucleus per bud	>2 nuclei	>2 nuclei in mother cell	>2 nuclei in **either bud**
				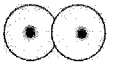	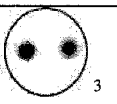	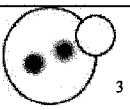	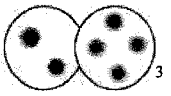
KMCa6a -MC	8h (n=354)	49.6	7.6	40.3	1.0	1.0	0.5
KMCa6a +MC	8h (n=407)	14.4	6.5	34.7	5.4	28.5	10.5
KMCa6a -MC	24h(n=344)	68.8	5.4	24.5	1.1	0	0.2
KMCa6a +MC	24h(n=481)	13.7	4.9	17.2	29.3	23.8	11.1
KMCa6e -MC	8h (n=348)	44.5	20.7	34.8	0	0	0
KMCa6e +MC	8h (n=353)	44.3	21.3	34.4	0	0	0
KMCa6e -MC	24h(n=321)	84.9	3.4	11.7	0	0	0
KMCa6e +MC	24h(n=325)	92.5	1.6	5.9	0	0	0

[1] media either –MC (-MUH) or +MC (-MUH+MC)
[2] enlarged cells demonstrated a much larger bud size compared to the "regular" size
[3] dots represent nuclei, but do not represent the exact location or number of the nuclei in each cell counted
Values are expressed as percentage.
Cells from strain KMCa6a or KMCa6e were inoculated in either inducing (-MC) or repressing (+MC) media for 8 hours or 24 hours, fixed and strained with DAPI. Results represent two individual trials that were combined.

Growth of the *TRS120* regulated strain under inducing conditions is temperature sensitive at 37°C

We next attempted to determine the effects of depleting *TRS120* in hyphal cells. Cells from strains KMCa6a and KMCa6e were inoculated into inducing media overnight, the diluted with inducing media that contained 10% serum to an $O.D._{600nm}$ of 0.15 at 37°C. The control strain formed hyphae after 4 hours, whereas the regulated strain was unable to form hyphae, even after a prolonged exposure time to the hyphal inducing media (data not shown). These results suggested that either the regulated strain is unable to form hyphae, even under inducing conditions, or the strain is temperature-sensitive.

To determine the effect of high temperature on growth, cells from strain KMCa6a and control strain KMCa6e were plated on solid inducing and repressing media for two days at 37°C. Under both inducing and repressing conditions, strain KMCa6a was unable to grow (Appendix 2 Figure 7A). In contrast, the control strain KMCa6e demonstrated normal growth in both conditions (Appendix 2 Figure 7A). Therefore, this suggests that the *TRS120*-regulated strain is temperature-sensitive.

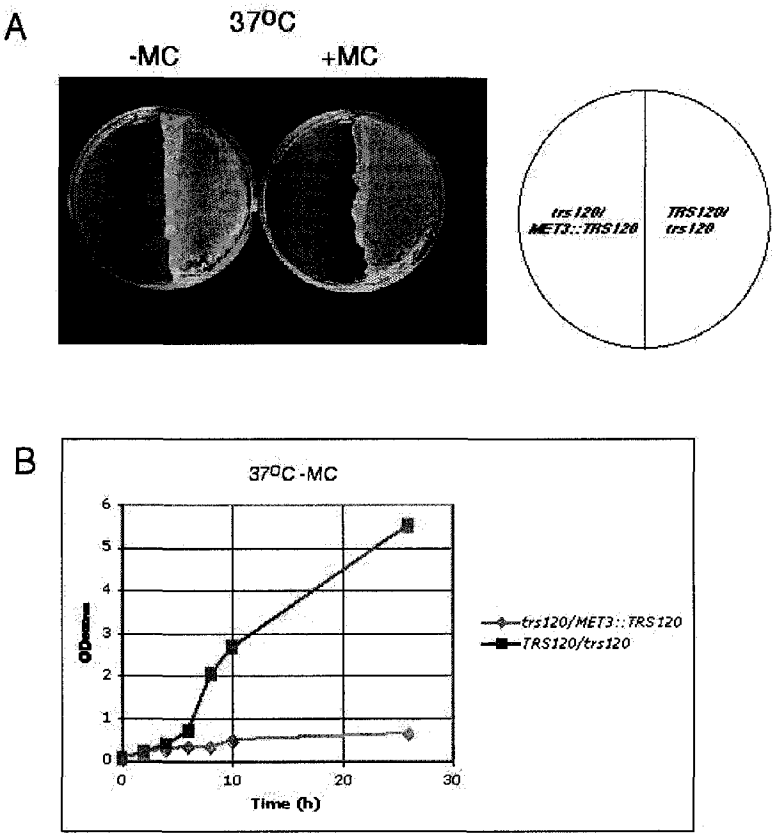

Appendix 2 Figure 6: Growth of the *TRS120*-regulated strain under *TRS120*-inducing conditions is temperature-sensitive at 37° C.

(A) Strains KMCa6A *(trs120::URA3/MET3::TRS120-HIS1)* and KMCa6E *(trs120::URA3/TRS120, HIS1)* were plated on SD media with (+MC) and without (-MC) 2.5 mM methionine and 0.5 mM cysteine, and incubated at 37°C for 48 h.

(B) Exponential-phase cells of strains KMCa6A and KMCa6E were diluted to an $O.D._{600nm}$ of 0.15 in –MC SD media, and the $O.D._{600nm}$ was recorded every 2h for 10h, and again at 26h.

In order to confirm that the strain was temperature sensitive, another growth curve was created. This time, cells from strain KMCa6a and control strain KMCa6e were inoculated overnight, and then diluted to an $O.D._{600nm}$ of 0.15 in inducing media only at 37°C. Cells were collected every two hours for 10 hours and subsequently at 26 hours. Cells from strain KMCa6a did not appear to grow, since no change in O.D. was recorded other than the initial inoculation (Appendix 2 Figure 7B). In contrast, the control strain KMCa6e was able to grow and had a normal doubling time (Appendix 2 Figure 7B). Thus, this suggests that the *TRS120* regulated strain is temperature-sensitive.

Cell morphology and nuclear division in the *TRS120*-regulated strain under inducing conditions are temperature sensitive at 37°C

In order to determine the effect that higher temperature might have on cell growth, cells from strains KMCa6a and KMCa6e were inoculated overnight in liquid inducing media. The next day, cells in exponential phase were inoculated in inducing liquid media at an $O.D._{600nm}$ of 0.15. Cells were collected after 10 and 24 hours, and fixed with 70% EtOH. Cells from stain KMCa6a were found to be abnormally large at 10 hours and even larger at 24 hours (Appendix 2 Figure 8). The cells had a similar phenotype to those in repressing medium at 30°C. In contrast, the control strain KMCa6e was morphologically normal (Appendix 2 Figure 8).

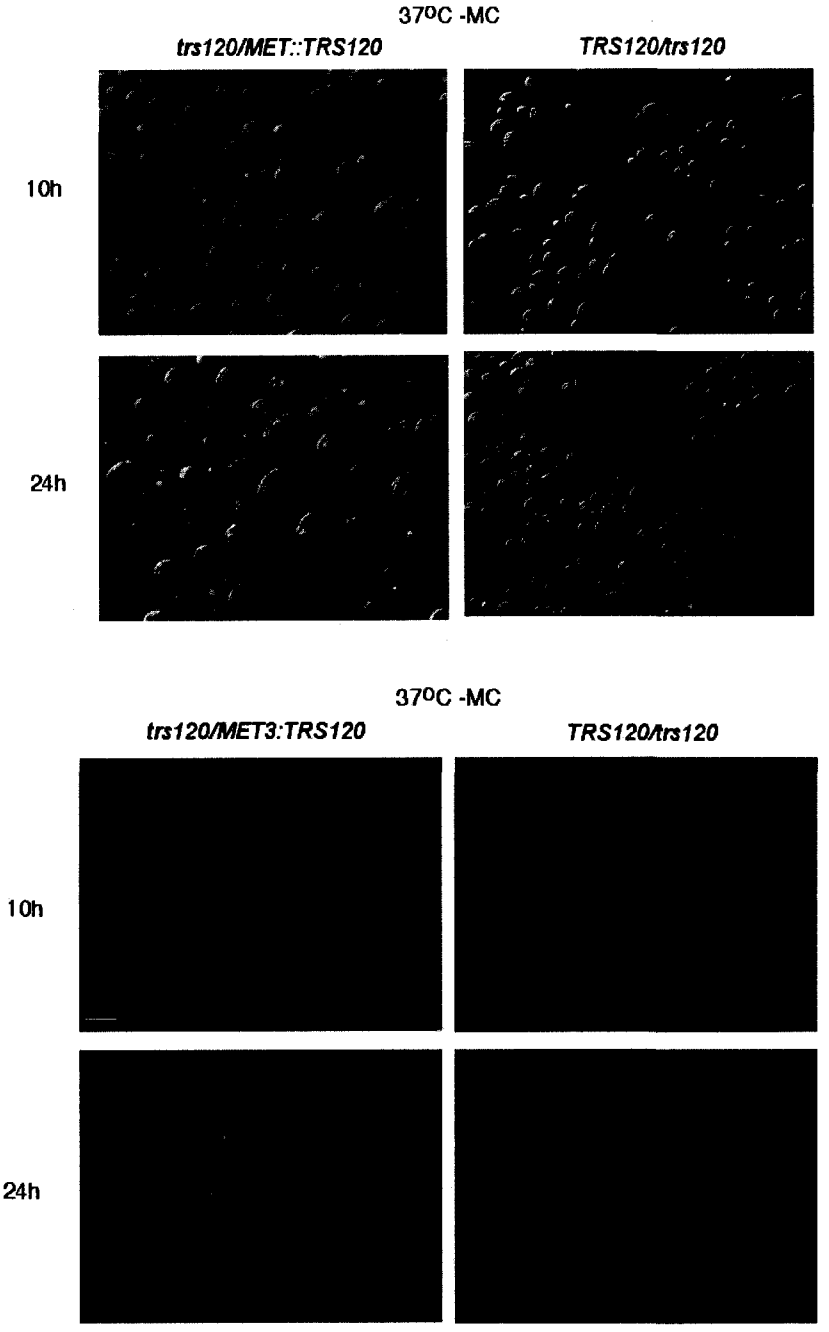

Appendix 2 Figure 8: Cell morphology and nuclear division in the *TRS120*-regulated strain under *TRS120*-inducing conditions are temperature sensitive at 37°C.

Strains KMCa6A *(trs120::URA3/MET3::TRS120-HIS1)* and KM Ca6E *(trs120::URA3/TRS120, HIS1)* were grown overnight, diluted to an $O.D._{600nm}$ of 0.15 in –MC SD media, and incubated for 10 h and 24 h. Cells were fixed, and nuclei and septa were stained with DAPI and Calcofluor, respectively. Bar: 10 μm.

In order to determine the effect that higher temperature might have on nuclear division, the same cells collected at 10 and 24 hours were stained with DAPI. Cells from KMCa6a demonstrated multiple nuclei at both time points, similar to what was observed at 30°C in repressing conditions (Appendix 2 Figure 8). In contrast, the control strain KMCa6e demonstrated a single nucleus per cell at both time points (Appendix 2 Figure 8). Thus, cells lacking *TRS120* are temperature-sensitive, and incubation at 37°C in inducing medium results in similar isometric cell expansion and nuclear uncoupling as seen in repressing medium at 30°C.

Addition of 1M Sorbitol rescues the temperature sensitivity of the *TRS120*-regulated strain under inducing conditions, but does not rescue growth of cells under repressing conditions

Since studies on the HYPA homologue in *A. nidulans* demonstrated cell wall defects (Shi et al., 2004), we investigated whether this was occurring in the *TRS120*-regulated strain by testing the effect of sorbitol. Sorbitol provides an osmotic support to cells that have defects in their cell wall. Cells from strain KMCa6a and the control strain KMCa6e were inoculated overnight in inducing media, diluted, and 8000 cells were spread on solid inducing or repressing media containing 1M sorbitol. The plates were subsequently incubated at 30°C or 37°C for 2 days. At 30°C on inducing solid media, both strains KMCa6a and KMCa6e were able to grow (Appendix 2 Figure 9). In contrast, in repressing solid media at 30°C, only the control strain KMCa6e was able to grow (Appendix 2 Figure 9). These results were similar to those obtained in the absence of sorbitol. Surprisingly, at 37°Cin inducing media, cells from strain KMCa6a were able to

grow, albeit not to the same degree as cells from the control strain (Appendix 2 Figure 9). In contrast, in repressing solid media at 37°C, only the control strain KMCa6e was able to grow (Appendix 2 Figure 9). Thus, sorbitol was able to rescue the effect of temperature-sensitivity only under inducing conditions, whereas under repressing conditions when cells lack *TRS120*, sorbitol was not able to rescue the temperature-sensitivity or growth defects.

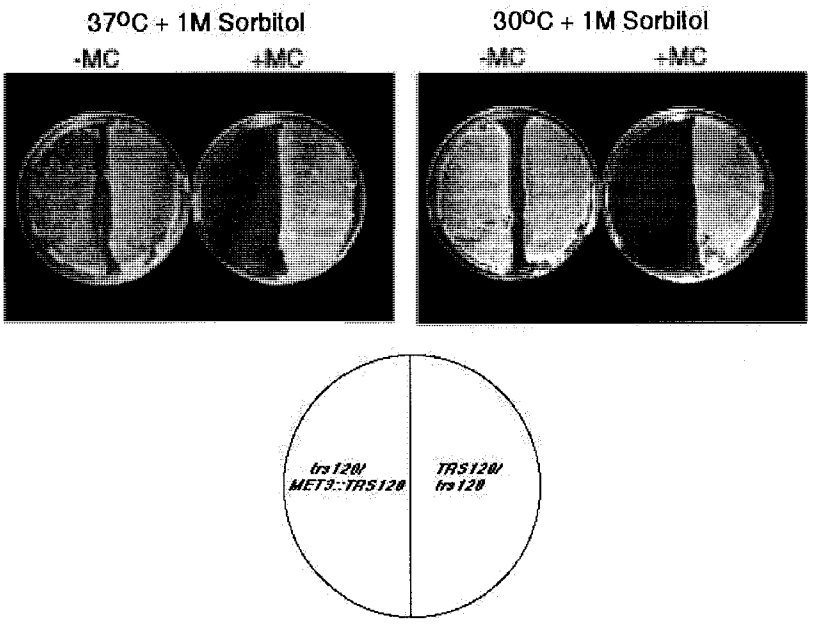

Appendix 2 Figure 9: Addition of 1M sorbitol rescues the temperature-sensitivity of the *TRS120*-regulated strain under inducing conditions, but does not rescue growth of cells under repressing conditions at 30° C.
Strains KMCa6A *(trs120::URA3/MET3::TRS120-HIS1)* and KMCa6E *(trs120::URA3/TRS120, HIS1)* were plated on SD media with (+MC) and without (-MC) 2.5mM methionine and 0.5 mM cysteine, supplemented with 1M sorbitol, and incubated at 37°C or 30 °C for 48h.

Discussion

We have demonstrated that *TRS120* is essential in *C. albicans*. This was determined by shutting off *TRS120* expression in repressing media, and observing no growth in either liquid or solid SD media. The lack of growth was confirmed with a growth curve, which demonstrated that after 10 hour in repressing media, cells lacking *TRS120* stopped growing. The slight increase in growth observed after 10 hours is most likely due to the cells increasing in diameter rather than doubling. However, cells in inducing media had only a slight decrease in growth rate compared to the controls. *TRS120* is also essential in *S. cerevisiae*, and mutants accumulate irregular membrane structures that resemble Berkeley bodies (Cai et al., 2005). As well, mutants have a disruption in the recycling of proteins from the endosome to the late Golgi (Cai et al., 2005). In contrast, the *TRS120* homologue in *A. nidulans*, HYPA, was found to not be essential in this filamentous fungus. The phenotype of the *hypA* mutants consisted of depolarized growth of the subapical hyphal compartments, while the apical cell stopped growing completely (Shi et al., 2004). Our results with Trs120p in *C. albicans* share similarities with both Trs120p in *S. cerevisiae* and HYPA in *A. nidulans*.

Trs120p is required for normal cell growth and nuclear division

It was quite surprising to discover that cell growth and nuclear division was affected when Trs120p was depleted. By 10 hours, over 30% of cells became enlarged and contained separated chromatin in the mother cell. The effect was more drastic by 24

hours, where over 50% of cells were enlarged and had up to four separated chromatin masses in one cell. This role is surprising considering that this gene is involved in the TRAPP complex and is required in the secretory pathway and not the cell cycle. In *hypA* mutants of *A. nidulans*, multiple nuclei were also found within enlarged cells, but the cells were very abnormally-shaped hyphae, and the increase in nuclear division could have been a secondary effect of increase in cell mass. In contrast, *C. albicans* cells depleted of Trs120p were showing defects in nuclear division very early, when cells were not yet enlarged. This suggests a more direct effect of Trs120p on the cell cycle in *C. albicans,* by unknown mechanisms. Thus, Trs120p may have some cell cycle-related function in addition to its role in secretion.

Trs120p is cold sensitive and unable to switch to hyphal form

To address the role of Trs120p in hyphal vs yeast cells, cells depleted of *TRS120* were incubated at 37°C with serum to study hyphal growth. Surprisingly, even in inducing conditions, cells were unable to grow and hypha could not form. The phenotype was similar to that in repressing conditions at 30°C. DAPI staining confirmed that cell division was also impaired. When cells were plated on 1M sorbitol to provide osmotic support, cells were able to grow in inducing media, but not in repressing media. Similar results were seen with *hypA* in *A. nidulans*, where cells lacking *hypA* required osmotic support to grow at higher temperatures (Shi et al., 2004). Therefore, a critical level of *TRS120* expression might be required at higher temperature for cell wall integrity.

Future experiments will focus on defining the mechanisms by which Trs120p influences secretion, the cell cycle and hyphal growth. Electron microscopy could be

used to obtain a better picture of what is happening to the cells in the absence of *TRS120*, and to determine if there is an accumulation of Berkeley bodies. Northern analysis would need to be done to ensure that the *MET3* promoter is completely repressing *TRS120*.In addition, other TRAPP complex genes, such as *TRS130*, should also be investigated for roles in cell growth and nuclear division.